

**PYRAZOLE AND PYRAZOLYL PALLADIUM(II) AND  
PLATINUM(II) COMPLEXES: SYNTHESIS AND *IN VITRO*  
EVALUATION AS ANTICANCER AGENTS.**



**FRANKLINE KIPLANGAT KETER**

**A Thesis Submitted In Partial Fulfillment Of The Requirements For The Degree Of  
Masters In Science In The Department Of Chemistry, University Of The Western  
Cape.**

**DATE: November 2004**

**SUPERVISOR: PROFESSOR JAMES DARKWA**

**CO-SUPERVISOR: PROFESSOR D. JASPER G. REES**

## ABSTRACT

The use of metallo-pharmaceuticals, such as the platinum drugs (e.g. cisplatin), for cancer treatment illustrates the utility of metal complexes as therapeutic agents. Platinum group metal complexes therefore offer potential as anti-tumour agents to fight cancer. Our study was aimed at synthesizing and evaluating the effects of palladium(II) and platinum(II) complexes as anticancer agents. The synthesis of water soluble pyrazole ligands (**L1-L3**) were performed by means of alkylaminoalkylation reactions. This was achieved by reacting either pyrazole or 3,5-dimethylpyrazole with formaldehyde and ethylamine or isopropylamine. The reactions were performed *in situ*. The preparation of the corresponding palladium(II) and platinum(II) complexes of **L1-L3** were performed by reacting the ligands with  $[\text{PdCl}_2(\text{NCMe})_2]$  and  $[\text{K}_2\text{PtCl}_4]$  respectively. The products obtained were insoluble in common organic solvents. Another class of compounds (**1-5**), palladium and platinum complexes with pyrazole and pyrazolyl ligands, were synthesized directly by using the already available ligands. Palladium complexes, **1**, **2**, **5**, were obtained by reacting pyrazole, 3,5-dimethylpyrazole and 3,5-dimethylpyrazolylacetic acid ligands with  $[\text{PdCl}_2(\text{NCMe})_2]$  while platinum complexes, **3** and **4** were obtained by reacting pyrazole, 3,5-dimethylpyrazole with  $[\text{K}_2\text{PtCl}_4]$ . All compounds were characterized by multinuclear NMR, IR, Mass spectroscopy, microanalysis and X-ray crystallography in the case of **L4**.

Compounds **1-5** were then evaluated for their activity as anticancer agents and have been discussed in chapter 4. All the cells were cultured in their respective media (e.g. for CHO cells, Hams F-12 medium was used) at 37 °C in a humidified 5% CO<sub>2</sub> atmosphere for 24

h. The compounds to be tested were dissolved in water (or DMSO in some cases) and added to media to make a final concentration ranging from 0.02 to 1.00 mM. Cisplatin was analysed as the positive control. All experiments were performed for duration of 24 h. The activity was found to be both dose- and time-dependent. This was achieved by performing preliminary analysis of their cytotoxicity on chinese hamster ovary (CHO) and normal human fibroblast (NHF) cell-lines using the APOPercentage<sup>TM</sup> assay with the help of Fluorescence Activated Cell Sorter (FACS) techniques. Palladium compounds **1** and **2** did not show any significant activity on these cell lines while **5** showed activity at IC<sub>50</sub> value of 0.67 mM after 24 h of treatment. Platinum complexes were more active than palladium compounds, with **3** and **4** showing significant activity at IC<sub>50</sub> values of 0.13 and 0.035 mM after 24 h of treatment.

The DNA fragmentation of cells treated with compound **3** and **5** was achieved by electrophoresis of the DNA extracted from the treated cells. This was performed on a 2% agarose gel at 100V for 1 h and visualized by ethidium bromide staining. The fragments of approximately 200 bp observed indicated cell death via apoptosis. Cell cycle studies was performed on CHO cells treated with compound **5** (at 0.60 mM), by staining the cells with acridine orange (AO) and subsequently evaluating cells FACS techniques. It was observed that DNA replication was inhibited at G<sub>1</sub>- phase with cells (ca. 31%) undergoing cell death (via apoptosis) after 24 h. Analysis of interaction of these compounds with biomolecules *in vitro* was achieved by studying the interaction of complex **3** and glutathione by <sup>1</sup>H NMR spectrum for 24 h at room temperature, indicating ligand substitution of the pyrazole ligand by glutathione.

## DECLARATION

I declare that *pyrazole and pyrazolyl palladium(II) and platinum(II) complexes: synthesis and evaluation in vitro as anticancer agents* is my own work, that it has not been submitted for any degree or examination in any other university, and that all the sources I have used or quoted have been indicated and acknowledged by complete references.

**FRANKLINE KIPLANGAT KETER**

.....

Signature

.....

Date

## **ACKNOWLEDGEMENTS**

I wish to express my sincere appreciation to my supervisors, Professors Darkwa and Rees for their constant support through the period of pursuing this work. Their contributions both material and in service were of great help. I would also like to acknowledge Sylvester Lyantage and Mervin Meyer, both of biochemistry department, for their support and advices in biochemical assays. Many thanks go to the Organometallics research group, especially Professor Mapolie, for the constant consultations that were fruitful. The same goes to apoptosis group. I would also like to thank Dr. Ilia Guzei of Wisconsin University, USA, for having helped in solving the crystal structure reported herein, I thank him for that. I would not forget to thank the Chemistry department and the University of the Western Cape as a whole for giving me an opportunity to pursue my studies. Finally I thank my family for their invariable support through the entire period, and most of all I thank the almighty God for his guidance and protection.

## **DEDICATION**

This work is dedicated to my family

## **Table of contents**

<b>ABSTRACT</b>	<b>ii</b>
<b>DECLARATION</b>	<b>iv</b>
<b>ACKNOWLEDGEMENTS</b>	<b>v</b>
<b>DEDICATION</b>	<b>vi</b>
<b>Table of contents</b>	<b>vii</b>
<b>List of figures</b>	<b>xi</b>
<b>List of Tables</b>	<b>xiv</b>
<b>ABBREVIATIONS</b>	<b>xv</b>
<i>Preface</i>	<b>xvi</b>
<b>Chapter 1</b>	<b>1</b>
<b>GENERAL INTRODUCTION TO APPLICATION OF METALS IN RESEARCH FOR ANTICANCER AGENTS</b>	<b>1</b>
<i>1.1 Introduction</i>	<b>1</b>
<i>1.2 Non-metal containing cancer drugs</i>	<b>3</b>
<i>1.3 Metal based anticancer drugs (metallo-drugs).</i>	<b>7</b>
<i>1.4 Platinum based anticancer agents.</i>	<b>13</b>
<i>1.5 Platinum-DNA interactions.</i>	<b>15</b>
<i>1.5.1 DNA: The biological cellular target of cisplatin.</i>	<b>15</b>
	<b>vii</b>

1.5.2 <i>Effects of platination on structure.</i>	18
1.5.3 <i>Conformational-activity related study.</i>	24
<b>1.6 <i>The kinetics of platinum(II) drugs.</i></b>	<b>26</b>
<b>1.7 <i>Interaction of platinum complexes with biomolecules.</i></b>	<b>27</b>
<b>1.8. <i>Pyrazole and Nitrogen containing Ligands in synthesis of anticancer agents.</i></b>	<b>31</b>
<b>1.9 <i>Rationale and Objectives.</i></b>	<b>37</b>
<b>Chapter 2</b>	<b>43</b>
<b>INTRODUCTION TO BIOCHEMICAL PROCESSES INVOLVED IN CELL DEATH</b>	<b>43</b>
<b>2.1 <i>Introduction to cancer</i></b>	<b>43</b>
<b>2.2 <i>Cytotoxicity</i></b>	<b>44</b>
<b>2.3 <i>Apoptosis</i></b>	<b>48</b>
2.3.1 <i>Cell membrane alteration.</i>	48
2.3.2 <i>Cell-cycle and its interruption</i>	50
2.3.3 <i>DNA fragmentation</i>	55
2.3.4. <i>p53, mitochondria, caspases, and other DNA damage responses in apoptosis</i>	57
<b>2.4 <i>References:</i></b>	<b>61</b>
<b>Chapter 3</b>	<b>64</b>
<b>SYNTHESIS OF PYRAZOLE LIGANDS AND THEIR COMPLEXATION WITH LATE TRANSITION METALS</b>	<b>64</b>
<b>3.1 <i>Introduction</i></b>	<b>64</b>
<b>3.2 <i>Experimental</i></b>	<b>65</b>



3.2.1 <i>Materials and methods.</i>	65
3.2.2 <i>Crystallographic structure determination</i>	66
3.2.3 <i>Synthesis of Ligands</i>	66
3.2.4 <i>Synthesis of complexes</i>	68
<b>3.3. <i>Spectroscopic data of the complexes used</i></b>	<b>69</b>
3.3.1 <i>Cis-dichloro-bis-(pyrazole)palladium(II) (1).</i>	69
3.3.2 <i>Cis-dichloro-bis-(3,5-dimethylpyrazole)palladium(II) (2).</i>	69
3.3.3 <i>Cis-dichloro-bis-(pyrazole)platinum(II) (3).</i>	69
3.3.4 <i>Cis-dichloro-bis-(3,5-dimethylpyrazole)platinum(II) (4).</i>	70
3.3.5 <i>Dichloro-bis-((3,5-dimethylpyrazolyl)acetic acid )palladium(II) (5)</i>	70
<b>3.6 <i>Results and discussions</i></b>	<b>70</b>
<b>3.7 <i>Molecular structure of L3</i></b>	<b>80</b>
<b>3.8 <i>Conclusion</i></b>	<b>88</b>
<b>3.9 <i>References</i></b>	<b>89</b>
<b>Chapter 4</b>	<b>90</b>
<b>EVALUATION OF PALLADIUM AND PLATINUM COMPLEXES AS ANTICANCER AGENTS AND OTHER EXPERIMENTS.</b>	<b>90</b>
<b>4.1 <i>Introduction</i></b>	<b>90</b>
<b>4.2 <i>Biological tests</i></b>	<b>91</b>
4.2.1 <i>Cell culture and drug treatment</i>	91
4.2.2 <i>Evaluation of cell death and apoptosis</i>	91
4.2.3 <i>Evaluation of cell cycle arrest using acridine orange</i>	92
4.2.4 <i>DNA fragmentation</i>	92

<b>4.3 Dichloro-bis-(pyrazole)platinum(II)-glutathione, 1:2 reaction</b>	<b>92</b>
<b>4.4 Results and discussion</b>	<b>93</b>
4.4.1 Morphological changes	93
4.4.2 Concentration effect on the cell death, dose response	96
4.4.3 Time-dependent reaction courses of the compounds on the treated cells	106
4.4.4 Evaluation of mechanism of cell death by DNA and RNA content measurement	109
4.4.5 Induction of genomic DNA cleavage	112
<b>4.5 Reactions of platinum(II) complex with glutathione monitored by <sup>1</sup>H NMR spectroscopy</b>	<b>115</b>
<b>4.6 Conclusions</b>	<b>119</b>
<b>4.7 References.</b>	<b>122</b>

## List of figures

<b>Figure 1.1.</b> Structures of compounds among the clinically useful drugs. <b>a.</b> Taxol, <b>b.</b> Vincristine, <b>c.</b> Podophyllotoxin, <b>d.</b> Camptothecin.	5
<b>Figure 1.2.</b> Structure of Tamoxifen ( $R=H$ ) and its derivative Hydroxytamoxifen ( $R=OH$ ).	6
<b>Figure 1.3.</b> Structures of $\text{trans-[Na][Ru(Im)(Me}_2\text{SO)Cl}_4]$ and $\text{trans-[ImH][Ru(Im)(Me}_2\text{SO)Cl}_4]$ .	8
<b>Figure 1.4.</b> Structures of gold(I) complexes. <b>(a)</b> Gold(I) complexes with 1,2-bis(diphenylphosphino)ethane and 1,2-bis(dipyridylphosphino)ethane ligands. <b>(b)</b> Tetrakis-(trishydroxymethyl)-phosphine)gold(I) complex.	9
<b>Figure 1.5.</b> Vanadocene dichloride.	11
<b>Figure 1.6.</b> Six-coordinate cage complex of rhodium(II) carboxylates, $[(\text{RCOO})_4\text{L}_2\text{Rh}_2(\text{II})]$ .	13
<b>Figure 1.7:</b> Isomeric forms of dichlorodiammineplatinum(II) complex.	14
<b>Figure 1.8.</b> DNA structures showing the forms a DNA molecule assume.	17
<b>Figure 1.9.</b> Heterocyclic bases of DNA.	17
<b>Figure 1.10.</b> The cellular uptake of cisplatin and its targets.	19
<b>Figure 1.11.</b> Diagram of cisplatin-DNA adducts.	20
<b>Figure 1.12.</b> Cis-diammine-1,1'-cyclobutane dicarboxylate platinum(II), carboplatin.	22
<b>Figure 1.13.</b> Cis-dichloroamine-2-methylpyridineplatinum(II), AMD-473.	23
<b>Figure 1.14.</b> <i>trans</i> -L-diaminocyclohexaneoxalatoplatinum(II), eloxatin.	24
<b>Figure 1.15.</b> Monodentate versus chelate amine based complexes. <b>(a)</b> Bis(acetato)ammine-dichloro(cyclohexylamine)platinum(IV) and <b>(b)</b> bis(acetateo)-N-cyclohexyl-1,3-propanediamineplatinum(IV).	25
<b>Figure 1.16.</b> Representation of possible reaction mechanisms for interaction of cisplatin with glutathione	30
<b>Figure 1.17.</b> A new ligand, bis-[(3,5-diisopropylpyrazolyl)ethyl]ether	32
<b>Figure 1.18.</b> The synthesis of ligands and their complexes. Benzimidazole (Bim), Methylbenzimidazole (Mbim) and Aminobenzimidazole (Ambim).	33

<b>Figure 1.19.</b> The synthesis of 1,5-bis(3,5-dimethylpyrazol-1-yl)-3- [bis(imidazol-2-yl)methyl]-3-pentane ( <i>bdpbiap</i> ).	34
<b>Figure 1.20.</b> Examples of water-soluble nitrogen ligands.	36
<b>Figure 2.1.</b> Apoptotic programmed cell death.	46
<b>Figure 2.2.</b> Structures of (a) <i>trans</i> -[PtCl <sub>2</sub> (isopropylamine)(dimethylamine)], (b) <i>trans</i> -[PtCl <sub>2</sub> (isopropylamine)(butylamine)].	47
<b>Figure 2.3.</b> The asymmetric phospholipids composition of a transformed mammalian cell.	488
<b>Figure 2.4.</b> Analysis of cells dying apoptotically using a fluorescence-activated cell sorter.	500
<b>Figure 2.5.</b> The four phases of a standard eukaryotic cell cycle culminating in cell division.	52
<b>Figure 2.6.</b> Cell cycle statistical histogram showing the apoptotic cells appearing at the left of G1 peak.	54
<b>Figure 2.7.</b> DNA fragmentation pattern. Separation of DNA fragments of different sizes by using different concentrations of agarose gel in electrophoresis.	566
<b>Figure 3.1.</b> <sup>1</sup> H NMR spectrum of 3,5-dimethyl-4-(isopropylamino)methylpyrazole ( <b>L3</b> )	711
<b>Figure 3.2</b> Mass spectrum of ligand, <b>L3</b> .	722
<b>Figure 3.3.</b> Mass spectrum of <b>L3</b> .	744
<b>Figure. 3.4.</b> <sup>1</sup> H NMR spectrum of 1 <i>N</i> -triphenylchloromethane-3,5-dimethylpyrazole.	777
<b>Figure 3.5.</b> IR spectrum of <b>L4</b> .	78
<b>Figure. 3.6.</b> One possible fragmentation pattern of <b>L4</b> .	79
<b>Figure 3.7.</b> Molecular structure of compound <b>L4</b> .	800
<b>Figure 3.8.</b> <sup>1</sup> H NMR spectrum of compound <b>1</b> .	85
<b>Figure 3.9.</b> <sup>1</sup> H NMR spectrum of compound <b>2</b> .	86
<b>Figure 3.10.</b> IR spectrum of compound <b>1</b> .	87
<b>Figure 4.1.</b> The morphological effects exerted by complexes on CHO and NHF cells.	94
<b>Figure 4.2.</b> Photographs of treated and untreated CHO cells, APOP dye staining.	95
<b>Figure 4.3.</b> FACS Analysis. Typical acquisition histograms obtained by FACS when quantifying the amount of live and dead cells.	97

<b>Figure 4.4.</b> Graphical representation of concentration-dependent effect of the compounds 3, 4, and 5 on the treated CHO cells (24 h) respectively.	99
<b>Figure 4.5.</b> Comparison of the effects of ligand and the metal in the overall activity of the complexes.	102
<b>Figure 4.6.</b> Graphical representation of concentration-dependent effect of the compounds 1 and 2 on CHO cells treated for 24 h.	105
<b>Figure 4.7.</b> Graphical representation of time-dependent effect of the compounds on treated CHO cells.	108
<b>Figure 4.8.</b> Differential staining of RNA and DNA with acridine orange of control. Cell cycle progression of the untreated CHO cells after 24 h.	110
<b>Figure 4.9.</b> Differential staining of RNA and DNA with acridine orange of treated cells. Cell cycle progression of CHO cells treated with compound 5 (0.60 mM), for 24 h.	111
<b>Figure 4.10.</b> DNA fragmentation pattern of CHO cells treated with complex 2.	113
<b>Figure 4.11.</b> DNA fragmentation pattern of CHO cells treated with complex 5.	114
<b>Figure 4.12.</b> <sup>1</sup> H NMR spectra showing the reaction of complex 3 with GSH (ratio 1:2) at room temperature, as monitored by <sup>1</sup> H NMR spectroscopy.	116
<b>Figure 4.13.</b> Cis-dichloro-bis(pyrazole)platinum(II), 3	118

## List of Tables

<b>Table 3.1.</b> <i>Crystal data and structure refinement for L4.</i>	84
<b>Table 3.2.</b> <i>Selected bond lengths [<math>\text{\AA}</math>] and angles [<math>^\circ</math>] for L4.</i>	85
<b>Table 4.1.</b> <i>IC<sub>50</sub> values (mM) for the complexes tested in CHO cells.</i>	103
<b>Table 4.2.</b> <i>Showing the disappearance of the complex and emerging of the ligand (pyrazole) substituted by GSH.</i>	122

## ABBREVIATIONS

NMR = Nuclear magnetic resonance

FTIR = Fourier transform infra red

GC-MS = Gas Chromatography-Mass Spectrometry

SARs = Structural activity relationships

Cisplatin = Cis-dichlorodiammineplatinum(II) complex

IC<sub>50</sub> = Concentration of compound needed to inhibit cell growth by 50% against a single cell line

FACS = Fluorescence Activated Cell Sorter

APOP = Apoptosis Percentage<sup>TM</sup>

AO = Acridine orange

DNA = Deoxyribonucleic acid

RNA = Ribonucleic acid

GSH = Glutamylcysteinylglycine, glutathione

CHO = Chinese hamster ovary cell line

NHF = Normal human fibroblast

Hela = Human cervix epitheloid carcinoma

MG = Human osteosarcoma

ca = Approximately

## *Preface*

Many a times, a project of this nature is hard to categorise as to whether it is under chemistry, biology, or a combination of all, biochemistry. Thanks to bioinorganic chemistry. Bioinorganic chemistry constitutes the discipline at the interface of the more classical areas of inorganic chemistry and biology. Although biology is generally associated with organic chemistry, inorganic elements are also essential to life processes e.g. sodium and potassium as charge carriers in osmotic balance, vanadium in nitrogen fixation (oxidase), manganese in photosynthesis among others.

Bioinorganic chemists study inorganic species, with special emphasis on how they function in the biological systems, *in vivo*. Inorganic elements have also been artificially introduced into biological systems as probes of structure and function. Metal containing compounds have been used not only as biological probes, but also as diagnostic and therapeutic pharmaceuticals. The mechanisms of action of platinum anticancer drugs, gold antiarthritic agents, and technetium radiopharmaceuticals are some of the currently active topics of investigation in bioinorganic chemistry. The potential applications of inorganic compounds to improve human health are boundless and therefore this area continues to grow rapidly.

Bioinorganic chemistry has two major components: the study of naturally occurring inorganic elements in biology and the introduction of metals into biological systems as probes and drugs. Peripheral but essential aspects of the discipline include investigations of inorganic elements in nutrition, toxicity of inorganic species and ways of overcoming them and of course metal ion transport and storage in the body. It is worth noting that



bioinorganic chemistry is extensive and as a consequence, my focus was to evaluate palladium and platinum pyrazole and pyrazolyl compounds as anticancer agents.

# Chapter 1

## GENERAL INTRODUCTION TO APPLICATION OF METALS IN RESEARCH FOR ANTICANCER AGENTS

### *1.1 Introduction*

Medicinal applications of metals can be traced to almost 5000 years back but the lack of experience of traditional medicinal chemists and pharmacologists in dealing with biologically active metal complexes, poses a substantial activation energy barrier to their identifying active metal complexes and shepherding them to the clinic. This factor retards the development of metallo-pharmaceuticals. However, it provides enterprising transition metal chemists with opportunities to pioneer the development of exciting new drugs.<sup>1</sup>

Along with an increased understanding of metallo-protein function and some excellent models of metal ion active sites, recent advances in understanding how naturally-occurring metal ions are delivered to these active sites and how metal ions are involved in curbing some diseases indicate new roles for metal ions in therapeutic strategies.<sup>2</sup> Although some of the biological functions are also showed by non-metal species e.g. tamoxifen and taxol, it is clear that metal ions play a major role in biochemical process. Metal ions are known to exert an inductive effect by coordination to the site of reaction and serve as redox sites that function by either electron or atom transfer.<sup>3</sup> The current development of successful metallo-pharmaceuticals, which include the platinum anticancer drugs,<sup>4</sup> radio-diagnostic agents,<sup>5</sup> all indicate the utility of complexes as both therapeutic and diagnostic agents.

Cancer is one of the diseases that contribute to the high mortality rate globally. Thus there has been need for continuous research to develop drugs to curb this disease. Cancer is fundamentally a disease at the cellular level, in which cell proliferates indefinitely. Consequently, cancer cells continue to grow and divide yielding an ever increasing mass referred to as a tumour.<sup>6</sup> The tumour grows invasively, destroying surrounding body tissues. Cancer cells from this primary tumor may then spread, or metastasize, to other parts of the body, where new tumors may begin to grow. Eventually the tumor load will cause death, often by physically blocking or compressing blood vessels or organs such as the brain. Based on the activities of metal ions in the biological systems as mentioned above, development of metal-containing compounds, as therapeutic agents has therefore been stimulated and is underway. One of such compounds is cisplatin developed a quarter of a century ago.

In the mid 1970s initial antitumour studies with *cis*-diamminedichloroplatinum(II) (cisplatin) indicated considerable activity against some of the cancer cell-lines e.g. leukemia L1210 tumours. Cisplatin remains the most effective drug in clinical treatment of testicular, ovarian, bladder, head and neck cancers. It is widely used in combination with other anticancer drugs such as doxorubicin, and 5-fluorouracil, in treatment of neck cancer among others. However, there is an intrinsic and acquired resistance that limits the organotropic profile of the drug. Some of the reasons that lead to this acquired resistance include; reduced cellular uptake and deactivation of cisplatin by thiol containing biomolecules e.g. glutathione.<sup>7</sup>

Nevertheless, today platinum complexes belong to the most promising class of drugs to tackle the problem of oncology. A mechanistic understanding of how these metal complexes achieve their activities is crucial to their clinical success, as well as to the rational design of new compounds with improved potency. However it goes without saying that non-metal containing drugs which are considered to be precursors for drug development and even as medicines, are still in use even though not easily isolated. The next section highlights on some of these organic compounds (natural products) and their application in cancer treatment.

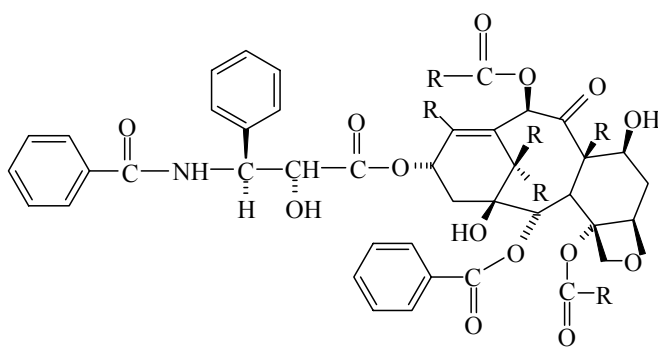
### ***1.2 Non-metal containing cancer drugs***

Natural products once served humankind as the source of most drugs, and higher plants provided most of these therapeutic agents. At present, natural products, their derivatives and analogues are used as remedies and represents over 50% of all drugs in clinical use, with higher plant-derived natural products representing approximately 25% of the total.<sup>8</sup>

In the war on cancer, and through the history of combating the disease of cancer, natural products have played an important role in the development of contemporary cancer chemotherapy. Between 1960 and 1982 the National Cancer Institute (NCI) screened around 114,000 extracts from an estimated 35,000 plant samples for anticancer activity.<sup>9</sup> A major group of these products are the powerful antioxidants, others are phenolic in nature, and the remainder includes reactive groups that confer protective properties.<sup>10</sup> *In vitro* studies done on these compounds have resulted in a number of clinically useful drugs that are now available. Among these clinically useful drugs are paclitaxel (Taxol<sup>®</sup>) vincristine (Oncovin<sup>®</sup>)<sup>11</sup> podophyllotoxin (a natural product precursor)<sup>12</sup> and

camptothecin<sup>11, 12</sup> (a natural product precursor for water-soluble derivatives of cancer drugs).

Besides natural products that have found direct application as drug entities, e.g. Taxol (Fig. 1.1a), there are many others that have served as chemical models or templates for the design, synthesis, and semi-synthesis of novel substances for treating diseases some of them include (1-pyrenylmethyl)amino alcohol derivatives, 2-amino-1,3-propanediol<sup>13</sup> and camptothecin (Fig.1.1d).



**a**

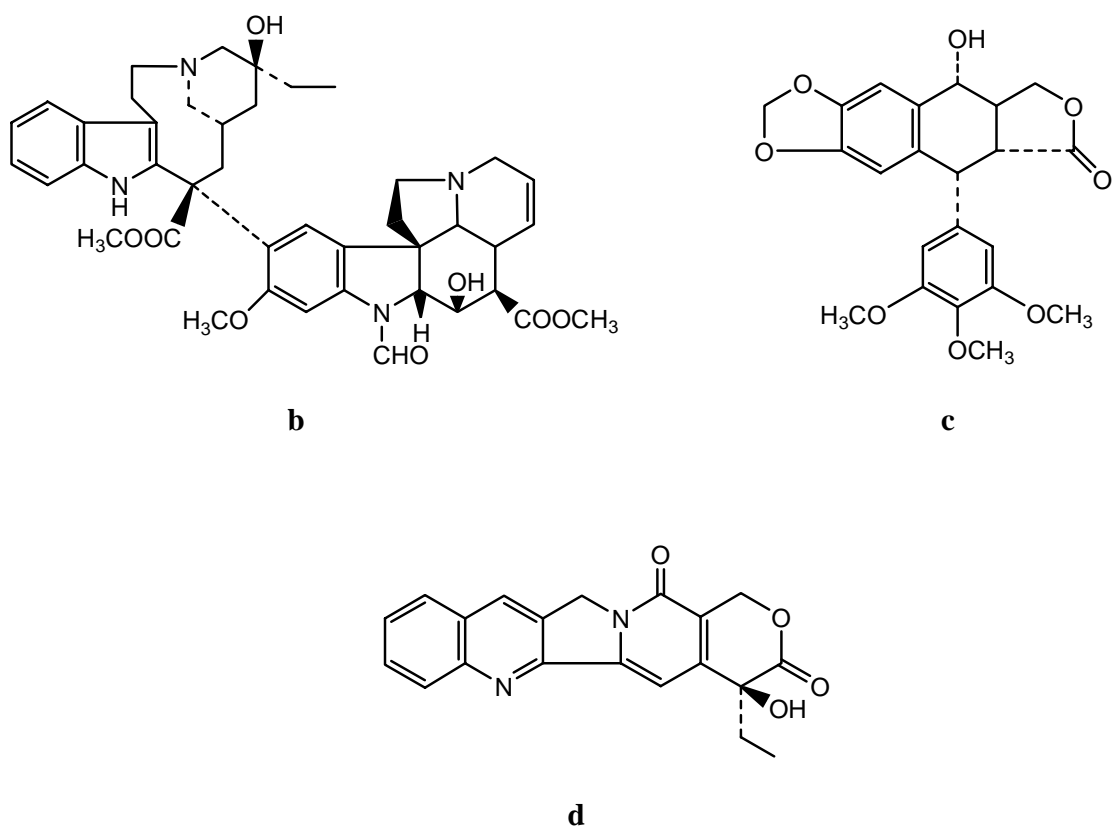


**Figure 1.1.** Structures of compounds among the clinically useful drugs. **a.** Taxol, **b.** Vincristine, **c.** Podophyllotoxin, **d.** Camptothecin.

Although significant progress has been made in cancer chemotherapy, current drugs are ineffective against many common cancers (colon, rectum, lung, prostate) <sup>14</sup> and are often very toxic. Paclitaxel (Fig. 1.1a) and tamoxifen (Fig. 1.2) are exceptions to ineffective drugs.

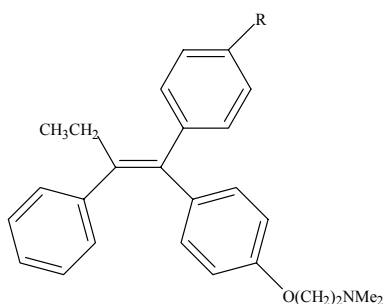


**Figure 1.2.** Shows the structure of Tamoxifen (R= H) and its derivative Hydroxytamoxifen (R= OH).

It is worth noting that inorganic based drugs (metal-containing drugs) still remains superior to other drugs especially anti-tumour agents. This is for the simple reason that whereas for organic drugs fractional guided assays are performed to identify the active compound, inorganic compounds are target specific (synthesized with specific design so as to bind to the DNA; hence their activity as anti-cancer drugs). In addition, the organic compounds are found in smaller quantities in nature and their synthesis in the laboratory is very challenging, i.e. it took 12 years to fully synthesise taxol. Even though these

drugs, e.g. taxol and tamoxifen, have shown anti-cancer activity, cisplatin is currently the most widely used anticancer drug. As a consequence, further research on more effective drugs can be achieved by synthesis of other new metal containing compounds.

### ***1.3 Metal based anticancer drugs (metallo-drugs).***

The development of modern medicinal inorganic chemistry, stimulated by the serendipitous discovery of cisplatin, has been facilitated by the inorganic chemist's extensive knowledge of the coordination and redox properties of metal ions. Metal centers being positively charged, are favoured to bind to the negatively charged biomolecules. The constituents of proteins and nucleic acids offer excellent ligands for binding to metal ions. The pharmaceutical use of metal complexes therefore has excellent potential that can be exploited.<sup>15</sup>

Ruthenium and gold complexes with antitumour activity are such examples. Many ruthenium complexes with oxidation state 2+ or 3+ display antitumour activity, especially against metastatic cancers. Ru(III) complex *trans*-[Na][Ru(Im)(Me<sub>2</sub>SO)Cl<sub>4</sub>] (Im = Imidazole) and its analogue, *trans*-[ImH][Ru(Im)(Me<sub>2</sub>SO)Cl<sub>4</sub>], (Fig. 1.3) are currently in a clinical trial.<sup>16</sup> For ruthenium(III) compounds, *in vivo* reduction to Ru(II) is required for activity. This facilitates its binding to the highly electrostatically charged DNA molecule. Cellular uptake of many ruthenium complexes appears to be mediated by the iron transport protein transferring process (stimulated by protein transferrin) into the tumor cells where upon it is reduced. In general, the cytotoxicity of ruthenium complexes and other metals correlates with their ability to bind DNA following intracellular activation by their reduction. However other researchers have reported complexes to have



shown different mode of action. No conclusive explanation as to its mode of action is known but it is reported that it does not involve DNA binding rather it interferes with type IV collagenolytic activity and reduce the metastatic potential of the tumors.<sup>16</sup>

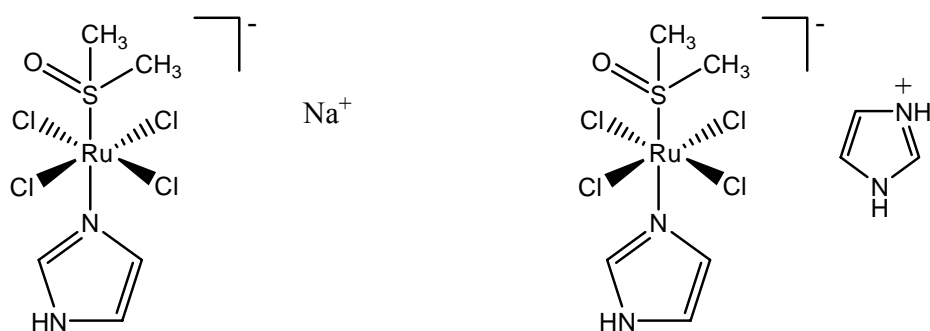


**Figure 1.3.** Structures of *trans*-[Na][Ru(Im)(Me<sub>2</sub>SO)Cl<sub>4</sub>] and *trans*-[ImH][Ru(Im)(Me<sub>2</sub>SO)Cl<sub>4</sub>].

Gold complexes on the other hand are mainly known to treat rheumatoid arthritis. Surprisingly they have also been reported to show antitumour activity.<sup>17</sup> Tetrahedral gold(I) complexes with 1,2-bis(diphenylphosphino)ethane and 1,2-bis(dipyridylphosphino)ethane ligands (Fig 1.4a) display a wide spectrum of antitumour activity *in vivo*, especially in some cisplatin-resistant cell lines. However mechanistic studies suggest that, in contrast to cisplatin, DNA is not the primary target of these complexes. Rather, their cytotoxicity is mediated by their ability to alter mitochondrial function by binding to receptive ligands and inhibit protein synthesis. Very recently, a hydrophilic tetrakis-((tris(hydroxy-methyl))phosphine)gold(I) complex (Fig 1.4b) was

reported to be cytotoxic to several tumor cell lines e.g. HCT-15 cells, derived from human colon carcinoma.<sup>18</sup>

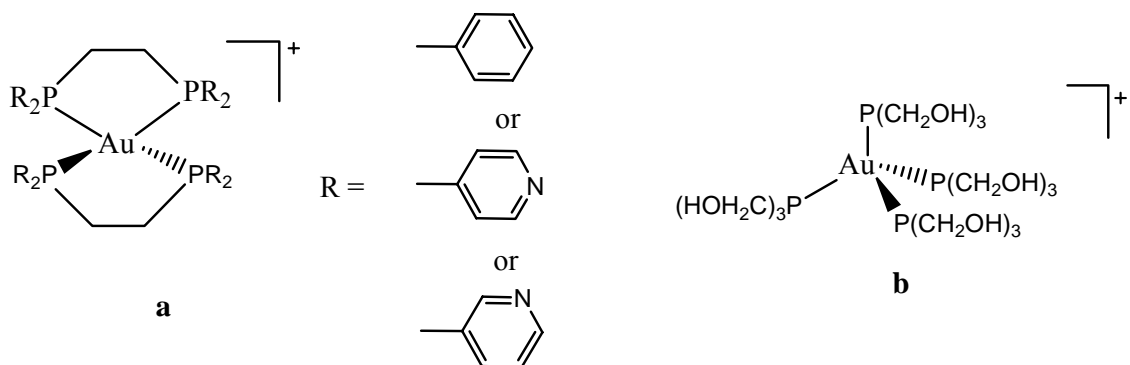


**Figure 1.4.** Structures of gold(I) complexes. **(a)** gold(I) complexes with 1,2-bis(diphenylphosphino)ethane and 1,2-bis(dipyridylphosphino)ethane ligands. **(b)** Tetrakis-(trishydroxymethyl)-phosphine)gold(I) complex.

In general much has been done on gold(I) complexes. The logical extension of phosphine gold(I) species as reported by Cookson *et al.* was to couple it to biologically active thiols e.g. 6-mercaptopurine and 6-thioguanine.<sup>19</sup> It is clear that the presence of the phosphine gold(I) entity enhance the potency of the biologically-active thiols. As part of the improvement on gold(I) systems, there have been on-going attempts to alter the solubility characteristics of phosphine gold(I) thiolates discussed above so as to improve on their activity. However, an area of research gaining prominence, with respect to gold compounds, based on recent publications, features gold(III) compounds.

Gold(III) would normally be regarded as oxidizing, and this property could be exacerbated in the reducing mammalian environment. However, judicious choice of donor atoms in the ligand donor set can impart stability to the higher oxidation state; gold(III) is regarded as a “harder” acid than gold(I) and hence, is more likely to form stable compounds with donor atoms such as nitrogen and oxygen whereas gold(I) exhibits a distinct preference for sulfur and phosphorous donor atoms. The gold(III) compounds investigated for potential anti-tumour activity are inevitably four coordinate and feature square planar geometries, as found for cisplatin so that, perhaps, a similar mechanism of action, i.e. interaction with DNA and disruption of normal cellular processes, may be assumed for these compounds. In this connection, evidence has been provided showing that some species bind DNA.<sup>20</sup> This fact is supported or related to the fact that gold in the +3 oxidation state has the same electronic configuration and structural characteristics as the world’s most widely-used anti-cancer drug, cisplatin.

Other significant metal complexes that have been studied are vanadium complexes. Although speculation (which has been proven) that these metal complexes may possess antitumour activity had existed since the beginning of the 20<sup>th</sup> century, these complexes were not tested until 1967. Since then the chemopreventive and antitumour effects of vanadium compounds have been widely investigated, especially on experimental animal models and various types of malignant cell-lines e.g. B cell lymphoma, T cell leukemia human ovary carcinoma and testicular cancer.<sup>21</sup> The first evidence that vanadium may exert chemopreventive effects on experimental carcinogenesis was provided by Thompson *et al.* on 1-methyl-1-nitrosourea (MNU-1) -induced mammary carcinogenesis

in female Sprague-Dewley rat.<sup>22</sup> They then proposed that the chemotherapeutic action of vanadium, in biological terms, was found to be mediated through inhibition of altered liver cell foci and hepatic nodule growth during the early stages of neoplastic transformation as reported elsewhere by Bishaye and co-workers.<sup>23</sup> Such compounds are the vanadocenes. They are organometallic complexes, with the vanadium(IV) linked to organic ligands by direct carbon metal bonds. They have been found to exhibit significant antitumour properties both *in vitro* and *in vivo*. Like Bis-(cyclopentadienyl)vanadium(II)chloride,  $[(\eta^5\text{-C}_5\text{H}_5)_2\text{VCl}_2]$  (Fig. 1.5), which belongs to the metallocene class of antitumour agents, has turn out to be one of the most promising compounds as a drug among the various non-platinum complexes.

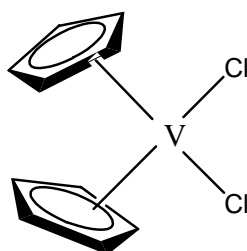


**Figure 1.5.** Bis(cyclopentadienyl)vanadium(II)chloride (vanadocene dichloride).

Vanadocene dichloride has been shown to be a potent antitumour agent against mouse tumours and its activity is due to its ability to interact at a molecular level with nucleic acids, especially DNA. Furthermore, the antitumor effects of vanadocene dichloride against human colon and lung carcinomas were shown to be due to the vanadium accumulation in nucleic acid-rich regions and to the inhibition of DNA and RNA synthesis in tumor cells,<sup>24</sup> suggesting the binding of this compound to the DNA.

Rhodium compounds have also been studied extensively. In spite of the fact that these compounds are analogous to platinum and ruthenium compounds, their antitumour activities have since been reported as insignificant due to their toxic effects.<sup>25</sup> However dimeric  $\mu$ -acetato dimers of rhodium(II) as well as monomeric square planar rhodium(I) and octahedral rhodium(III) complexes have shown interesting antitumour properties. The dirhodium tetraacetate complex,  $[(\text{CH}_3\text{COO})_4(\text{H}_2\text{O})_2\text{Rh}_2(\text{II})]$ , (Fig. 1.6) is much more inhibitory towards *Escherichia coli* DNA polymerase I and exhibits good antitumour activity against P388 lymphocytic leukemia and sarcoma 180 but little activity against L1210 and B16 melanoma.<sup>26</sup>

Recent structural studies suggest that the antitumour activity of di-rhodium(II) carboxylates may bear analogy to that of cisplatin by binding to adjacent guanines on DNA.<sup>27</sup> Antitumour activity has also been found to increase in the series  $[(\text{RCOO})_4(\text{H}_2\text{O})_2\text{Rh}_2(\text{II})]$  (R=alkyl group) with the lipophilicity of the R group and is independent of its reduction potential.<sup>26</sup> Thus rhodium(II) acetate (R = CH<sub>3</sub>), propionate (R = CH<sub>3</sub>CH<sub>2</sub>), butyrate (R = CH<sub>3</sub>CH<sub>2</sub>CH<sub>2</sub>), pentanoate (R = CH<sub>3</sub>CH<sub>2</sub>CH<sub>2</sub>CH<sub>2</sub>) show a considerable variation in their antitumour activity against Ehrlich ascites tumour cells in mice, with the pentanoate complex being the most active. Lengthening the carboxylate alkyl (R) chain beyond the pentanoate was found to reduce the drugs' therapeutic efficacy.

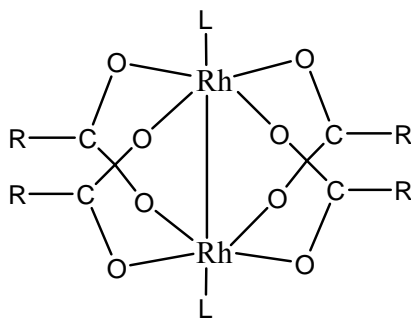


**Figure 1.6.** Six-coordinate cage complex of rhodium(II) carboxylates,  $[(\text{RCOO})_4\text{L}_2\text{Rh}_2(\text{II})]$ , R = alkyl group, L =  $\text{H}_2\text{O}$  or other donor solvent.

#### ***1.4 Platinum based anticancer agents.***

Platinum anticancer compounds are currently in widespread use for the treatment of many tumors, including genitourinary cancer. This class of interesting chemotherapeutic agents arose as a result of experiments performed by Rosenberg in the 1970s. The experiments were initially designed to study the effects of electric fields upon the growth of bacterium *Escherichia coli* in ammonium chloride solution over platinum electrodes.<sup>28</sup> To their surprise, they observed an unusual phenomenon of filamentous (long threadlike) growth. The bacteria cells, which normally divide rapidly, grew to 300 times their usual size and did not divide as expected. This observation was eventually found to result from the presence of platinum(II) and platinum(IV) ammine chloride complexes formed *in situ* by electrolysis at the platinum electrodes.



**Figure 1.7:** Isomeric forms of dichlorodiammineplatinum(II) complex.

Further studies showed one cause of the filamentation to be specifically *cis*-dichloro-diamine platinum(II) complex (cisplatin) (Fig. 1.7a). Interestingly this is a classic coordination compound, of which the synthesis and its structure had been known for more than a century.<sup>29</sup> Subsequent investigations of the effects of cisplatin on rapidly dividing mammalian tumor cells indicated significant antitumour activity against sarcoma 180 and leukemia L1210 in mice.<sup>30</sup> The relationship between structure and activity was found to fulfill the Structure Activity Relationships (SARs) as reported by Kelemu *et al.*<sup>31</sup> The requirements are: (i) A *cis* geometry with the general formula  $cis-[PtX_2(amine)_2]$  for platinum(II) compounds and  $cis-[PtY_2X_2(amine)_2]$  for platinum(IV) compounds. (ii) The X ligand should be an anion with intermediate binding strength such as chloride or oxalate. In the case of platinum(IV) Y can be chloride, hydroxide, or carboxylate oriented *trans* to each other. (iii) The amine ligands should possess at least one NH moiety necessary for hydrogen bonding interactions.

Several clinical trials on cisplatin as a drug commenced soon thereafter, and in 1979, it was approved by the Food and Drugs Administration (FDA) for the treatment of several human cancers. Since then much research attention has been paid not only to cisplatin, but also to cisplatin mimics as potential anticancer drugs because of the success of cisplatin. Indeed cisplatin, (Fig. 1.7a), one of the most widely used anticancer drugs, is effective in treating a variety of cancers, especially testicular cancer.<sup>32</sup> As a result, its importance in current clinical research towards drug discovery includes emphasis on the need to understand its biological chemistry with the ultimate goal of using this information to design even more effective drugs.

### ***1.5 Platinum-DNA interactions.***

#### ***1.5.1 DNA: The biological cellular target of cisplatin.***

After the discovery of the anticancer properties of cisplatin, work began to investigate its mechanism of action. One of the first issues that needed to be settled was its biological target, for there are many cellular components that can react with cisplatin e.g. RNA and glutathione. Attention has focused on deoxyribonucleic acid (DNA) molecule as the generally accepted target and as a consequence many studies have been performed to establish the nature of platinum binding to the DNA.<sup>33</sup>

Through intensive research efforts over the past several years, there is now a fairly detailed understanding of how cisplatin and its mimics bind to DNA and how the DNA is structurally modified as a result of this interaction.<sup>34</sup> One such experiment involved the treatment of *Escherichia coli* bacteria cells with cisplatin, which led to its lysis (disintegration), a condition associated with DNA-damaging agents.<sup>35</sup> DNA (Fig. 1.8) is a



biomolecule and is one of the many cellular components in the human body. It contains the complete genetic information that specifies the structure of all proteins and ribonucleic acids (RNA). In human cells, there are 46 chromosomes, each consisting of a single DNA duplex up to 4 cm long. Each DNA molecule is a polymer of monomeric units, the nucleotides, which consists of phosphate group, a 2-deoxyribose sugar, and a heterocyclic amine base (Fig.1.9). The deoxyribose sugar and phosphodiester repeating units are attached through the sugar moiety to the 9N atoms of adenine, **A**, and guanine, **G**, (purine bases) or the 1N atoms of cytosine, **C**, and thymine, **T**, (pyrimidine bases). The ordering of bases from 5' to 3' on the DNA strand defines the sequence of that particular strand. The sequence of nucleotides is arranged in a helix conformation and matches with a complementary one to form a double-helix. The bases point towards the centre of the double-helix, and are held together by hydrogen bonds and base stacking, while the phosphates are located on the more solvent accessible surface of the helix. In its simplicity, the base **A** pairs with **T**, and **G** pairs with **C**, and the sequence of these base-pairs determines the genetic coding.

The physical nature of DNA is important to consider due to its fundamental importance in metal DNA interactions. The low pKa value of the phosphate groups makes the DNA highly charged molecule in a large pH range. As a result, the charge density is high, and the DNA attracts oppositely charged ions and repels negatively charged ones. In this respect, the nucleobases acts as ligands and thus coordinates to the metal of an already positively charged species.<sup>31</sup>

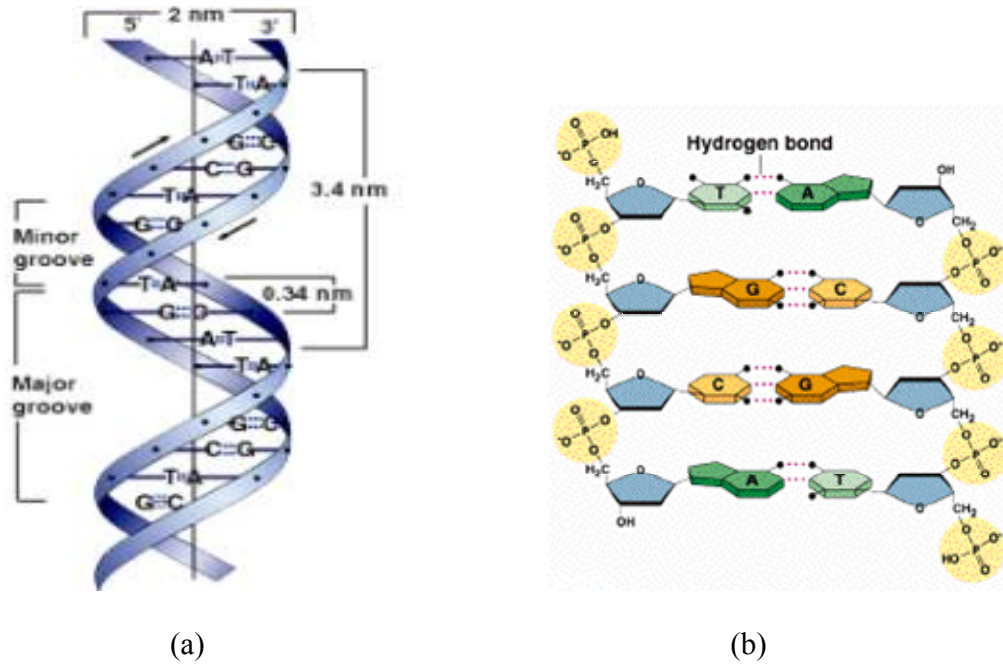


**Figure 1.8.** DNA structures showing the forms a DNA molecule assume i.e. (a) Helix shape together with the (b) hydrogen bonding in the pairing bases.

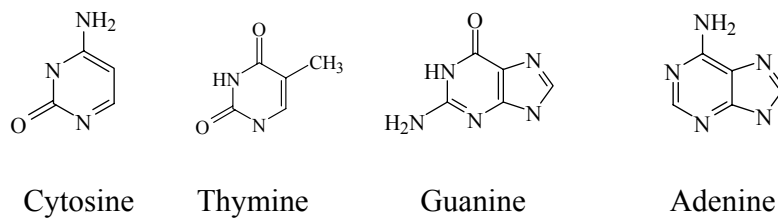


**Figure 1.9.** Heterocyclic bases of DNA.

### ***1.5.2 Effects of platination on structure.***

Based on the *cis*- and *trans*-platin complexes, there is need to understand the binding modes of these complexes to DNA macromolecule and what effects it has. Both complexes are neutral, thermodynamically stable, and known to retain their co-ordination environment in circulating blood plasma. The limiting factor for accumulating platinum in cells is its concentration. Indeed uptake does not have a pH optimum suggesting that the transport is not carrier-mediated.<sup>36</sup> These results indicate that cisplatin and its isomers enters cells by passive diffusion, although there is some evidence that uptake may in part occur by an active transport mechanism.<sup>36</sup> In the blood stream (plasma), cisplatin encounters a relatively high concentration of chloride ions (ca. 100 mM) that suppresses hydrolysis and maintains the compound in a neutral state. Interestingly in the cytoplasm of the cell the chloride ion concentration drops to 4 mM (Fig.1.10). The implication here is that when the drug (cisplatin) passes through the cell membrane into the cytoplasm, it undergoes hydrolysis.

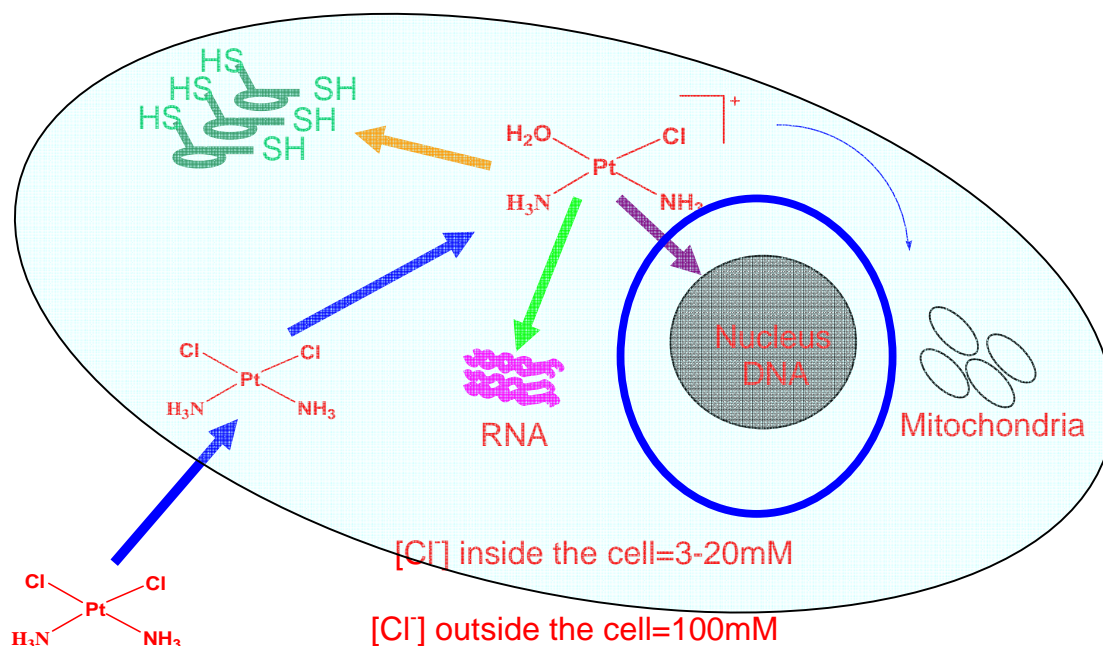


**Figure 1.10.** The cellular uptake of cisplatin and its targets. Reproduced from Encyclopedia of Cancer, J. R. Bertino, Ed. Academic Press: San Diego, CA, 1 (1997) p. 392.

This leads to a range of aquated and non-aquated products respectively being formed,<sup>37</sup>  $[\text{Pt}(\text{NH}_3)_2(\text{OH}_2)_2]^{2+}$ ,  $[\text{Pt}(\text{NH}_3)_2(\text{OH})(\text{OH}_2)]^+$ ,  $[\text{Pt}(\text{NH}_3)_2(\text{Cl})(\text{OH}_2)]^+$ ,  $[\text{Pt}(\text{NH}_3)_2(\text{OH})_2]$ ,  $[\text{Pt}(\text{NH}_3)_2(\text{OH})(\text{Cl})]$  and  $\text{Pt}(\text{NH}_3)_2\text{Cl}_2$ . It is the positively charged platinum hydrolysis product,  $[\text{Pt}(\text{NH}_3)_2(\text{Cl})(\text{OH}_2)]^+$ , that is electrostatically attracted by the DNA macromolecule. The coordination of these platinum species to DNA is known to occur in two steps. Formation of the monofunctional adducts primarily at the N7 position of guanine or adenine becomes the first intricate step. This monofunctional platinum-DNA

adduct then reacts further to form a bi-functional adduct (Fig. 1.11a, b). This occurs at the N7 position of the nearby guanine, and seldomly to the adenine base.<sup>38</sup>

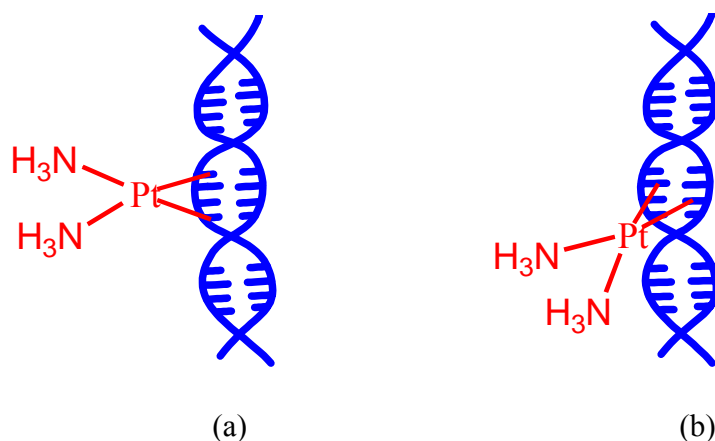


**Figure 1.11.** Diagram of cisplatin-DNA adducts. (a) depicts an intrastrand crosslink and (b) an interstrand crosslink.

Two forms of adduct are seen as a result of this binding. There is the intrastrand cross-link (Fig 1.11a), whereby the coordinated nucleotide bases are on the same DNA strand as opposed to an interstrand cross-link whereby the coordination occurs with the bases being on opposite DNA strands as shown in Figure 1.11b above. Normally the products are chromatographically separated and identified by their <sup>1</sup>H NMR spectra.<sup>39</sup> Generally 48-60% of cis-[Pt (NH<sub>3</sub>)<sub>2</sub>{d(GpG)}] and 23-28% of cis-[Pt (NH<sub>3</sub>)<sub>2</sub>{d(ApG)}] (d = sugar back bond of DNA molecule, A and G are bases as described in section 1.5.1) are found as the intrastrand crosslinks.<sup>40</sup> The transplatin analogue is stereochemically limited to form intrastrands. Nevertheless it has been shown to form kinetically stable adducts with DNA via the interstrand binding (Fig. 1.11b), thus indicating that the compound must not

necessarily be in a *cis* conformation (SARs rules) to be active. <sup>1</sup>H NMR analysis revealed an adduct spectrum of dG-Pt-dC (50%), dG-Pt-dG(40%) and dG-Pt-dA (10%)<sup>41</sup> (d = sugar back bond of DNA molecule, A, G, C are bases as described in section 1.5.1, interstrand binding). From these data, it is clear that both *cis* and *trans*-type drugs binds to DNA through N7 positions of guanine and adenine. The significant difference is that stereochemical factor limits *trans*-type from forming an intrastrand adduct, rather it forms interstrand. The type of ligand systems used determines the conformation of the complex to be formed. When the ligand is bulky, it favours *trans*-isomer, although there is a mixture of the two isomers in solution. The important thing to note is that they both form DNA-platinum adducts, thus inducing cytotoxicity.

However, significant acquired resistance has limited the clinical success of cisplatin. This is as a result of the factors mentioned in the previous section. Cisplatin also has large dose limiting side effects including signs of nephrotoxicity (kidney damage), neurotoxicity (nervous system damage) and ototoxicity (hearing loss). Therefore much attention has been focused on designing new second-generation platinum compounds with improved pharmacological properties and a broader range of antitumor activity. Several platinum complexes are currently in clinical trials.<sup>42</sup> Recent work suggests that there may be some biologically active *trans* platinum compounds, including platinum(II) complexes with planar ligands,<sup>43</sup> platinum(II) iminoether compounds,<sup>44</sup> and *trans*-ammine(ammine')platinum(IV) compounds.<sup>45</sup> However these new complexes have not yet demonstrated significant advantages over cisplatin either *in vitro* or *in vivo*.

Carboplatin (Fig. 1.12), developed by Johnson Matthey Technology, displays the same spectrum of activity against cancer cell-lines as cisplatin.<sup>44</sup> There is little or no nephrotoxicity and neurotoxicity as the side effects compared to cisplatin. However bone marrow toxicity is the known dose-limiting factor. The reduced toxicity is attributed to the slow nucleophilic substitution (by water) of the chelated dicarboxylate leaving group, with the low reactivity of the complex itself being attributed to its slow ring opening.<sup>39</sup> As a result, carboplatin can be administered at much higher doses ( $900 \text{ mg/m}^2$ ) than cisplatin ( $60\text{-}120 \text{ mg/m}^2$ ). It is worth noting that carboplatin is the only metal containing cancer drug, other than cisplatin, to obtain worldwide approval for clinical use to date.<sup>46</sup>

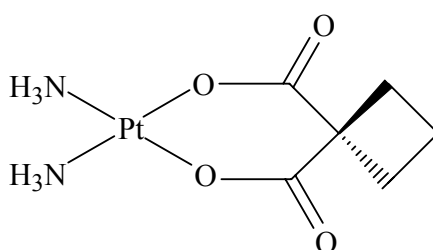


**Figure 1.12.** Cis-diammine-1,1'-cyclobutane dicarboxylate platinum(II), carboplatin.

Another interesting complex is cis-dichloroamine-2-methylpyridineplatinum(II), (popularly known as AMD-473) (Fig. 1.13). It is known to be a sterically hindered platinum complex. Crystal structure of the complex has shown that the pyridine ring is tilted  $102.7^\circ$  with respect to the  $\text{PtN}_2\text{Cl}_2$  square plane.<sup>47</sup> The sterically hindered non-leaving group slows associative substitution reactions on the square planar platinum. This is important for biological nucleophiles that are able to bind platinum without prior

hydrolysis of the chloro-ligand (e.g. thiol groups of proteins or peptides). AMD-473 hydrolyses more slowly (two fold) than cisplatin and also shows reduced rates of reaction with thiourea and methionine while maintaining reactivity towards DNA.<sup>38</sup>

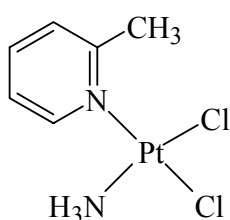


**Figure 1.13.** Cis-dichloroamine-2-methylpyridineplatinum(II), AMD-473.

AMD-473 also displays (*in vitro*) cytotoxicity intermediate between cisplatin and carboplatin. In a growth inhibition assay using 11 human ovarian cancer cell-lines, the mean concentration that kills 50% of the cells,  $IC_{50}$ , of AMD-473 was 8.1  $\mu\text{M}$ , higher than the mean for cisplatin (2.6  $\mu\text{M}$ ) but lower than the mean for carboplatin (20.3  $\mu\text{M}$ ).<sup>15</sup> Its superiority to carboplatin has been attributed to its structure which is a distorted square planar geometry and the presence of the aromatic ligand hinders thiol-mediated detoxification. It has also been shown to overcome other modes of resistance such as reduced cellular uptake and enhanced DNA repair.<sup>48</sup>

While maintaining the structure activity relationships (SARs) features, another complex, *trans*-L-diaminocyclohexaneoxalatoplatinum(II), oxaliplatin (eloxatin), possessing a rigid non leaving group and chelated dicarboxylato as leaving group was synthesized (Fig.



1.14). The synthesis is based on the fact that having bidentate ligands, which imparts a specific stereochemistry to the compound, (*cis*- conformation) could lead to formation of DNA adducts that could not be translablized or in other words form kinetically stable adducts. Oxaliplatin is administered in combination with 5-Fluorouracil plus leucovorin (5FU/LV) (these are cancer therapy drugs). It is used to treat patients with colorectal cancer (cancer of the colon and rectum) whose disease has recurred or become worse following initial therapy with a combination of other drugs.<sup>49</sup> It has an improved efficacy i.e. it shrinks tumours (in some patients) and delay resumed tumour growth.<sup>49</sup>

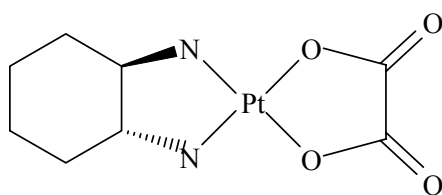


**Figure 1.14.** *trans*-L-diaminocyclohexaneoxalatoplatinum(II), eloxatin.

### 1.5.3 Conformational-activity related study.

There has been a debate concerning the effect of particular compounds being attributed to their rigid geometries i.e. *cis*- and *trans*- geometry. Young *et al.* investigated the effects of monodentate versus chelate conformation by a direct comparison of bis(aceto)amminedichloro(cyclohexylamine)platinum(IV) (**a**), with its N-cyclohexyl-1,3-propanediamine analogue (**b**), (Fig. 1.15).<sup>50</sup> Compound **a** showed selective cytotoxicity toward cisplatin-resistant human ovarian tumour cell-lines. The preliminary antitumour activity of compound **a** was found to be inferior to that of **b**.

The variation in their activities may be ascribed to the difference between the monodentate amines in the former and the rigid chelating *N*-cyclohexyl-1,3-propanediamine (chpda) in the latter. It is possible that the rigid chelating complex forms intrastrand specifically, whereas complex exhibiting monodentate character would have both isomers, *cis*- and *trans*- in solution and would form both intra- and inter-strand platinum-DNA adducts; hence its high cytotoxic effect. The chelating effects of neutral amine observed both *in vitro* and *in vivo* gives a clear indication of the features that can be used to control the physicochemical properties of a particular drug during its development so as to exhibit desirable biological activity.<sup>50</sup>

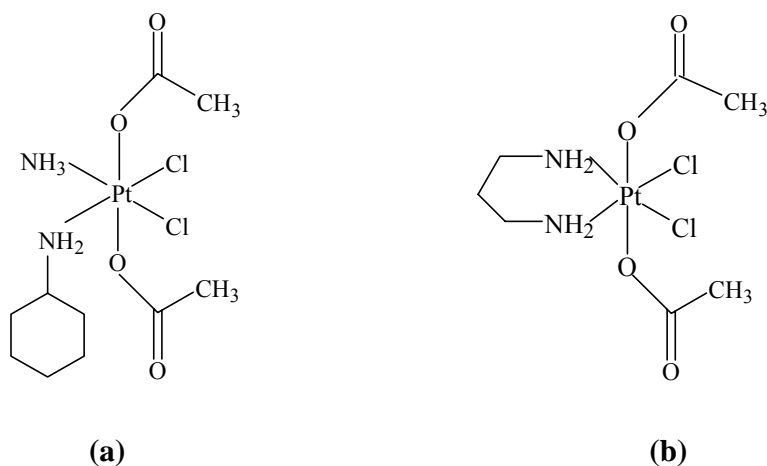


**Figure 1.15.** Monodentate versus chelate amine based complexes. **(a)** Bis(acetato)amminedichloro(cyclohexylamine)platinum(IV) and **(b)** bis(acetateo)-*N*-cyclohexyl-1,3-propanediamine platinum(IV).

### ***1.6 The kinetics of platinum(II) drugs.***

In an attempt to understand the difference in the activity spectra of the two isomer, *cis* and *trans*, kinetic studies have been undertaken. As a result, several observations have been proposed to explain the difference in the activities of the two isomers. For instance, the half-lives of the intermediate platinum-DNA products formed (monofunctional adduct), (see section 1.5.2) have been reported to be different for the two isomers. Conversion of the monofunctional adduct to a bifunctional adduct is slow for *trans*-isomer (30 h) as compared to *cis*-isomer (15 h). The monofunctional adduct of *trans*-isomer would then be susceptible to thiol binding by glutathione (GSH) rendering it not to be active.<sup>51</sup>

Generally it has been found that the rates of reaction of *cis*- and *trans*-platin with DNA are governed mainly by their rates of hydrolysis. This has been monitored by use of <sup>195</sup>Pt-radiolabelled analogues to investigate the binding reactions directly. The reaction rates of both isomers were also found to be the same on double and single stranded DNA, implying that local DNA conformation was not a major factor in binding.<sup>51</sup> Recent studies which employed <sup>195</sup>Pt NMR spectroscopy to check the formation of monofunctional adducts of *cis*- and *trans*-platin and their respective closure to bifunctional adducts, gave  $t_{1/2} = 1.9$  h and  $t_{1/2} = 2.0$  h as respective half-lives for initial binding to DNA.<sup>52</sup> These values were found to be identical to the half-lives for hydrolysis of these compounds.

### ***1.7 Interaction of platinum complexes with biomolecules.***

The biomolecules present in blood and cells are varied in their structure and chemical reactivity. Many small molecules, proteins and enzymes have the potential to react with platinum complexes.<sup>53</sup> The sulfur containing molecules can therefore easily coordinate to the metal, with sulfur as the binding site to give other forms of metal complexes, which leads not only to the inactivity of the drug but also its toxicity in the body system.

The sulfur containing tripeptide glutamylcysteinylglycine, glutathione (GSH), is one such example and is the most prevalent sulfur containing molecule in cells. This intracellular non-protein thiol is found to have a concentration of up to 8 mM.<sup>54</sup> It is known to be one of the primary defenses against toxins and oxidants present in the cell. It can deactivate electrophilic drugs including chemotherapeutic agents, and is known to scavenge for heavy metals in the body. Thus although cellular DNA is considered to be the therapeutic target of platinum drugs, a large part of the platinum reacts with cysteine groups of proteins instead, which are also constituents of GSH.<sup>55</sup> These reactions may induce toxic side effects that occur in cancer chemotherapy. More importantly, the reaction with these sulfur containing proteins are associated with cellular resistance against platinum drugs.<sup>56</sup> A lot of studies have been done to this effect.

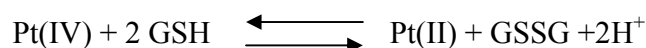
Hall and co-workers<sup>52</sup> have considered the reaction rates for reduction of platinum(IV) complexes versus substitution when reacted with biomolecules.<sup>52</sup> Even though none of the platinum(IV) compounds that have been put on clinical trial have revealed any significantly greater activity in human than of cisplatin and their platinum(IV) analogues e.g. carboplatin,<sup>57</sup> they found it important in this instance to use platinum(IV) complexes

because it was hypothesized that they are activated on reduction by glutathione. Their reduction by such biological reductants is in agreement with the assumption that these compounds act as pro-drugs to their platinum(II) analogues.<sup>58</sup> Hall *et al.* observed that sulfhydryl group of glutathione is readily oxidized, with  $E^{\circ}$  value reported as  $-240$  mV at pH 7.0 (close to biological pH).<sup>31</sup>



This was found to be in the range for oxidation by platinum(IV) complexes, which have  $E^{\circ}$  values up to  $-1000$  mV.<sup>59</sup> Using *trans*-[PtCl<sub>2</sub>(CN)<sub>4</sub>]<sup>2-</sup>, Hall and workers also showed by using stopped-flow techniques that *trans*-[PtCl<sub>2</sub>(CN)<sub>4</sub>]<sup>2-</sup> was reduced by glutathione, a reaction that proceeded directly without substitution at platinum(IV). The reduction was found to be pseudo-first-order, and variation of chloride concentration had no effect on the rate of reduction. The rate of reduction was also found to increase with increasing pH, suggesting that a deprotonated thiol group is a more reactive species towards platinum(IV) complexes.<sup>52</sup>

The above phenomenon was supported by other research findings, which showed that the reaction of tetra-platin with DNA is slow *in vitro*, but the reaction become rapid upon addition of two stoichiometric equivalents of GSH, indicating reduction of the platinum(IV) complex to its platinum(II) analogue.<sup>60</sup>



The binding of this biomolecule appears to be irreversible suggesting that a strong bond is formed between the central platinum atom of the complex and one or more of such molecules.<sup>61</sup> This is supported by the fact that platinum complexes, in this case platinum(IV), are soft acids and are more likely to form a stable bond with sulfur, a soft base. Unfortunately one failure of this study is the fact that it does not clearly indicate the reaction at cellular level or when the complex has already penetrated the cell membrane. As mentioned earlier, platinum(IV) compounds act as pro-drugs and as a prerequisite need to be reduced to platinum(II) before penetrating the cell. In fact structure-activity relationship (SAR) rules defined for platinum(II) compounds are significant factors in determining the activity of platinum(IV) analogues. While extensive work has been carried out on the interaction of platinum(IV) complexes with GSH, very little has been reported on its interaction with the platinum(II) analogues. In their attempts, Odenheimer and Wolf reacted cisplatin with glutathione in a 1:2 mole ratio respectively.<sup>61</sup> They postulated possible reaction mechanisms and products for this interaction (Fig. 1.16).

With this in mind, it is then important to investigate the interaction of GSH with platinum(II) compounds, because it is actually these compounds that cross the cell membrane and react with DNA. Our attempt to do this kind of studies is based on pyrazole platinum(II) complexes.

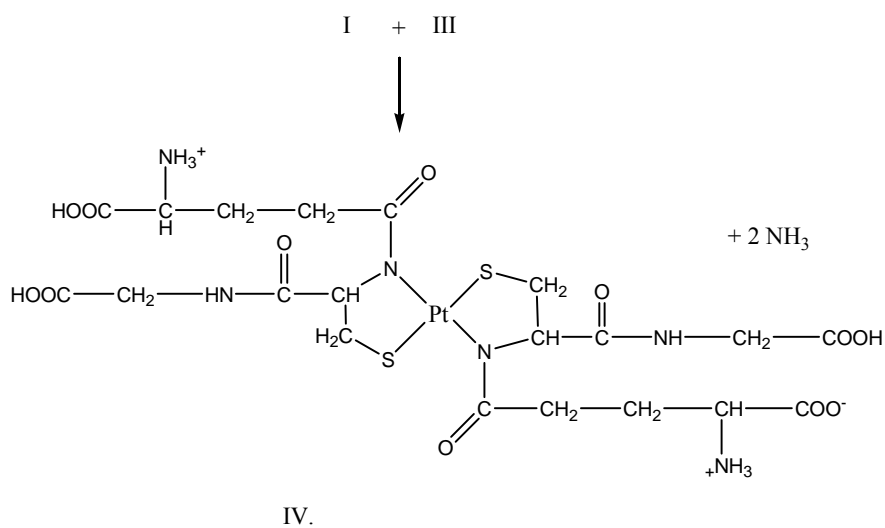
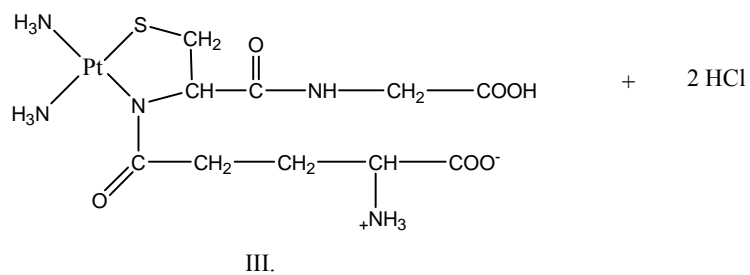
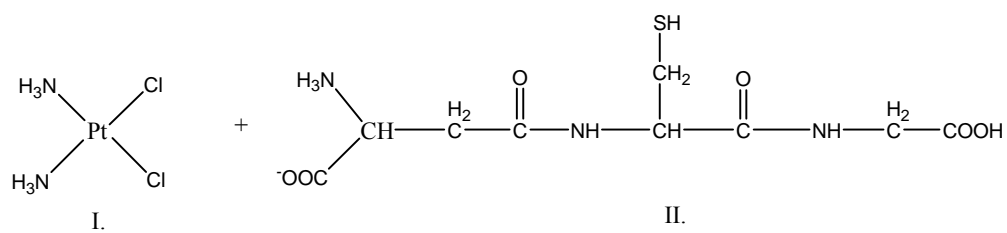


**Figure 1.16.** Representation of possible reaction mechanisms for interaction of cisplatin with glutathione

### ***1.8. Pyrazole and Nitrogen containing Ligands in synthesis of anticancer agents.***

The properties of metal-coordinated compounds, whether in classical inorganic coordination complexes or in organometallic compounds or in bioinorganic compounds, are determined in large measure by the nature of ligands bound to the metal ion.<sup>62</sup> Most ligands are based on nitrogen-containing heterocyclic compounds with exception of a few having sulfur and oxygen moieties. The key feature of these heterocycles is their  $\pi$ -electron deficiency. This is a common feature with bidentate and tridentate nitrogen-heterocyclic compounds containing 6-membered rings such as 1,10-phenanthroline (phen) and 2,2'-bipyridine (bipy). On the other hand, the  $\pi$ -electron excessive five-membered nitrogen heterocycle, pyrazole is a poorer  $\pi$ -electron acceptor. In fact, it is a better  $\pi$ -donor and hence acts as hard donor site. In drug design, especially inorganic based, such information is vital.<sup>63</sup>

The ease of synthesis of variously substituted pyrazoles is the most interesting feature in the incorporation of pyrazole groups in the design of new ligands and hence offers the opportunity of both electronic and steric control of the properties of the metal complexes. Thus pyrazole-based chelating ligands are good in the development of systematic coordination chemistry. It is important therefore to have a critical analysis of the molecular structural aspects of the resulting complexes. In so doing, understanding electronic structural aspects and the reactivity is important.

A new ligand bis[3,5-diisopropylpyrazolyl]ether has recently been specifically designed<sup>64</sup> to model the binding aspects of zinc to protein backbones in enzymes. (Fig. 1.17). This demonstrates that the geometries, nuclearities and reactivity properties of a



particular compound can be controlled by the change in the coordination mode of chelating ligands in the coordination sphere of metal ions; by the placement of substituent groups near donor site of a ligand.

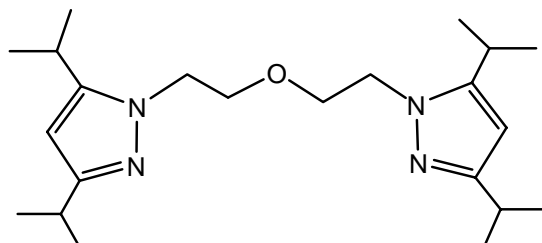


**Figure 1.17.** A new ligand, bis-[(3,5-diisopropylpyrazolyl)ethyl] ether

Second generation platinum(II) antitumour complexes that carry “non-leaving ligands” other than simply ammonia are of interest for their ability to modulate drug metabolism and target binding through steric and electronic effects on the substitution mechanism.<sup>65</sup> Several platinum complexes with N-heterocyclic ligands such as imidazole, thiazole, benzimidazole, benzoxazole and benzothiazole have been reported, of which some showed significant cytotoxicity.<sup>66</sup> The use of amines more compatible to the human system has been another important area. For this purpose, naturally occurring substances like amino acids, peptides, and glucosamines whose uptake is increased in malignant cells have been used as non-leaving ligands in some platinum complexes.<sup>67</sup> In a study performed by Fatma *et al.*, benzimidazole ligands having hydrogen, methyl or amino-methyl groups at position 2 were used as non-leaving ligands of the platinum(II) complexes that they synthesized (Fig.1.18). This was in consideration of three main reasons: firstly the sterically hindered ligands were seen to reduce rapid detoxification by thiol-containing molecules in the cells. Secondly the use of bidentate ligands such as 2-

aminomethylbenzimidazole instead of simple ammonia could lead to prevention of translabilization and undesired displacement of the non-leaving ligand by sulfur and nitrogen donors that are present in the cell. Thirdly, the hydrophobic properties (which is one of the important factors)<sup>68</sup> whereby the presence of aminomethyl groups makes the ligand water soluble and so (by extension) is the resultant complex. Ultimately the solubility of the drug will facilitate drug administration.

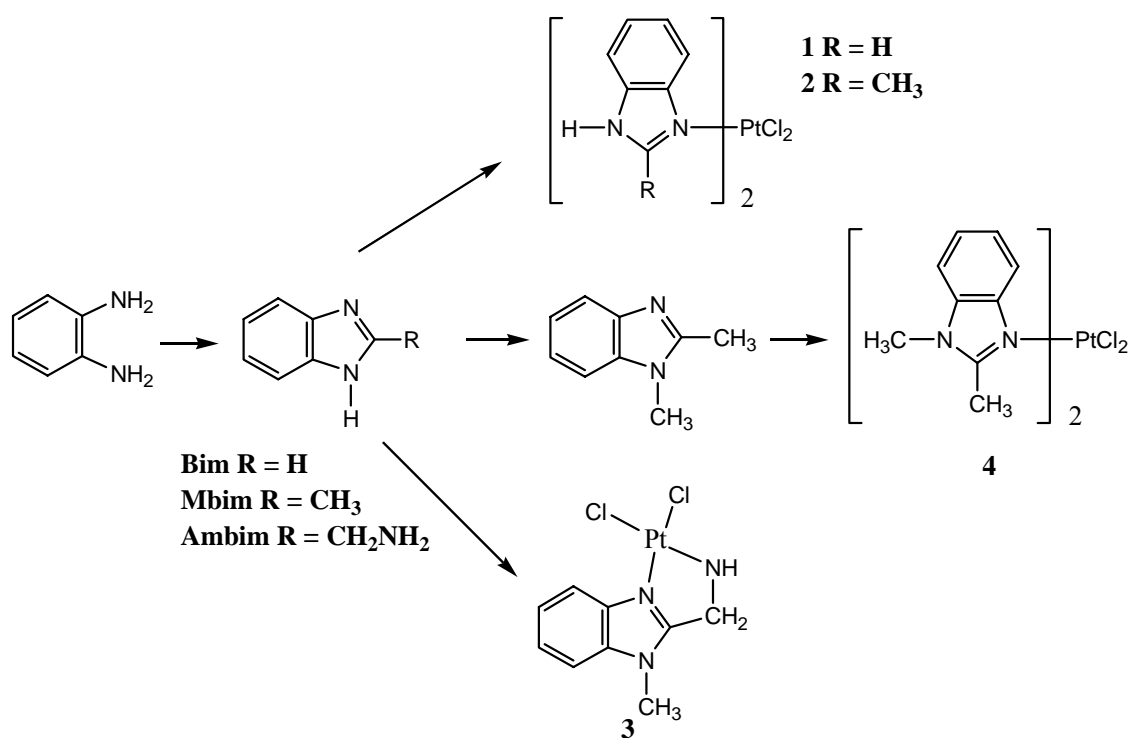


**Figure 1.18.** The synthesis of ligands and their complexes. Benzimidazole (Bim), Methylbenzimidazole (Mbim) and Aminobenzimidazole (Ambim). Reproduced from J. Med. Chem. 38 (2003) 473.

Fatma and co-workers observed that complex **2** (Fig.1.18), with the ligands having free N-H moiety in the structure, was found to be slightly more active than its corresponding methylated derivative, complex **4**, to confirm the role of free N-H group of the benzimidazole ligands on the cytotoxic activity of the benzimidazole-platinum(II) complexes.<sup>68</sup>

The coordination environments of metal ions in biomolecules often consist of nitrogen-donor and oxygen donor atoms, which are provided by histidines and aspartates or glutamates. And since pyrazoles resemble imidazoles, it has been incorporated in stable chelates to obtain ligand systems applicable in the design of new drugs.<sup>69</sup> For example a new ligand containing both imidazole and 3,5-dimethylpyrazole moieties (Fig. 1.19) have been synthesized which may act as a pentacoordinating ligand.<sup>69</sup>

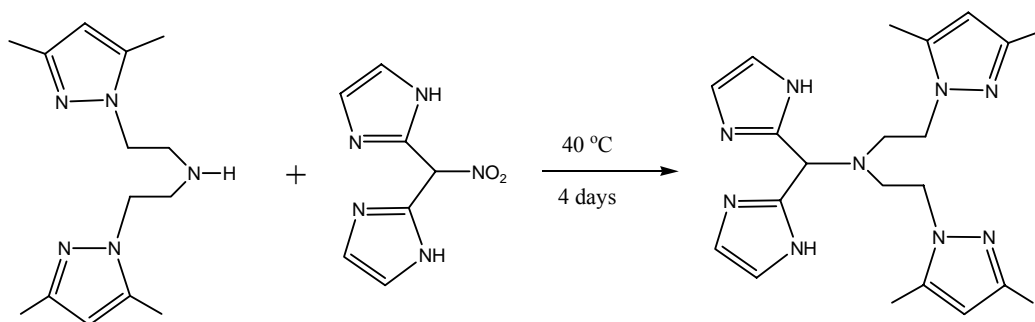


**Figure 1.19.** The synthesis of 1,5-bis(3,5-dimethylpyrazol-1-yl)-3-[bis (imidazol-2-yl) methyl]-3-pentane (bdpbiap).

The methylene chains allow a certain degree of flexibility to the ligand with the possibility to form five and six-membered chelate rings. The imidazole group, after loss of a proton may form an intramolecular imidazolato-bridge between two metal centers. The incorporation of metal ions e.g. palladium(II) and platinum(II) to such ligands (Fig. 1.19) allows formation of multinuclear complexes. Multinuclear platinum complexes (for example) contain two or more linked platinum centers that can each covalently bind to DNA, and hence are capable of forming a completely different range of DNA adducts compared to cisplatin and its analogues.<sup>70</sup> The rationale of the synthesis of this type of compounds is the likelihood of facile and selective uptake of the platinum-complexes which contain aminoacids/sugars as ligands because these natural products are normally taken up by the cell.<sup>71</sup> However, to date, there have been no clinically significant advances that have been developed from this design approach.

Over the past few years there have been efforts to develop water soluble, nitrogen based ligands for synthesis of metallo-drugs. There has been comparatively little attention paid to this type of ligands as well. In the limited number of examples published, the hydrophilicity has been introduced either through an ionic substituent (cationic or anionic) or a polyhydroxy substituent (such as carbohydrate). Sulfonated bipyridine ligands (Fig. 1.20A) were among the first examples of nitrogen ligands developed for applications in aqueous solution.<sup>72</sup>

Subsequently, several other monodentate and bidentate ligands either with ionic (Figs. 1.20B and 1.20C) or polyhydroxy (Fig.1.20D) substituents have been developed. Examples of multidentate ligands are the tridentate tris(pyrazolyl)methane (Fig.1.20E)

and tris(pyridyl)amine derivatives as well as tetradentate porphyrin ligands.<sup>73</sup> In general, the subject of nitrogen containing ligands is extensive and cannot be discussed fully; however these ligands continue to play a significant role in the design of new drugs.

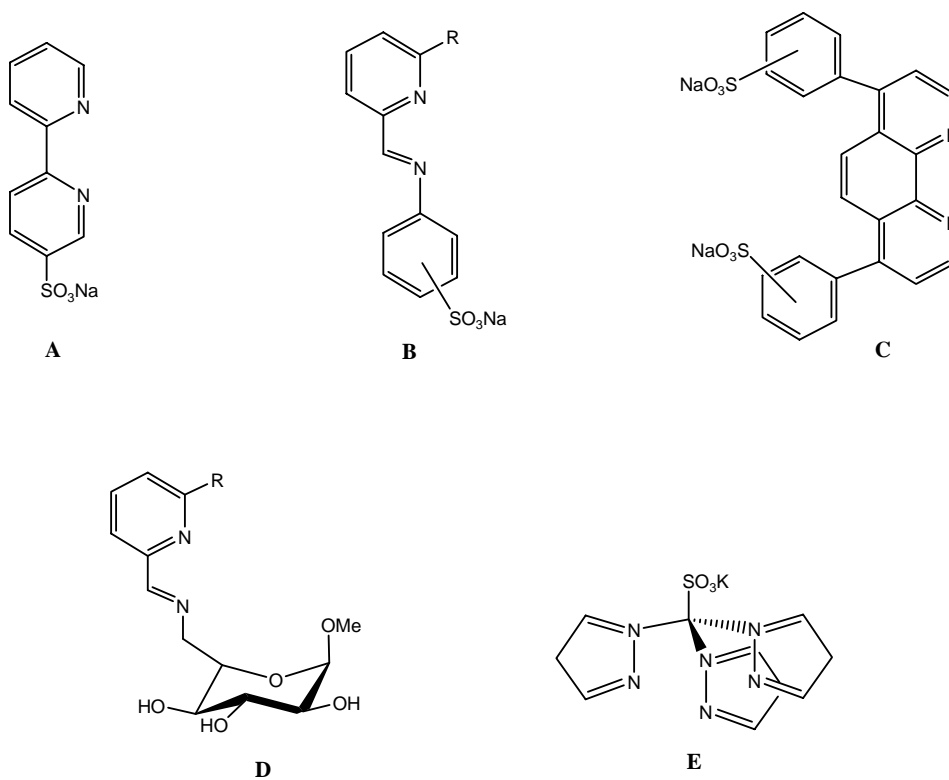


**Figure 1.20.** Examples of water-soluble nitrogen ligands.

### ***1.9 Rationale and Objectives***

Based on the extensive literature given above on the use of metal complexes as anticancer agents, it is clear that metal-containing compounds especially cisplatin are important in the research towards discovery of better anti-cancer drugs. The widely used ligands and complexes are based on imidazole. For instance, several complexes especially platinum containing, with N-heterocyclic ligands such imidazole, thiozole, benziimidazole, benzoxazole and benzothiozole have been reported. However it is noted that little has been done on complexes based on pyrazoles as the ligands. Since pyrazole belong to the same class of compounds as imidazole, it is therefore important to try and explore its chemistry as far as anti-cancer drugs are concerned.

Pyrazole-type heterocycles thus represent this important class of non-leaving ligands. This is because of their rich electronic property that can be altered by appropriate choice of substituents on 2-N, 3-C, 4-C, and 5-C atoms of the pyrazole. This in turn enables optimization of the electronic property of the metal center. It also boosts the efficiency of the drug. For instance, incorporation of aminomethyl groups or carboxylic groups improves the solubility of the complexes in water. The presence of the 1H proton in the pyrazole ring is ideal for hydrogen bonding in the DNA. In this study, pyrazole and 3,5-dimethylpyrazole have been used as ligands to synthesise palladium(II) and platinum(II) complexes. The choice of palladium as a one of the metals is based on two factors: (i) it is an homologue of platinum and thus is expected to show similar activity, (ii) it is cheap. The purpose of this research work is therefore to synthesise palladium(II) and platinum(II) complexes and evaluate them as anti-cancer agents.

### 1.9 Reference:

1. Gerard J., Siden T., Anne V., Roger A., *J. Organomet. Chem.* 600 (2000) 23.
2. Holford J., Raynaud F., Murrer B. A., Grimaldi K., Hartley J. A., Abrahams M., Kelland L. R., *Anticancer Drug Des.* 13 (1998) 1.
3. Keppler B. K., *Metal Complexes in Cancer Chemotherapy*, VCH, Weinheim, 1993.
4. Elizabeth R. J., Lippard S. J., *Chem. Rev.* 99 (1999) 2467.
5. Clarke M. J., Podbielski L., *Coord. Chem. Rev.* 78 (1987) 253.
6. Evans C. W., *The Metastatic Cell: Behaviour and Biochemistry*, 2<sup>nd</sup> Ed., Chapman and Hill, London, 1991.
7. Sakai K., Yasushi T., Takuma U., Koji G., Msakatsu O., Taro T., Kazuko M., Kenji O., Kazuyuki K., *Inorg. Chim. Acta.* 297 (2000) 64.
8. Balandrin N.F., Kinghorn A. D., Farnsworth N. R. in *Human Medicinal Agents from Plants* Kinghorn, A. D., Balandrin, N. F., Eds., *ACS Symposium Series 534* (1993) p. 2.
9. Cragg G. M., Boyd M. R., Cardellina II J. H., Grever M. R., Schepartz S. A., Snader K. M., Suffness M. Kinghorn A. D., Balandrin M.F., Eds., *ACS Symposium Series 534* (1993) p. 81.
10. Reddy L., Odhav B., Bhoola K.D., *Pharmacol. Ther.* 99 (2003) 1.
11. Gerzon K. in *Anticancer agents Based on Natural Products Models* Cassady J. M., Douros J. D., Eds., *Academic Press* (1980) p. 271.

12. Jardine I. in *Anticancer Agents Based on Natural Products Models* Cassidy, J. M., Eds., *Academic Press* (1980) p. 319.
13. Bair K. W., Tuttle R. L., Knick V. C., Cory M., McKee D. D., *J. Med. Chem.* 33 (1990) 2385.
14. Abdulla M., Gruber P., *Biofactors* 12 (2000) 45.
15. Holford J., Sharp S.Y., Murrer B.A., Abrams M., Kelland L.R., *Br. J. Cancer* 77 (1998) 366.
16. Clarke M. J. *Coord. Chem. Rev.* 236 (2003) 209.
17. Mckeage M. J., Maharaj L., Berners-Price S. J., *Coord. Chem. Rev.* 232 (2002) 127.
18. Pillarsetty N., Katti K. K., Hoffman T. J., Volkert W.A., Katti K. V., Kamei H., Koide T., *J. Med. Chem.* 46 (2003) 1130.
19. Cookson P. D., Tiekink E. R. T., Whitehouse M. W. *Aust. J. Chem.* 47 (1994) 577.
20. Carotti S., Guerri A., Mazzei T., Messori L., Mini E., Orioli P., *Inorg. Chim. Acta.*, 81 (1998) 90.
21. Kresja C. M., Nadler S. G., Esselstyn J. M., Kavanagh J. T., Ledbetter J. A., Scieven G. L., *J. Biol. Chem.* 272 (1997) 11541.
22. Thompson H. J., Chasteen D. N., Neeker L., *Carcinogenesis* 8 (1997) 51.
23. Bishaye A., Chatterjee M., *Br. J. Cancer.*, 71 (1995) 1214.
24. Angelos M. Evangelou, *Crit. Rev. Oncol. Hematol.* 42 (2002) 249.
25. Katsaros N., Anagnostopoulou A., *Crit. Rev. Oncol. Hematol.* 42 (2002) 297.
26. Howard R. A, Kimball A. P., *Cancer Res.*, 39 (1979) 2568.



27. Dunbar K. R., Matonic J. H., Saharan V. P., Crawford C. A., Christou G., *J. Am. Chem. Soc.* 116 (1994) 2201.
28. Norman R. E. and Sadler P. J., *Inorg. Chem.*, 27 (1988) 3583.
29. Andrews P. A., Murphy M. P., and Howell S. B., *Cancer Res.* 45 (1985) 6250.
30. Lippard S. J., *Prog. Inorg. Chem.*, John Wiley & Sons, Inc, 38(1990) pg 477.
31. Kelemu L., Tiesheng S., Lars I. E., *Inorg. Chem.*, 39 (2000) 1728
32. Yang K., Lachicotte R. J., Eisenberg R., *Organometallics* 16 (1997) 5234.
33. Mc A'Nulty M. M., Whitehead J. P., Lippard S. J., *Biochemistry* 35 (1996) 6089.
34. Admiraal G., Van der Veer J. L., de Graaff R. A. G., den Hartog J. H. J., Reedijk J., *J. Am. Chem. Soc.* 109 (1987) 592.
35. Fichtinger-Schepman A. M. J., Van der Veer J. L., Lohman P. H. M., Reedijk J., *J. Inorg. Biochem.* 21(1984) 103
36. Gately D. P., Howell S. B., *Br. J. Cancer* 67 (1993) 1171.
37. Howe-Grant M.E., Lippard S.J., *Metal Ions Biol. Syst.*, 20 (1980) 63.
38. Holford J., Raynaud F., Murrer B. A., Grimaldi K., Hartley J. A., Abrahams M., Kelland L. R., *Anticancer Drug Des.* 13 (1998) 1.
39. Neidle S., Ismail I. M., Sadler P. J., *J. Inorg. Biochem.* 13 (1980) 205.
40. Fichtinger-Schepman A. M. J., Van der Veer J. L., den Hartog J. H. J., Lohman P. H. M., Reedijk J., *Biochemistry*, 24 (1985) 707.
41. Eastman, *Biochemistry*, 25 (1986) 3912.
42. Lebwohl D., Canetta R., *Eur. J. Cancer* 34 (1998) 1522.
43. Van Beusichem M., Farrell N., *Inorg. Chem.* 31 (1992) 634.

44. Coluccia M., Nassi A., Loseto F., Boccarelli A., Marrigio M. A., Giordano D., Intini F. P., Caputo P., Natile G., *J. Med. Chem.* 36 (1993) 510.
45. Kelland L. R., Barnard C. F. J., Mellish K. J., Jones M., Goddard P. M., Valenti M., Bryant A., Murrer B. A., Harrap K. R., *Cancer Res.* 54 (1994) 5618.
46. Wong E., Giandomenico C. M., *Chem. Rev.* 99 (1999) 2451.
47. Chen Y., Guo Z., Parsons S., Sadler P.J., *Chem. Eur. J.* 4 (1998) 672.
48. Wheate N. J., Collins J. G., *Coord Chem. Rev.* 241 (2003) 133.
49. US Food and Drug Administration Drug Fact Sheet: *Eloxatin*, February 2003.
50. Young L., Shin W. K., Jong Y. P., Ok-sang J., *J. Mol. Str.* 659 (2003) 129
51. Johnson N. P., Hoeschele J. D., and Rahn R. O., *Chem. Biol. Interact.*, 30(1980) 157
52. Hall M. D., Hambley T. W., *Coord Chem. Rev.* 232 (2002) 49.
53. Mason W.R., *Coord. Chem. Rev.*, 7 (1972) 241.
54. Rabenstein D. L., Guevremont R., Evans C. A., *Metal Ions Biol. Syst.*, 9 (1979) 103.
55. Bart A. J., Jaap B., Reedijk J., *J. Inorg. Biochem.* 89 (2002) 197.
56. Reedijk J., *Chem. Rev.*, 99 (1999) 2499.
57. Kelland L. R., Murrer B. A., Abel G., Giandomenico C. M., Mistry P., Harap K. R., *Cancer Res.*, 52 (1992) 822.
58. Talman E. G, Bruning W, Reedijk J., Spek A. L, Veldman N., *Inorg. Chem.*, 36 (1997) 854.
59. Bierbach U., Qu Y., Hambley TW., Peroukta J., Nguyen HL., Doedee M., Farrell N., *Inorg. Chem.*, 38 (1999) 3535.

60. Iakovidis A., Hadjiliadis N., *Coord. Chem. Rev.*, 17 (1994) 135.
61. Odenheimer E., Wolf W., *Inorg. Chim. Acta.*, 66 (1982) L48.
62. Brown T. L., Lee K. J., *Coord. Chem. Rev.* 128 (1993) 89.
63. Comba P., *Coord. Chem. Rev.* 123 (1993) 1.
64. Dowling C., Murphy V. J., Parkin G., *Inorg. Chem.* 35 (1996) 2415.
65. Wang K., Lu J., Li R., *Coord. Chem. Rev.* 151 (1996) 53.
66. Mylonas S. S., Valavanidis A., Dimitropoulos K., Polissiou M., Tsiftoglou A. S., Vizirianakis I. S., *J. Inorg. Biochem.* 34 (1988) 265.
67. Iakovidis A., Hadjiliadis N., *Coord. Chem. Rev.* 135 (1994) 17.
68. Fatma G., Oztekin A., Gokcen E., Hatice E., *Eur. J. Med. Chem.* 38 (2003) 473.
69. Giovanni T., Willem L. D., Reedijk J., Nora V., Spek A. L., *Inorg. Chim. Acta.* 288 (1999) 239.
70. Hambley T. W., Jones A. R., *Coord. Chem. Rev.* 212 (2001) 35.
71. Colombo A., Di Gida R., Pasini A., Dasdia T., Zunino F., *Inorg. Chim. Acta.* 125 (1986) L1.
72. Britovsek G. J. P., Grace Woo Y. Y., Nitinan A., *J. Organomet. Chem.* 679 (2003) 110.
73. Ferrara M. L., Orabona I., Ruffo F., Funicello M., Panunzi A., *Organometallics* 17 (1998) 3832.

## **Chapter 2**

### **INTRODUCTION TO BIOCHEMICAL PROCESSES INVOLVED IN CELL DEATH**

#### ***2.1 Introduction to cancer***

Cancer is a disease caused by uncontrolled growth and spreading of abnormal cells. Cancer can seriously threaten human health and it is a leading cause of death. Since 1990, about 16 million new cancer cases have been diagnosed in the United States, where the overall costs for cancer in 2001 were estimated at \$156.7 billion. It is estimated that in 2002 about 1.3 million new cases were diagnosed.<sup>1</sup> Although the mechanisms of formation and spread of cancer are still not well understood, both external factors (e.g. tobacco smoking, chemicals, radiation, and infections) and internal factors (e.g. inherited metabolism mutations, hormones, and immune conditions) are believed to be relevant causative factors. These may act together or sequentially to initiate and promote carcinogenesis.<sup>2</sup>

Although there have been rapid advances in the development of anticancer drugs, there is a lack of proper cure for cancers. A worthy goal at present is to develop treatments that produce remission and/or palliation. A cancer is said to be in remission when all clinical evidence of cancer has disappeared. It is noteworthy, however, that microscopic foci of cancer cells may still remain. Effective treatments include surgery, radiotherapy, chemotherapy, hormone-therapy and immunotherapy. Each of these treatment modalities has advantages and disadvantages, and their combination is usually needed to produce the most effective results.<sup>2</sup>

The surgical removal of a cancerous tumor and the surrounding affected tissue is often effective and considered as the primary procedure for tumors large enough to manipulate. However it is difficult for surgery to be effective and it is usually unavoidable to have residual affected cells. In addition, surgery may have the undesirable side effect of changing the growth rate of the remaining cancer cells by triggering a faster metastatic process. In many cases, patients die of metastatic cancer after the primary tumor has been successfully removed.<sup>3</sup> Multimodal therapy that utilizes radiotherapy, chemotherapy and other forms of treatments to follow surgery provides a better chance to kill the metastatic cancer cells or, at least, to keep them in the remission state described earlier.

Thus cancer chemotherapy was first successfully practiced in the 1950s when nitrogen mustard, which was used as a war gas, was found to be effective in inhibiting tumor growth. Due to extreme toxicity, however, effective chemotherapy with anticancer drugs was not widely applied until the 1960s. However in the early 1980s, chemotherapy was introduced for treatment of carcinoma with a high expectation of reducing the incidence of distant metastases and increasing the possibility of local control. Thus chemotherapeutic agents become important as anticancer agents.

## ***2.2 Cytotoxicity***

For many biologists it came as a surprise to realize that the death of a cell is not necessarily a bad thing. Actually cell death in metazoans is required for development, maintenance and survival of the organism. Physiological cell death has been observed in different tissues and in various organisms. Cell death occurs throughout the life span of multi-cellular organisms and arguably represents the only irreversible cell fate decision.<sup>4</sup>

Cytotoxicity is the cell-killing property of a chemical compound. Cell death can occur by either of two distinct mechanisms, necrosis or apoptosis.<sup>5</sup> Necrosis is the pathological process, which occurs when cells are exposed to a serious physical or chemical damage, whereas apoptosis is the physiological process by which unwanted cells are eliminated during development and other normal biological processes.<sup>4,5</sup> Loss of viability, whether as a result of necrosis or apoptosis, is often defined experimentally as the loss of cell membrane integrity. The determination of whether a cell dies by apoptosis as opposed to necrosis is best made on the basis of (i) alterations in the cell membrane and cytoplasm and (ii) changes in the cells chromatin, both of which occur prior to the lysis (breakdown) of the membrane.<sup>6</sup>

In early stages of apoptosis, changes occur at the plasma membrane. Plasma membrane alteration involves the translocation of phosphatidylserine (PS) from the inner side of the plasma membrane to the outer layer and is best detected by flow-cytometry.<sup>7</sup> The cell chromatin condenses and forms aggregates near the nuclear membrane which, in turn becomes convoluted, whilst the nucleolus becomes enlarged and appears abnormally granular (Fig. 2.1).<sup>8</sup> It is generally assumed that these morphological changes result from a developmental programme for cell death that can be triggered by deprivation of a growth factor, or by addition of a xenobiotic compound such as cancer therapeutic drug. In addition, apoptosis involves the fragmentation of the genomic DNA, an irreversible event that commits the cell to die and occurs before changes in plasma membrane permeability. This DNA fragmentation has been shown to result from activation of endogenous  $\text{Ca}^{2+}$  and  $\text{Mg}^{2+}$  -dependent nuclear endonuclease. This enzyme selectively cleaves DNA at sites located between nucleosomal units (linker DNA) generating mono-

and oligonucleosomal DNA fragments. It occurs in a predictable pattern in which the cell nucleus becomes condensed; the cell itself shrivels forming small apoptotic bodies. They are engulfed and digested i.e. phagocytosis. Other key elements signifying apoptosis includes protease cascade and mitochondrial changes.<sup>6</sup>

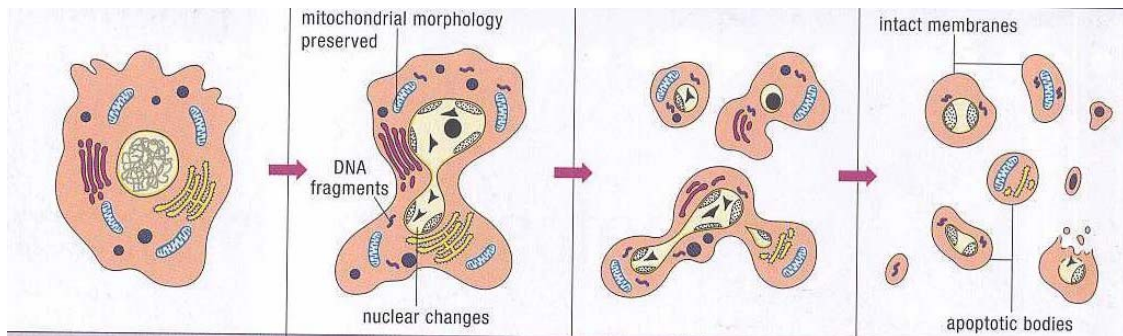


**Figure 2.1.** Apoptotic programmed cell death. Reproduced from Apoptosis and Cell Proliferation, 2<sup>nd</sup> Ed. 1998, Germany, p.2.

*In vivo*, these apoptotic bodies are rapidly recognized and phagocytized by either macrophages or adjacent epithelial cells.<sup>4</sup> As a result of this, no inflammatory response is elicited on the adjacent cells, in contrast to necrosis whereby the cellular contents are released into the extracellular fluid thereby causing inflammation, and hence triggering the release of chemokines and cytokines which then activates the inflammatory response of the nearby cells.

To the extent that most traditional anticancer chemotherapy drugs exert their cytotoxic effects by inducing apoptosis, apoptosis-modulating drugs for treating cancer have been available for many years.<sup>9</sup> However, these agents initially act nonspecifically by either damaging DNA or disrupting the cytoskeleton, and do so in both tumor and normal cells.

As a result of this apoptosis research in cancer drug discovery is paramount in that we not only synthesize new drugs, but we also probe them for their ability to kill the tumours without side effects on the neighbouring cells.<sup>10</sup> Metallo-drugs fortunately have been found to induce apoptosis. Two complexes of the type *trans*-[PtCl<sub>2</sub>(isopropylamine)(amine<sup>o</sup>)] evaluated by Perez and coworkers (Fig 2.2), showed apoptotic activity on *Pam 212-ras* murine keratinocytes cells.<sup>11</sup>

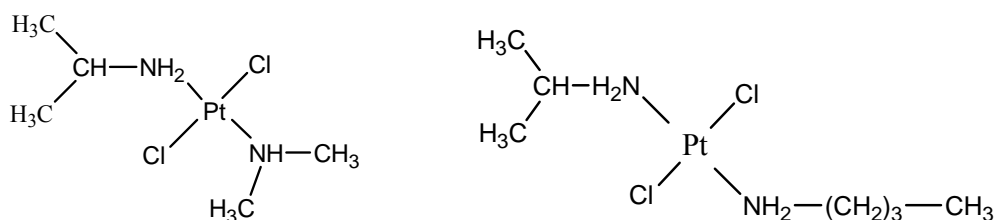


**Figure 2.2.** Structures of (a) *trans*-[PtCl<sub>2</sub>(isopropylamine)(dimethylamine)], (b) *trans*-[PtCl<sub>2</sub>(isopropylamine)(butylamine)] which have shown apoptotic activity (reference herein). *J. Inorg. Biochem.* 77 (1999) 37.

This paves way for more research to be done on cisplatin analogues. Of interest is the fact that there is the expectation that elucidation of the cellular mechanisms that lead to apoptosis may allow this form of cell death to be included more effectively by cancer therapeutic agents.<sup>12</sup> In addition, the apoptotic mechanism of cell death is fundamental to the normal development of tissues and organisms, in contrast to cell death by necrosis which is usually accidental and therefore do not have such significance but is primarily pathological.



## 2.3 Apoptosis

### 2.3.1 Cell membrane alteration.

Apoptosis is a distinct form of cell death that proceeds along a genetically determined execution programme. It exhibits a characteristic morphology i.e. shrinking of cells (Fig. 2.1). There are other unique biochemical alterations that lead to this process. One such process is the alteration of the cell membrane. The cell membrane is described as a semi-fluid mosaic structure composed of phospholipids with a diverse group of inserted proteins and some cholesterol. The phospholipids in the membrane are arranged in the form of a 'bi-layer' i.e. an asymmetric membrane in composition, structure and function. (Fig. 2.3).

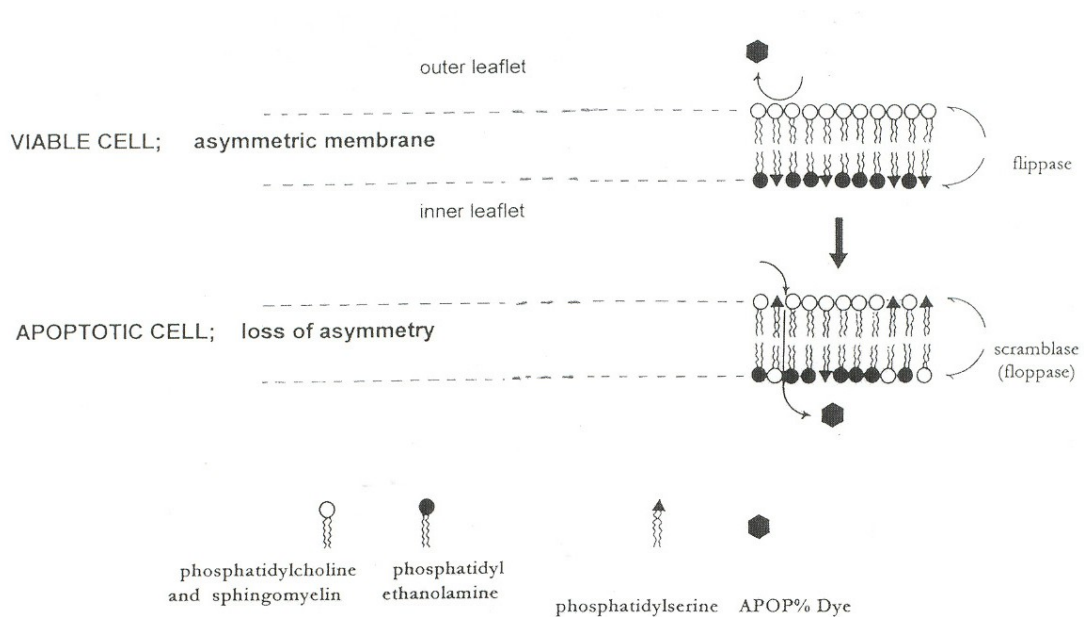


**Figure 2.3.** The asymmetric phospholipids composition of a transformed mammalian cell. Reproduced from APOPercentage Assay Manual, 2<sup>nd</sup> Ed. Ireland, 2002, p.10.

The outer leaflet of the lipid membrane is composed of choline containing phospholipids, (phosphatidylcholine and sphingomyelin), that is in contact with the extra-cellular matrix, (*in vivo*), or with cell culture medium, (*in vitro*). The inner leaflet of the membrane is composed of phosphatidylethanolamine and phosphatidylserine and is in contact with the cell's cytoplasm. The non-polar, hydrophobic fatty acid tails of the phospholipids of both leaflets make up the interior volume of the membrane, giving the typical bi-layer structure, as seen by electron microscopy.

The asymmetric composition of the membrane phospholipids is essential in maintaining a viable cell. The membrane and its components selectively control the exchange of molecules and the generation of concentration gradients between the cytoplasm and the extra cellular fluid. To ensure normal trans-membrane functions the phospholipids must be maintained in an asymmetric distribution. The process is regulated by 'flippases' that catalyse the active transport of aminophospholipids from the outer to inner monolayer.<sup>13</sup> In cells undergoing apoptosis, flippase is counteracted by the action of another enzyme known as 'floppase'.<sup>14</sup> The net effect of floppase action is the scrambling of the phospholipid distribution between the inner and outer monolayers, better known as the flip-flop mechanism. The flipping of phosphatidylserine molecules to the surface of the membrane permits the transport of a dye into the cell (as shown in the Fig. 2.3) allowing it to accumulate within the cell. This is a biochemical alteration that is unique with cells dying by apoptosis, and by extension allows the investigation of the cell death mechanism by monitoring and quantifying the dye uptake.

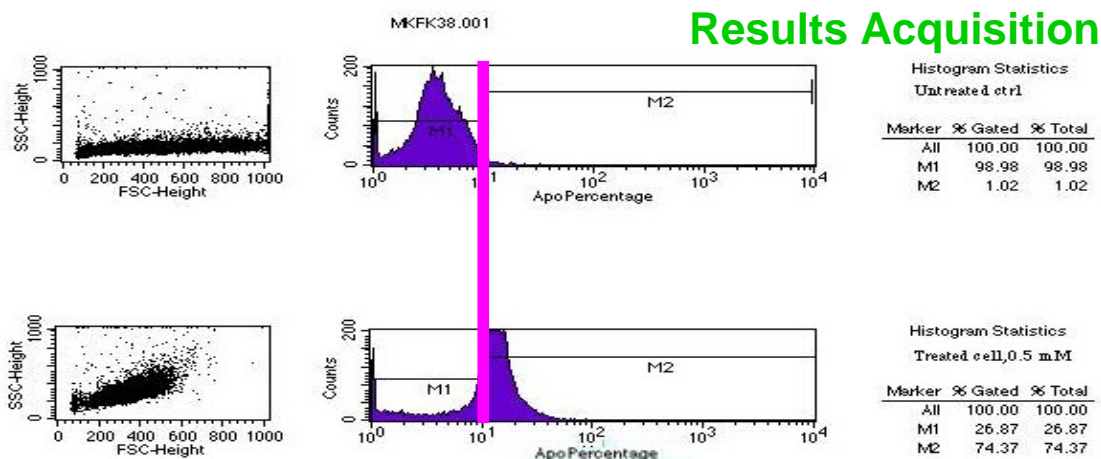


**Figure 2.4.** Analysis of cells dying apoptotically using a fluorescence-activated cell sorter.

The above figure shows typical results obtained for both the untreated and the treated cells respectively. The fluorescence-activated cell sorter is used to make measurements on individual cells. The cells that take up dye become fluorescent, and thus the intensity of fluorescence observed is directly proportional to the amount of cell death in a given population of cells. The cells in category **M1** are regarded as normal cells and **M2** as apoptotic cells. The Forward Scatter and the Side Scatter plots (FSC, SSC) of the treated cells shows that they have condensed (shrunk) while the untreated cells have maintained their morphology.

### ***2.3.2 Cell-cycle and its interruption***

Apart from the anticancer agents binding to the DNA hence its activity, there are many other processes that culminate to the demise of the treated cells, e.g. cell division interruption. Cell division is responsible for DNA replication.<sup>15</sup> It is important to try and

understand what these chemical agents do at a cellular level, i.e. disrupting the cell cycle which regulates cell division and multiplication concurrently.

Cells reproduce by duplicating their contents and then dividing into two. This happens by means of cell division.<sup>4</sup> It is principally the way by which all living things are propagated. The cell cycle is an ordered set of events, involving cell growth and division into two daughter cells. In unicellular species, such as bacteria, each cell division produces an additional organism whereas in multicellular species many rounds of cell-division are required to not only make new individuals but also to replace cells that are damaged.<sup>16</sup> The vast majority of cells doubles their mass and duplicates all their cytoplasmic organelles in each cell-cycle. Thus there is a set of cytoplasmic and nuclear processes to be coordinated with one another during the cell cycle and this is achieved through a cell-cycle control system that coordinates the cycle as a whole.<sup>5</sup>

The cell cycle is divided into several distinct phases, of which the most dramatic is *mitosis*, the process of nuclear division, which precedes to cell division itself. In mitosis the chromosomes condense into visible structures. In addition, the cells microtubules are reorganized to form the mitotic spindle that will eventually separate the chromosomes.<sup>17</sup> As mitosis proceeds, the cell seems to pause briefly in a state called metaphase, in which the chromosomes, already duplicated, are aligned on the mitotic spindle, poised for segregation.<sup>18</sup> The separation of the duplicated chromosomes marks the beginning of anaphase, during which the chromosomes move to the poles of the spindle, where they de-condense and reform intact nuclei. The cell is then pinched into two (daughter cells)

by a process called cytokinesis, which marks the end of mitosis better referred to as **M phase**.<sup>15</sup>

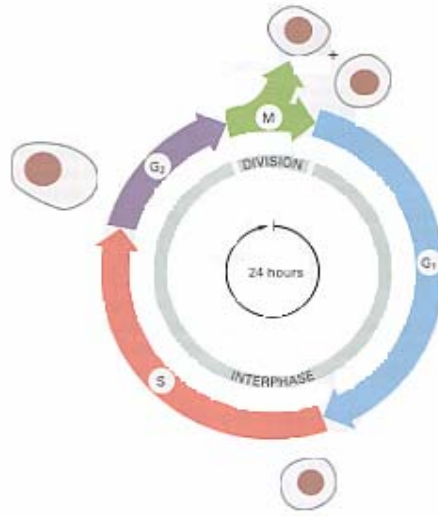


**Figure 2.5.** The four phases of a standard eukaryotic cell cycle culminating in cell division. Reproduced from *Molecular Biology of the Cell*, 3<sup>rd</sup> Ed. Garland Publishing, Inc. New York and London, p. 863.

The much longer period that elapses between one M phase and the next is known as *interphase*. By microscopy the cell appears to be in a dormant phase which is a deceptive observation as other techniques have revealed that it is a stage during which elaborate preparations for cell division takes place in an orderly sequence i.e. the DNA in the nucleus is replicated. DNA replication occurs in a small portion of interphase called the **S phase** (S for synthesis).<sup>19</sup> The interval between the completion of M phase and beginning of S phase is called the **G<sub>1</sub> phase** (G for gap) whereas the interval between the end of DNA synthesis and the beginning of mitosis is called the **G<sub>2</sub> phase**. G<sub>1</sub> is known to

regulate and control the cell cycle. During  $G_1$  the cell monitors its environment and its own size and when ready, it takes a decisive step that commits it to DNA replication and completion of a division cycle. The  $G_2$  phase provides a safety gap, allowing the cell to ensure that DNA replication is complete before getting into mitosis. However if the cells in  $G_1$  phase do not encounter DNA replication, they pause their progress in the cycle and subsequently enter a special resting state which is referred to as  $G_0$  phase indefinitely. Other research scientists in this field have regarded this phase as a phase entered by apoptotic cells.

#### ***2.3.2.1 Simultaneous identification of $G_0$ - and apoptotic cells by DNA and RNA content measurement.***

In this kind of study, there is a need to reveal whether a particular agent or treatment administered may preferentially induce apoptosis of  $G_1$ - or  $G_0$ -cells in cell populations which consist of a mixture of cycling and quiescent  $G_0$ -cells.<sup>20</sup> During apoptosis as described earlier, calcium and magnesium-dependent nucleases are activated and as a result degrade the DNA. This means that within the DNA there will be nicks and breaks leading to its fragmentation. This can always be detected using a number of techniques which include: - using strand break labelling (TUNEL) technique to detect broken DNA, using Hoechst binding to detect DNA conformational changes, and DNA analysis by looking at a sub- $G_1$  peak.

The sub- $G_1$  peak analysis is one of the widely used techniques in determination of apoptosis. Cell dying apoptotically, undergo chromatin condensation and degradation of the genomic DNA respectively. The sub- $G_1$  method relies on the fact that after DNA

fragmentation there are small fragments (low molecular weight DNA) and therefore when cells are permeabilized, these fragments leak out in the subsequent rinsing and quantitative staining procedure. As a result, the cells that have lost DNA will take up less of the DNA-binding dye and thus the resultant Ap-peak appearing to the left of the G<sub>1</sub> peak (Fig. 2.6).

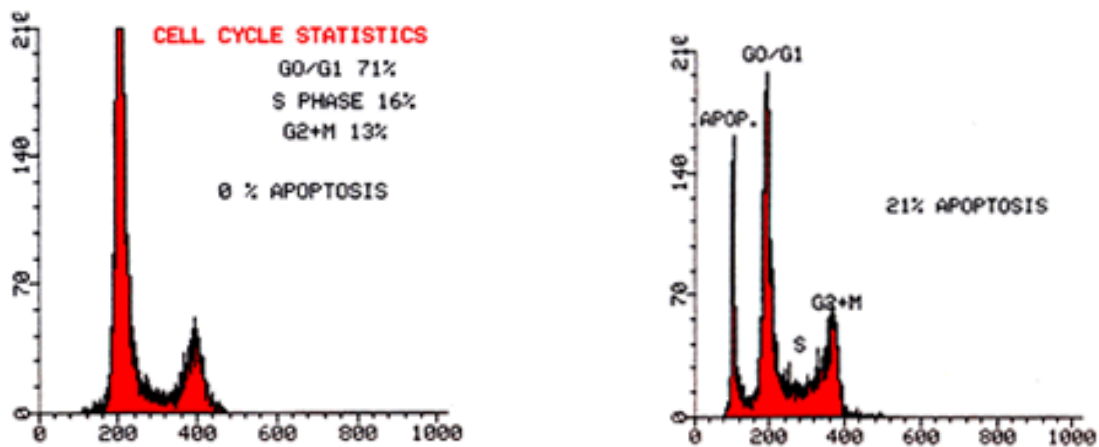


**Figure 2.6.** Cell cycle statistical histogram showing the apoptotic cells appearing at the left of G<sub>1</sub> peak.

The advantage of this method is that it is very rapid and will detect cumulative apoptosis and is applicable to all cell types. However, in order to be seen in the sub-G<sub>1</sub> area a cell must have lost enough DNA to appear there; so for example if cells enter apoptosis from the S or G<sub>2</sub>/M phase of the cell-cycle or if there is an aneuploid population undergoing apoptosis, they may not appear in the sub-G<sub>1</sub> peak. In conjunction with the above information, simultaneous measurement of cellular DNA and RNA can be done. This is

one of the sub-G<sub>1</sub> peak types of analysis. It has been shown that 90% of the cellular RNA is the rRNA. In this context the G<sub>0</sub>-cells (apoptotic) are known to contain a 5-10 fold lower rRNA content compared with their proliferating (growing) counterparts.<sup>21</sup> Thus flow cytometry measurement of cellular RNA content enables quiescent cells to be distinguished from cycling cells.<sup>21</sup>

The use of acridine orange, which has metachromatic properties, enables this type of analysis to be performed. At an appropriate concentration and ionic conditions, this dye intercalates into DNA and fluoresces green, whereas the product of its interaction with RNA fluoresces red. Thus cells with lower DNA staining than that of G<sub>1</sub>-cells (Sub-G<sub>1</sub> peak) are considered apoptotic.<sup>22</sup>

### ***2.3.3 DNA fragmentation***

Apoptosis as described earlier is morphologically characterized by early cell shrinkage, and chromatin condensation, among other changes. The nuclear fragmentation of such cells is one of the more extensively studied biochemical events in apoptosis. DNA double-strand cleavage occurs in the linker regions between nucleosomes, and produces DNA fragments that are multiples of approximately 185 base pairs (bp).<sup>23</sup> These DNA fragments can readily be detected by agarose gel electrophoresis. DNA fragmentation has long been used in distinguishing apoptosis from necrosis and is among the most reliable methods of detecting apoptotic cells. In pure cell populations, biochemical changes in chromatin and eventually DNA degradation provide useful and often quantifiable means of detecting apoptosis. In contrast, cells that undergo necrosis are normally accompanied by random DNA breakdown, and therefore exhibit diffuse smears in the agarose gel



instead of clear ladders. Nevertheless classical biochemical methods, such as gel electrophoresis, indicate the difference in DNA degradation content of the cells which have undergone apoptosis as opposed to necrosis. In apoptosis there is presence of oligonucleosome-sized fragments of DNA, which when analysed on agarose gels, produce 'ladders' (Fig. 2.7) whilst necrosis does not.

DNA fragmentation during apoptosis is considered to occur in two stages. Walker *et al.*<sup>24</sup> reported sequential degradation of genomic DNA, initially to high molecular weight DNA fragments of approximately 300 kb, followed by the appearance of 50 kb loop-size chromatin fragments which are detected using pulse-field gel electrophoresis. Oligonucleosomal DNA fragments that produce the characteristic 200 bp DNA ladder are released when the 50 kb fragments are further degraded.

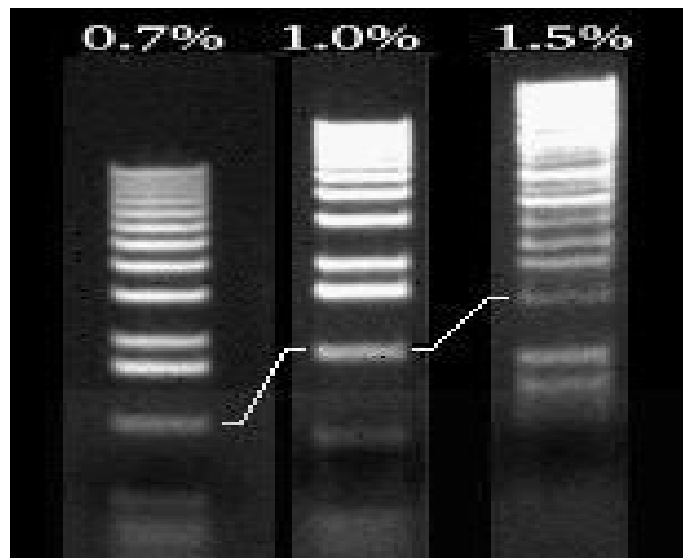


**Figure 2.7. DNA fragmentation pattern.** DNA laddering profile showing separation of DNA fragments of different sizes by using different concentrations of agarose gel in electrophoresis. Higher concentrations of agarose facilitate separation of small DNAs, while low agarose concentrations allow resolution of larger DNAs.

#### ***2.3.4. p53, mitochondria, caspases, and other DNA damage responses in apoptosis***

The definition of p53 is a nuclear protein that functions as a transcription factor capable of regulating genes.<sup>25</sup> It plays a central role in the coupling of cell damage to cell cycle arrest and hence induction of apoptosis. In response to cellular stress exerted by hypoxia or the presence of DNA damage, the cellular p53 level increases and p53 is activated by modification<sup>26</sup> and turns on the transcription of its target genes.<sup>25</sup> The p53 cell cycle arrest pathways involve p21 gene (WAF1, CIP-1) and Growth Arrest and DNA damage-inducible gene, GADD45. The p21 is a cyclin-dependent-kinase (cdk) inhibitor. It binds to a number of cyclin-cdk complexes and proliferating cell nuclear antigen (PCNA) to block cell cycle progression in G<sub>1</sub> and G<sub>2</sub>. GADD45 also binds to PCNA and arrests the cell cycle in G<sub>2</sub>.<sup>26</sup>

The decision whether an individual cell undergoes growth arrest or apoptosis following p53 activation, appears to depend on a variety of factors, such as environmental conditions and the cell type. Depending on the cell type, augmentation of insulin like growth factor binding protein 3 (IGF-BP3) and Bax expression contribute to apoptosis induction by p53.<sup>27</sup> Bax, a mammalian cell death protein that targets mitochondrial membranes, binds to and thereby antagonizes Bcl-2 (anti-apoptotic protein) and probably facilitates cytochrome c release by forming pores into mitochondria membrane.<sup>28</sup> In the context of cellular DNA damage following p53 cell cycle arrest, some control mechanism evaluates whether the DNA can be repaired in a reasonable time or whether the damage is severe and hence the cell undergoes apoptosis in a p53 dependent manner.<sup>29</sup>

Caspases, a set of cysteine proteases that are activated specifically in apoptotic cells, are known to possess an active-site cysteine, and cleave substrates at Asp-Xxx bonds (i.e. after aspartic acid residues). Caspase is thought to be central component that triggers apoptotic pathway because of the visible changes it causes that suggests cell death via apoptosis. These enzymes participate in a cascade that is triggered in response to pro-apoptotic signals and culminates in cleavage of a set of proteins, resulting in the disassembly of the cell. Most of the morphological changes observed have been reported to be caused by a set of cysteine proteases that are activated specifically in apoptotic cells.<sup>30</sup>

One role of caspases is to inactivate proteins that protect living cells from undergoing apoptosis. For example, experiments performed by Nagata and co-workers<sup>31</sup> showed that the caspase-activated deoxyribonuclease (CAD), responsible for DNA fragmentation pre-exists in living cells as an inactive complex with an inhibitory sub-unit, called ICAD. The cleavage of CAD-ICAD complex i.e. activation of CAD, occurs by means of caspase-3-mediated cleavage of the inhibitory sub-unit (ICAD) hence fragmentation of DNA and apoptosis respectively.<sup>31</sup> Many other caspase substrates have been reported over years but the commonly discussed are caspases-2, 3, 7, 8, 9, and 10. Other negative regulators of apoptosis cleaved by caspases include, Bcl-2 proteins and nuclear lamins,<sup>32</sup> focal adhesion kinase (FAK) and p21-activated kinase 2 (PAK2).<sup>33</sup>

Mitochondria play an essential role in eukaryotic life and death. It is the power house of a cell but also plays a critical role in the control of apoptosis regulation. In fact a variety of key events in apoptosis focus on mitochondria, including the release of caspase activators e.g. cytochrome c, changes in electron transport, loss of mitochondrial trans-membrane potential, altered cellular oxidation-reduction, and participation of pro- and anti-apoptotic Bcl-2 family proteins. The different signals that converge on mitochondria to trigger or inhibit these events and their down-stream effects delineate several major pathways in physiological cell death.<sup>34</sup> It is understood that the effectors of apoptosis are represented by a family of intracellular cysteine proteases known as caspases. Inhibiting caspases, however, does not always inhibit cell death induced by pro-apoptotic stimuli. Although caspase inhibitors block some or all of the apoptotic morphology induced by growth factor withdrawal, actinomycin, ultraviolet (UV) radiation, staurosporine or glucocorticoids, they do not necessarily maintain replicate or clonogenic potential; ultimately, the cells die despite inactivation of caspases.<sup>35</sup> In addition, some pro-apoptotic proteins such as Bax, induce mitochondrial damage and cell death when caspases are inactivated. Such experimental observations support the fact that a caspase-independent mechanism of death exists. This mechanism is found to involve mitochondria.<sup>36</sup>

The importance of mitochondria in apoptosis was suggested by studies with a cell free system in which, spontaneous, Bcl-2-inhibitable nuclear condensation and DNA fragmentation were found to be dependent on the presence of mitochondria.<sup>37</sup> Subsequently, another study showed that induction of caspase activation by addition of deoxyadenosine triphosphate depended on the presence of cytochrome c released from mitochondria during extract preparation. During apoptosis (*in vitro* and *in vivo*)

cytochrome c is released from mitochondria and this is inhibited by the presence of Bcl-2 on the organelles. Cytosolic cytochrome c then forms an essential part of the vertebrate 'apoptosome' which is composed of cytochrome c, Apaf-1, and pro-caspase-9.<sup>36</sup> The result is activation of caspase-9, which then processes and activates other caspases and leads to cell death. Other apoptosis mediators released from mitochondria include pro-caspase-3 that is liberated into the cytosol during apoptosis and apoptosis inducing factor (AIF) which processes purified pro-caspase-3 *in vitro*. In general all these factors include the pathways and mechanisms involved in apoptosis when cells are treated with compounds being investigated.

## 2.4 References:

1. Feng S., Chien S., *Chem. Eng. Sci.* 58 (2003) 4087.
2. Schabel Jr. F. M., *Cancer*, 40 (1977) 558.
3. Baxter L. T., and Jain R. K., *Br. J. Cancer*, 73 (1996) 447.
4. Zörnig M., Hueber A., Baum W., Evan G., *Biochim. Biophys Acta*, 1551(2001) F1.
5. Kroemer G., Petit P., Zamzani N., Vayssiere J. L., Mignotte B., *FASEB J.* 9 (1995) 1277.
6. Nagata S., *Apoptosis by cell death factor*, 88 (1997) 355.
7. Boehringer M., *Apoptosis and cell proliferation*, 2<sup>nd</sup> Ed. Germany, 1998, p. 5.
8. Brown D. A., Rose J. K., *Cell* 68 (1992) 533.
9. Hengartner M. O., *Nature* 407 (2000) 770.
10. Alam J. J., *TRENDS in Biotechnology* 21 (2003) 479.
11. Perez J. M., Montero E. I, Gonzalez A. M., Alvarez-Valdes A., Alonso C., Navarro-Ranninger C., *J. Inorg. Biochem.* 77 (1999)37.
12. Bailly E., Bornens M., *Nature* 355 (1992) 300.
13. Sprong H., Van der Sluijs P., Van Meer G., *Nat. Rev.*, 2 (2001) 504.
14. Zhou Q., Zhao J., Stout J. G., Luhm R. A., Wedmer T., Sims P. J., *J. Biol. Chem.*, 272 (1997) 18240.
15. Alberts B., Bray D., Lewis J., Raff M., Roberts K., Watson J. D., *Molecular Biology of the Cell*, 3<sup>rd</sup> Ed. Garland Publishing, Inc. New York and London, p. 863.
16. Krishan A., *J. Cell Biol.* 66 (1975) 188.

17. Howard A., Pelc S. R., *Exp. Cell Res.* 2 (1951) 178.
18. McIntosh J. R., McDonald K. L., *Sci. Am.* 261 (1989) 48.
19. Sawin K. E., Scholey J. M., *TRENDS Cell Biol.* 1 (1991) 122.
20. Bruno S., Lassota P., Giaretti W., Darzynkiewicz Z., *Oncol. Res.* 4 (1992) 29.
21. Ringdahl M. H., and Cooper H. L., *J. cell Physiol.* 97(1978) 253.
22. Darzynkiewicz Z., Traganos, F., Sharpless T., Melamed M. R., *Proc. Natl. Acad. Sci. USA* 73 (1976) 2881.
23. Kosmider B., Osiecka R., Ewaciesielska, Szmigiero L., Zyner E., Ochocki J., *Mutat. Res.* 558 (2004) 169.
24. Walker P. R., Smith C., Youdale T., Leblanc J., Whitfield J. F. and Sikorska M., *Cancer Res.* 51 (1991) 1078.
25. Levine A. J., *Cell* 88 (1997)323.
26. Lohrum M. A. E., Vousden K H., *Cell Death Diff.* 6 (1999) 1162.
27. Amundson S. A., Myers T. G., Fornace A. J., *Oncogene* 17 (1998) 3287.
28. Shendel S. L., Montal M., Reed J. C., *Cell Death Diff.* 5 (1998) 372.
29. Barlow C., brown K. D., Deng C. X., Tagle D. A., Wynshaw-Boris A., *Nature Genet.* 17(1997) 453.
30. Alnemri E. S., Livingston D. J., Nicholson D. W., Salvesen G., Thornberry, N. A., Wong W. W., Yuan J., *Cell* 87 (1996) 171.
31. Nagata S., *Exp. Cell Res.* 256 (2000) 12.
32. Orth K., Chinnaiyan A. M., Garg M., Froelich C. J., Dixit V. M., *J. Biol. Chem.* 271 (1996) 16443.
33. Rudel T., Bokoch G. M., *Science* 276 (1997) 1571.

34. Douglas R. G., John C. R., *Science* 281 (1998) 1309.
35. McCarthy N. J., Whyte M. K. B., Gilbert C. S., Evan G. I., *J. Cell Biol.* 136 (1997) 215.
36. Xiang J., Chao D. T., Korsmeyer S. J., *Proc. Natl. Acad. Sci. U.S.A.* 93 (1996) 14559.
37. Newmeyer D., Forschorn D. M., Reed J. C., *Cell* 79 (1994) 353.



## Chapter 3

### SYNTHESIS OF PYRAZOLE LIGANDS AND THEIR COMPLEXATION WITH LATE TRANSITION METALS

#### *3.1 Introduction*

Cis-dichlorodiammineplatinum(II) complex (cisplatin), is one of the most effective drugs in clinical treatment of testicular, ovarian, bladder, head and neck cancers. However there are factors that limits its organotropic profile as a drug. That includes both the intrinsic and acquired resistances to the drug by patients. It has several side effects that include nephrotoxicity and neurotoxicity.<sup>1</sup>

Due to these reasons, there is a lot of research in the design of other drugs; platinum based (including other metals, i.e. palladium) anticancer complexes which possess improved clinical efficacy.<sup>2</sup> Hence the reason why second-generation platinum(II) antitumour complexes that carry non-leaving ligands other than simply ammonia are of interest for their ability to modulate drug metabolism and target binding through steric and electronic effects on the substitution mechanism.

In this study pyrazole and its derivatives were chosen as the non-leaving ligands of the palladium(II) and platinum(II) complexes in consideration of three main reasons. The sterically hindering ligands may reduce rapid detoxification by thiol-containing molecules and that the hydrophobic properties of the ligands taken into consideration.<sup>1</sup> The early SARs have defined the necessity of at least one NH moiety which is believed to be important for H-bonding interaction towards DNA.<sup>3</sup> While maintaining these factors,

the incorporation of aminomethyl groups at position 4 of the pyrazoles was adopted to afford an ideal ligand for synthesis of water soluble complexes. In this chapter we report the synthesis of this type of ligands together with attempts of their complexation. The preliminary *in vitro* antitumour activity of the complexes tested on mammalian CHO cell-lines is reported in chapter 4.

### **3.2 Experimental**

#### **3.2.1 Materials and methods.**

All chemicals and other reagents other than those described were used as received.  $[\text{PdCl}_2(\text{NCMe})_2]$  was prepared according to the literature methods.<sup>4</sup> All the palladium and platinum complexes used in this study were also synthesized as per literature procedures<sup>4,5</sup> and their characterization have just been reported (not discussed) to show the purity of the compounds. Glutathione used in some of the experiments performed was purchased from Acros Organics. The water used was double distilled. All manipulations of air- and/or moisture sensitive compounds were performed under a dry, deoxygenated nitrogen atmosphere using Schlenk techniques. IR spectra were recorded as NaCl cells on a Perkin-Elmer, paragon 1000 PC FTIR spectrophotometer.  $^1\text{H}$  NMR spectra were recorded on a Gemini 2000 instrument in  $\text{CDCl}_3$  and  $\text{DMSO-}d_6$  solution at room temperature (200 MHz).  $^1\text{H}$  chemical shifts were referenced to the residual signals of the protons of the solvents and are quoted in ppm. GC-MS was recorded in the electron impact mode, EI at 70 eV on a Finnigan-Matt GCQ equipped with 30 m HP-SMS capillary column with a stationary phase based on (5%-phenyl)-methylpolsiloxane. Elemental analysis was performed on a Carlo Erba NA analyzer in the department of

chemistry, University of the Western Cape and on a Fisons analyzer in the department of chemistry, University of Capetown.

### ***3.2.2 Crystallographic structure determination***

Crystal evaluation and data collection were performed on a Bruker CCD-1000 diffractometer with Mo K $_{\alpha}$  ( $\lambda = 0.71073 \text{ \AA}$ ) radiation and the diffractometer to crystal distance of 4.8 cm. The initial cell constants were obtained from three series of  $\omega$  scans at different starting angles. The reflections were successfully indexed by an automated indexing routine built in the SMART program. These highly redundant datasets were corrected for Lorentz and polarization effects. The absorption correction was based on fitting a function to the empirical transmission surface as sampled by multiple equivalent measurements. A successful solution by the direct methods provided all non-hydrogen atoms from the *E*-map. All non-hydrogen atoms were refined with anisotropic displacement coefficients. All hydrogen atoms were included in the structure factor calculation at idealized positions and were allowed to ride on the neighboring atoms with relative isotropic displacement coefficients.

### ***3.2.3 Synthesis of Ligands***

#### ***3.2.3.1. 3,5-dimethyl-4-(ethylamino)methylpyrazole (L1)***

A mixture of 3,5-dimethylpyrazole (1.00 g, 10.4 mmol), paraformaldehyde (0.48 g, 16 mmol), KOH (0.9 g, 16 mmol) and ethylamine (2 ml, 20 mmol) were dissolved in 50 ml of water. The mixture was kept under reflux conditions for ca. 51 h. The product was extracted from the aqueous solution using CHCl<sub>3</sub> (2 x 60 ml) and dried with anhydrous

MgSO<sub>4</sub> for one minute. The solids were separated by filtration and the colourless filtrate concentrated to dryness in vacuo. The product was isolated as oil. Yield = 1.25 g (78%).

IR (Nujol): 3250 ( $\nu_{\text{N-H}}$ ), 2970 ( $\nu_{\text{C-H}}$ ), 1589 cm<sup>-1</sup> ( $\nu_{\text{C-N}}$ ). <sup>1</sup>H NMR (CDCl<sub>3</sub>):  $\delta$  4.62 (br, 1H, NHEt), 3.53 (br s, 2H, CH<sub>2</sub>NHEt), 2.81 (q, <sup>3</sup>J<sub>HH</sub> = 7.4 Hz, 2H, NCH<sub>2</sub>CH<sub>3</sub>), 2.21 (s, 6H, CH<sub>3</sub>), 1.07 (t, <sup>3</sup>J<sub>HH</sub> = 7.4 Hz 3H, NCH<sub>2</sub>CH<sub>3</sub>). <sup>13</sup>C {<sup>1</sup>H}NMR (CDCl<sub>3</sub>):  $\delta$  143.6 (C(CH<sub>3</sub>)), 114.2 (C(CH<sub>2</sub>NHEt)), 44.3 (CH<sub>2</sub>NHEt), 39.8 (CH<sub>2</sub>CH<sub>3</sub>), 17.2 (CH<sub>2</sub>CH<sub>3</sub>), 10.1 (C(CH<sub>3</sub>)).

### 3.2.3.2. 4-isopropylaminopyrazole (**L2**)

Pyrazole (1.00 g, 14.70 mmol), paraformaldehyde (0.67 g, 11.35 mmol) and KOH (0.9 g, 16 mmol) were transferred to a Schlenk tube, dissolved in 50 ml of water and stirred for 2 min. before adding isopropylamine (1.88 ml, 43.24 mmol). The reaction mixture was kept under reflux conditions for 4 days. The product was then extracted as in 3.2.3.1 above. Yield: 1.12 g (71%) <sup>1</sup>H NMR (CDCl<sub>3</sub>):  $\delta$  7.59 (s, 1H, 5-Pz); 6.33 (s, 1H, 3-Pz); 4.99 (br s, 2H, CH<sub>2</sub>NH*i-Pr*), 3.67 (br, 1H, NH*i-Pr*), 2.65 (m, 1H NCH(CH<sub>3</sub>)<sub>2</sub>), 1.04 (d, 6H, NCH(CH<sub>3</sub>)<sub>2</sub>). Anal. Calc. for C<sub>7</sub>H<sub>13</sub> N<sub>3</sub>: C, 60.40; H, 9.41; N, 30.19%. Found: C, 59.95; H, 9.28; N, 29.62%.

### 3.2.3.3. 3,5-dimethyl-4-(isopropylamino)methylpyrazole (**L3**).

A mixture of 3,5-dimethylpyrazole (1.00 g, 10.4 mmol), paraformaldehyde (0.48 g, 16 mmol), KOH (0.9 g, 16 mmol) and isopropylamine (1.3 g, 20 mmol) were dissolved in 50 ml of water and refluxed for 48 h. Extraction was done as in 3.2.3.1 above. The product was isolated as clear oil. Yield = 1.53 g (87%). IR (Nujol): 3272 ( $\nu_{\text{N-H}}$ ), 2962 ( $\nu_{\text{C-H}}$ ), 1571 cm<sup>-1</sup> ( $\nu_{\text{C-N}}$ ). <sup>1</sup>H NMR (CDCl<sub>3</sub>):  $\delta$  4.80 (br, 1H, NH*i-Pr*), 3.53 (br s, 2H, CH<sub>2</sub>NH*i-Pr*),

2.81 (m, 1H,  $\text{NCH}(\text{CH}_3)_2$ ), 2.04 (s, 6H,  $\text{CH}_3$ ), 1.06 (d,  $^3J_{\text{HH}} = 5.8$  Hz, 6H,  $\text{NCH}(\text{CH}_3)_2$ ).  $^{13}\text{C}\{^1\text{H}\}$ NMR ( $\text{CDCl}_3$ ):  $\delta$  144.8 ( $\text{C}(\text{CH}_3)$ ), 113.2 ( $\text{C}(\text{CH}_2\text{NH}i\text{-Pr})$ ), 48.3 ( $\text{CH}(\text{CH}_3)_2$ ), 39.2 ( $\text{CH}_2\text{NH}i\text{-Pr}$ ), 20.2 ( $\text{CH}(\text{CH}_3)_2$ ), 11.1 ( $\text{C}(\text{CH}_3)$ ). MS, EI (70 eV);  $m/z$  167  $[\text{1}]^+$ . Anal. Calc. for  $\text{C}_9\text{H}_{17}\text{N}_3$ : C, 64.63; H, 10.25; N, 25.12%. Found: C, 62.18; H, 10.46; N, 23.03%.

#### 3.2.3.4. Synthesis of *1N*-triphenylchloromethane-3,5-dimethylpyrazole. (**L4**)

3,5-dimethylpyrazole (1.00 g, 10.4 mmol) was transferred to a Schlenk tube. Triphenylchloromethane (2.90 g, 10.4 mmol) was also transferred to the same Schlenk tube. Toluene (40 ml) and triethylamine (2 ml) was added respectively and the solution degassed with  $\text{N}_2$  gas for about 1 min. The solution was stirred under reflux conditions at 80 °C overnight. The salt was then filtered and the solvent evaporated to obtain a brown solid as the product. Chromatography was performed to purify the product with  $\text{CH}_2\text{Cl}_2$ :Hexane (5:1 ratio). The product crystallized upon slow evaporation of the solvent to give X-ray quality crystals. Yield: 2.57 g (73%) IR (Nujol):  $1701\text{ cm}^{-1}$  ( $\nu_{\text{C}=\text{C}}$ )  $1571\text{ cm}^{-1}$  ( $\nu_{\text{C}=\text{N}}$ ).  $^1\text{H}$  NMR ( $\text{CDCl}_3$ )  $\delta$  7.45, 7.143 (15 H,  $(\text{C}_6\text{H}_5)_3$ ); 6.03 (s, 1H, 4-Pz); 2.23 (s, 3H, 5-Me); 1.46 (s, 3H, 3-Me).

#### 3.2.4 Synthesis of complexes

##### 3.2.4.1 Bis-(3,5-dimethyl-4-(ethylamino) methylpyrazole)palladium(II) (**C1**)

3,5-dimethyl-4-(ethylamino)methylpyrazole (0.12 g, 0.77 mmol) was dissolved in about 3 ml of dichloromethane in a Schlenk tube. Then 0.1 g (0.385 mmol) of  $[\text{PdCl}_2(\text{NCMe})_2]$  was dissolved in dichloromethane (20 ml) and transferred to the same Schlenk tube. The reaction mixture was degassed and stirred at room temperature for a period of 6 h. to

obtain the product as an insoluble precipitate in dichloromethane. Yield: 0.14 g (75%) IR (Nujol): 3349  $\text{cm}^{-1}$  ( $\nu_{\text{N-H}}$ ), 1701  $\text{cm}^{-1}$  ( $\nu_{\text{C=C}}$ ) 1566 $\text{cm}^{-1}$  ( $\nu_{\text{C=N}}$ ). Anal. Calc. for  $\text{C}_{16}\text{H}_{30}\text{N}_6\text{PdCl}_2$ : C, 36.90; H, 5.75; N, 18.44%. Found: C, 37.81; H, 5.90; N, 15.05%.

#### 3.2.4.2 Attempted synthesis of palladium and platinum complexes of ligands **L2** and **L3**

Attempts to synthesise these complexes were performed. Unfortunately full characterization of the compounds obtained could not be performed as most of the reactions produced insoluble solids e.g. reaction **C1** above.

### 3.3. Spectroscopic data of the complexes used

#### 3.3.1 *Cis-dichloro-bis-(pyrazole)palladium(II)* (**1**).

$^1\text{H-NMR}$  ( $\text{CDCl}_3$ ):  $\delta$  11.69 (br s, 2H, N-H); 8.12 (s, 2H, 5-Pz); 7.59 (s, 2H, 3-Pz); 6.38 (s, 2H, 4-Pz). IR (Nujol): 3299  $\text{cm}^{-1}$  ( $\nu_{\text{N-H}}$ ), 1500 $\text{cm}^{-1}$  ( $\nu_{\text{C=N}}$ ). Anal. Calc. for  $\text{C}_6\text{H}_8\text{N}_4\text{PdCl}_2$ : C, 22.99; H, 2.57; N, 17.87%. Found: C, 23.59; H, 2.15; N, 17.78%.

#### 3.3.2 *Cis-dichloro-bis-(3,5-dimethylpyrazole)palladium(II)* (**2**).

$^1\text{H-NMR}$  ( $\text{CDCl}_3$ ):  $\delta$  11.83 (br s, 2H, N-H); 5.70 (s, 2H, 4-Pz); 2.67 (s, 6H, 5-Me); 1.92 (s, 6H, 3-Me). IR(Nujol): 3188  $\text{cm}^{-1}$  ( $\nu_{\text{N-H}}$ ), 1568  $\text{cm}^{-1}$  ( $\nu_{\text{C=N}}$ ). Anal. Calc. for  $\text{C}_{10}\text{H}_{16}\text{N}_4\text{PdCl}_2$ : C, 32.50; H, 4.36; N, 15.16%. Found: C, 33.47; H, 4.50; N, 15.26%.

#### 3.3.3 *Cis-dichloro-bis-(pyrazole)platinum(II)* (**3**).

$^1\text{H NMR}$  ( $\text{CDCl}_3$ ):  $\delta$  7.93 (d, 2H, 5-Pz,  $^2J_{\text{HH}} = 2.2\text{Hz}$ ); 7.48 (d, 2H, 3-Pz); 6.40 (s, 2H, 4-Pz). IR (Nujol): 3217  $\text{cm}^{-1}$  ( $\nu_{\text{N-H}}$ ), 1520  $\text{cm}^{-1}$  ( $\nu_{\text{C=N}}$ ). Anal. Calc. for  $\text{C}_6\text{H}_8\text{N}_4\text{PtCl}_2$ : C, 17.92; H, 2.01; N, 13.93%. Found: C, 18.31; H, 1.34; N, 13.84%.

#### 3.3.4 *Cis-dichloro-bis-(3,5-dimethylpyrazole)platinum(II) (4)*.

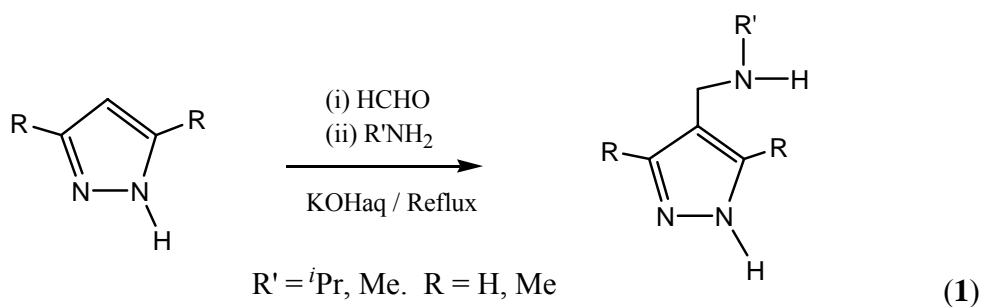
$^1\text{H}$  NMR ( $\text{CDCl}_3$ ):  $\delta$  12.08 (br s, 2H, N-H); 5.75 (s, 2H, 4-Pz); 2.37 (s, 6H, 5-Me); 2.12 (s, 6H, 3-Me). IR (Nujol):  $3210\text{ cm}^{-1}$  ( $\nu_{\text{N-H}}$ ),  $1568\text{ cm}^{-1}$  ( $\nu_{\text{C-N}}$ ). Anal. Calc. for  $\text{C}_{10}\text{H}_{16}\text{N}_4\text{PtCl}_2$ : C, 26.20; H, 3.52; N, 12.23%. Found: C, 26.70; H, 3.16; N, 12.13%.

#### 3.3.5 *Dichloro-bis-((3,5-dimethylpyrazolyl)acetic acid)palladium(II) (5)*

$^1\text{H}$  NMR ( $\text{DMSO-d}_6$ ):  $\delta$  2.31 (s, 6H,  $\text{CH}_3$ , pz); 2.42 (s, 6H,  $\text{CH}_3$ , pz); 5.61 (s, H, CH); 6.04 (s, 2H, pz). IR (Nujol):  $1756\text{ cm}^{-1}$  ( $\nu_{\text{C=O}}$ ),  $3410\text{ cm}^{-1}$  ( $\nu_{\text{O-H}}$ ). Anal. Calc.  $\text{C}_{12}\text{H}_{16}\text{N}_4\text{O}_2\text{PdCl}_2 \cdot 0.5\text{CH}_2\text{Cl}_2$ : C, 32.25; H, 3.23; N, 12.04%. Found. C, 32.27; H, 3.41; N, 12.25%.

### 3.6 Results and discussions

Compounds **L1** – **L3** were synthesized according to equation 1 below by reacting the appropriate pyrazole with formaldehyde and an appropriate secondary amine (either isopropylamine or ethylamine).



The pyrazole ligands e.g. **L3**, were prepared by alkylaminoalkylation of the dimethylpyrazole (eq.1). The formaldehyde-amine mixture under reflux conditions leads to aminomethylation of pyrazole at position 4 resulting in thermodynamically stable

product of the reaction. The product is isolated as an oil. These ligands were found to be soluble in dichloromethane.  $^1\text{H}$  NMR spectrum of the ligand is a spectroscopic evidence of the formation of the new pyrazole. The missing peak at 5.72 ppm of the starting material, 3,5 dimethylpyrazole, confirms substitution in position 4 of the pyrazole. Further presence of  $\text{CH}_2\text{NHR}$  signals at 3.53 ppm supports.

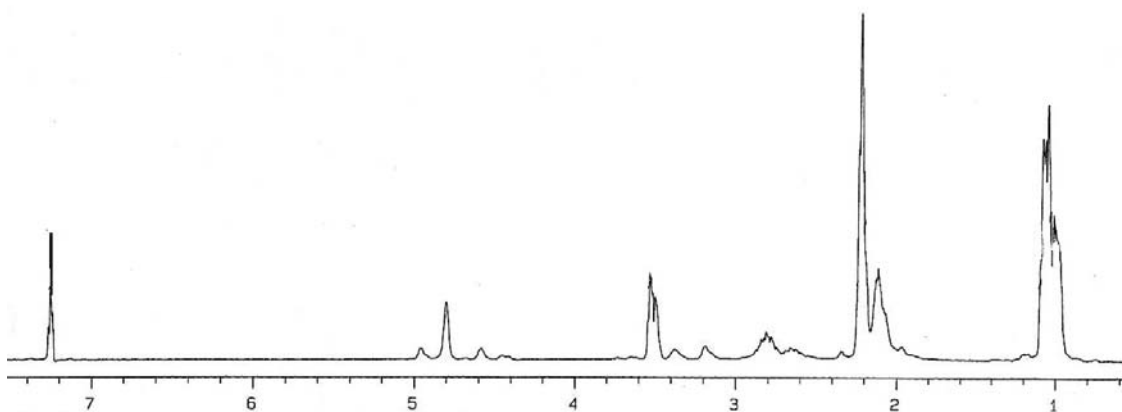


**Figure 3.1.**  $^1\text{H}$  NMR of 3,5-dimethyl-4-(isopropylamino)methylpyrazole (**L3**)

Infrared Spectroscopy was a useful technique in further characterization of the ligands. As most of these ligands were oils, recording of spectra was performed on the neat oil between NaCl plates. For ligand **L3** the most important stretching frequencies to note are the  $\nu(\text{N-H})$  (in the aromatic ring) and  $\nu(\text{N-H} + \text{C-H})$  (in the alkyl chain) (eq. 1) which appeared at 3272 and 2962  $\text{cm}^{-1}$  respectively. The latter frequency confirms the incorporation of the alkylamino chain in position 4 of the parent pyrazole. The stretching frequencies found at 1571 and 1710  $\text{cm}^{-1}$  correspond to  $\nu(\text{C=C})$  and  $\nu(\text{C=N})$  respectively.



The  $\nu(\text{C}=\text{C})$  is a strong sharp band as opposed to  $\nu(\text{C}=\text{N})$  which in this case is moderate though more than often is variable.

The gas chromatography coupled with Mass Spectrophotometer (GC-MS) was run to investigate the purity and subsequently obtain the fragmentation pattern of the ligands. The gas chromatograph (GC trace) of **L3** obtained, indicated 80% purity of the ligand (Fig. 3.2). The mass spectrum of ligand **L3**, obtained from the Mass Spectrometry component of the GC-MS, showed molecular ion peak at  $m/z = 167[\text{HL}]^+$  with a base peak at  $m/z = 109$  (Fig. 3.3) along with other pyrazole fragments.

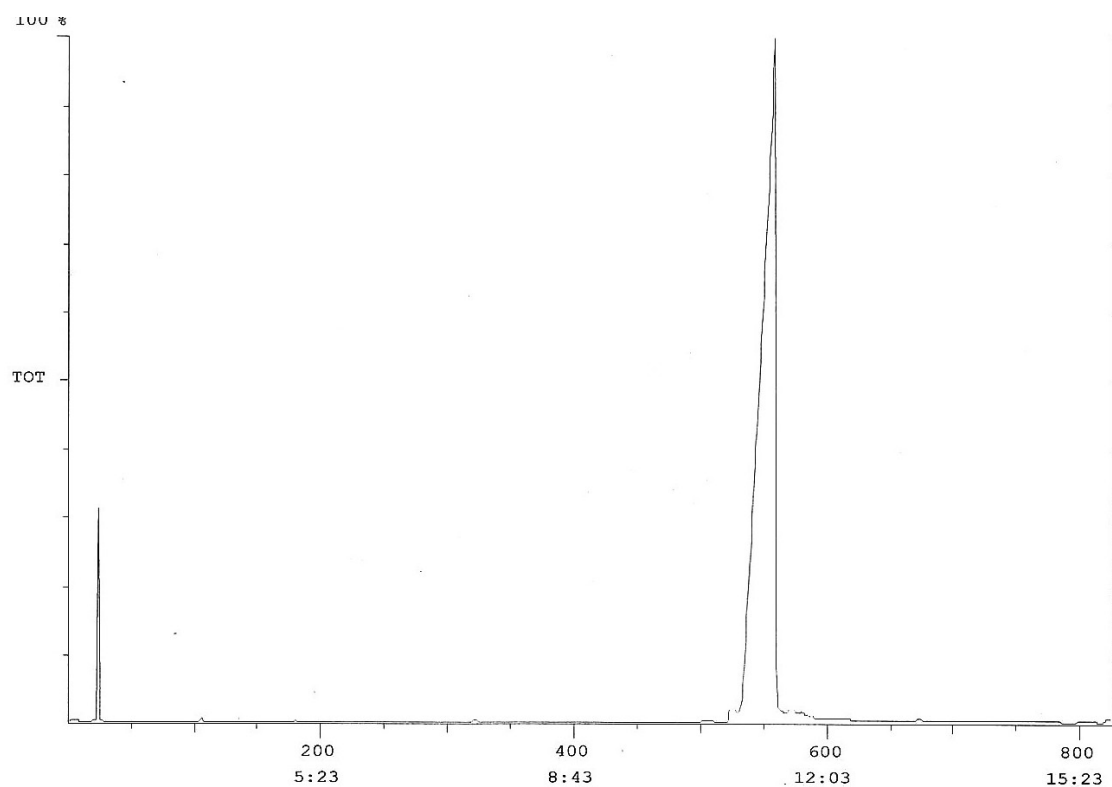


**Figure 3.2** Mass spectrum of ligand, **L3**. This is a typical GC trace obtained for pure compounds.

Fragmentation patterns of the ligands were obtained by mass spectrometry which is coupled with GC component as mentioned above. Normally the mass spectral fragmentation of the compound is found to give a characteristic pattern. Each kind of fragment has a particular ratio of mass to charge, or  $m/z$  value. For most ions, the charge is 1, so that  $m/z$  is simply the mass of the fragment. Thus for ligand **L3** it exhibited a systematic fragmentation pattern (Scheme 1). It gave a molecular ion peak of  $m/z = 167$  with a corresponding base peak (the most intense peak signifying a stable fragment) of  $m/z = 109$ . This corresponds with a methyl-substituted heterocycles that loses a H to produce the corresponding tropylium ions, which are frequently the base peak. Ethyl and higher substituted heterocycles will undergo  $\beta$ -cleavage, losing alkyl and producing a tropylium ion.<sup>7</sup> The fragmentation of the heterocycle rings, which includes pyrazole ring, is as a result of small and stable, neutral molecules, which are analogous to HCN, such as C=NH as well as HC $\equiv$ CH and thus is not discussed herein.

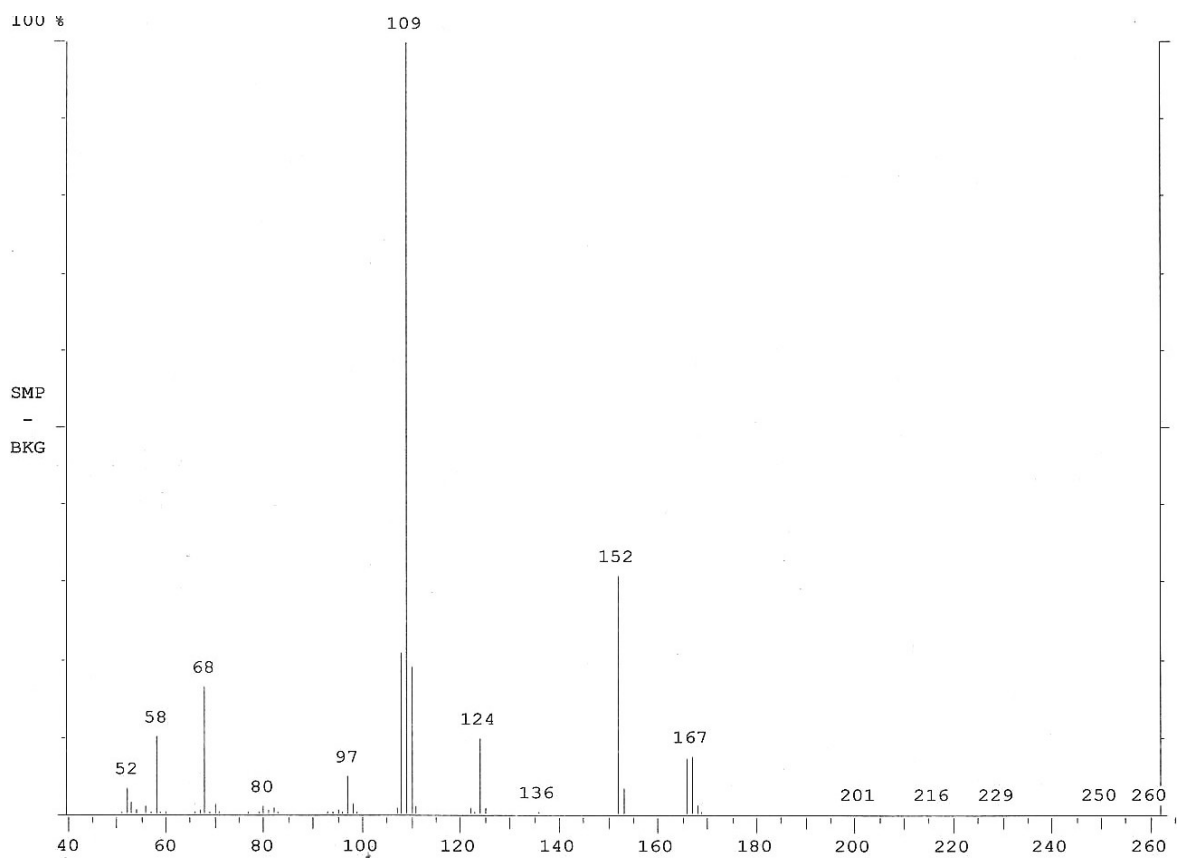
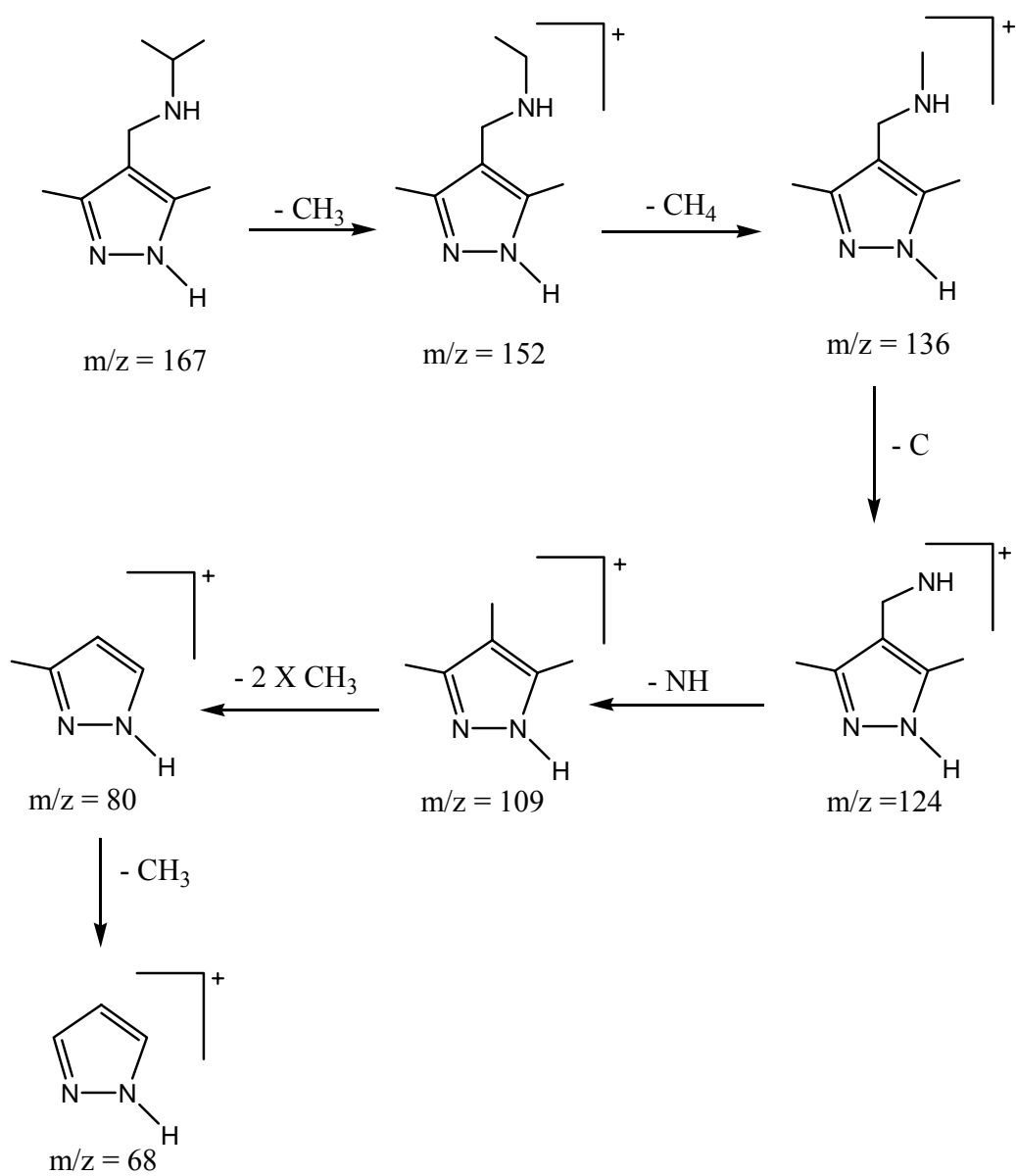
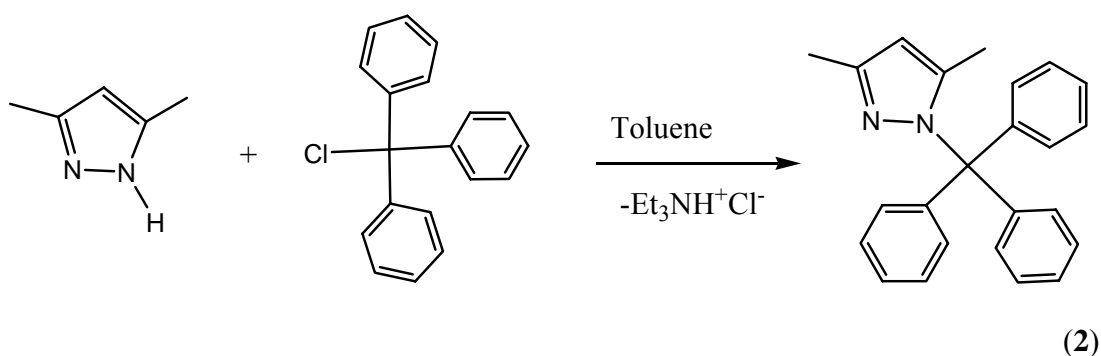


**Figure 3.3.** Mass spectrum of L3.



**Scheme 1.** Fragmentation pattern of L3.

The pyrazole ligand **L4** was prepared by reacting the two starting material. The product isolated was a brown solid. It is very soluble in organic solvents e.g. dichloromethane. These were efforts to establish another synthetic route other than the *in situ* synthesis that was used. Our hypothesis was that, with the new route we would improve both the yields and purity. This was also to avoid the possibility of obtaining side reaction product i.e. 3,5-dimethyl-1-(isopropylamino)methylpyrazole instead of 3,5-dimethyl-4-(isopropylamino)methylpyrazole, which was the desired product. This was achieved by protecting position 1 of the parent pyrazole with triphenylchloromethane (eq. 2). The  $^1\text{H}$  NMR spectrum of the ligand gave an indication of the formation of the new ligand. The peaks at  $\delta$  2.23 and 1.45 ppm (Fig. 3.4) shows that as opposed to the 3,5-dimethylpyrazole parent ligand where protons of both methyl groups resonate at same frequency, those of the new ligand synthesized resonate at different frequency suggesting different chemical environments.



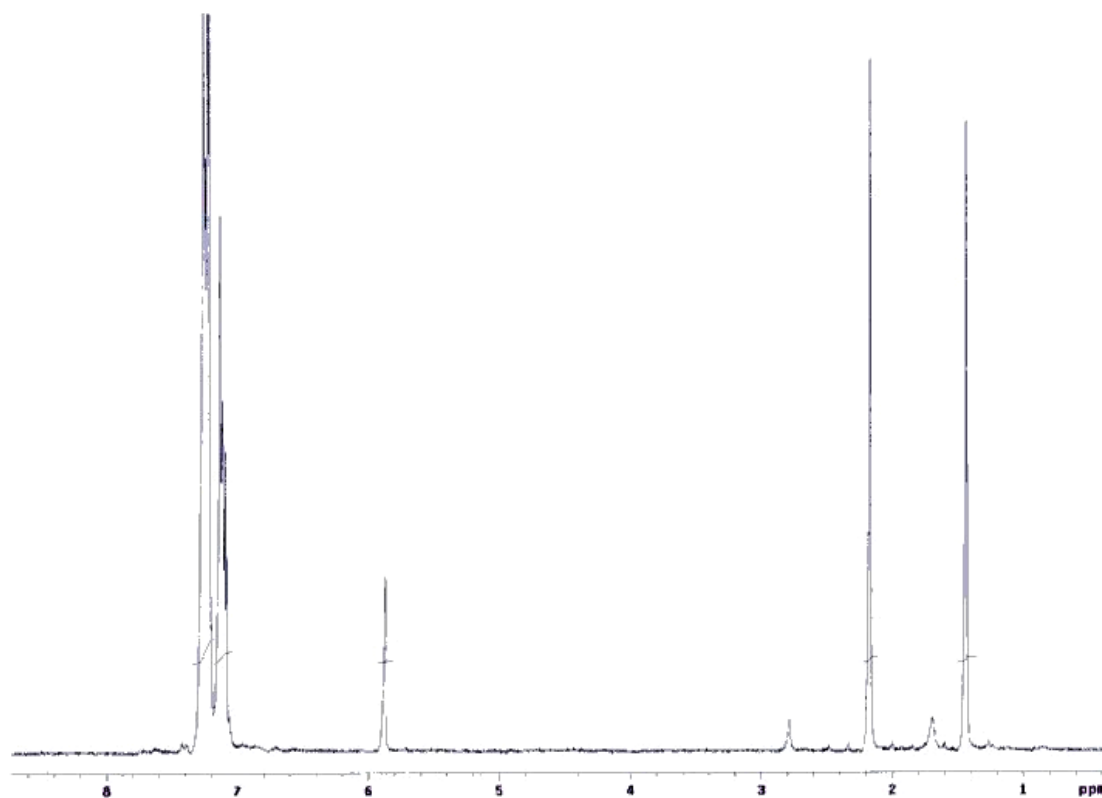


**Figure 3.4.**  $^1\text{H}$  NMR spectrum of 1N-triphenylchloromethane-3,5-dimethylpyrazole.

Infrared spectroscopy of **L4** revealed the stretching frequencies of the functional groups present together with those of the phenyl rings. They were found at  $1701\text{ cm}^{-1}$  for  $\nu(\text{C}=\text{N})$  and  $1550\text{ cm}^{-1}$  for  $\nu(\text{C}=\text{C})$ . The stretching frequencies of the protons in the phenyl rings,  $\nu(\text{C}-\text{H})$  were significant at  $2800\text{-}3000\text{ cm}^{-1}$  accompanied by the strong bending frequencies at  $696\text{-}886\text{ cm}^{-1}$ . Of interest was the absence of  $\nu(\text{N}-\text{H})$  frequency at ca.  $3200\text{ cm}^{-1}$  suggesting full derivatization of the parent pyrazole.

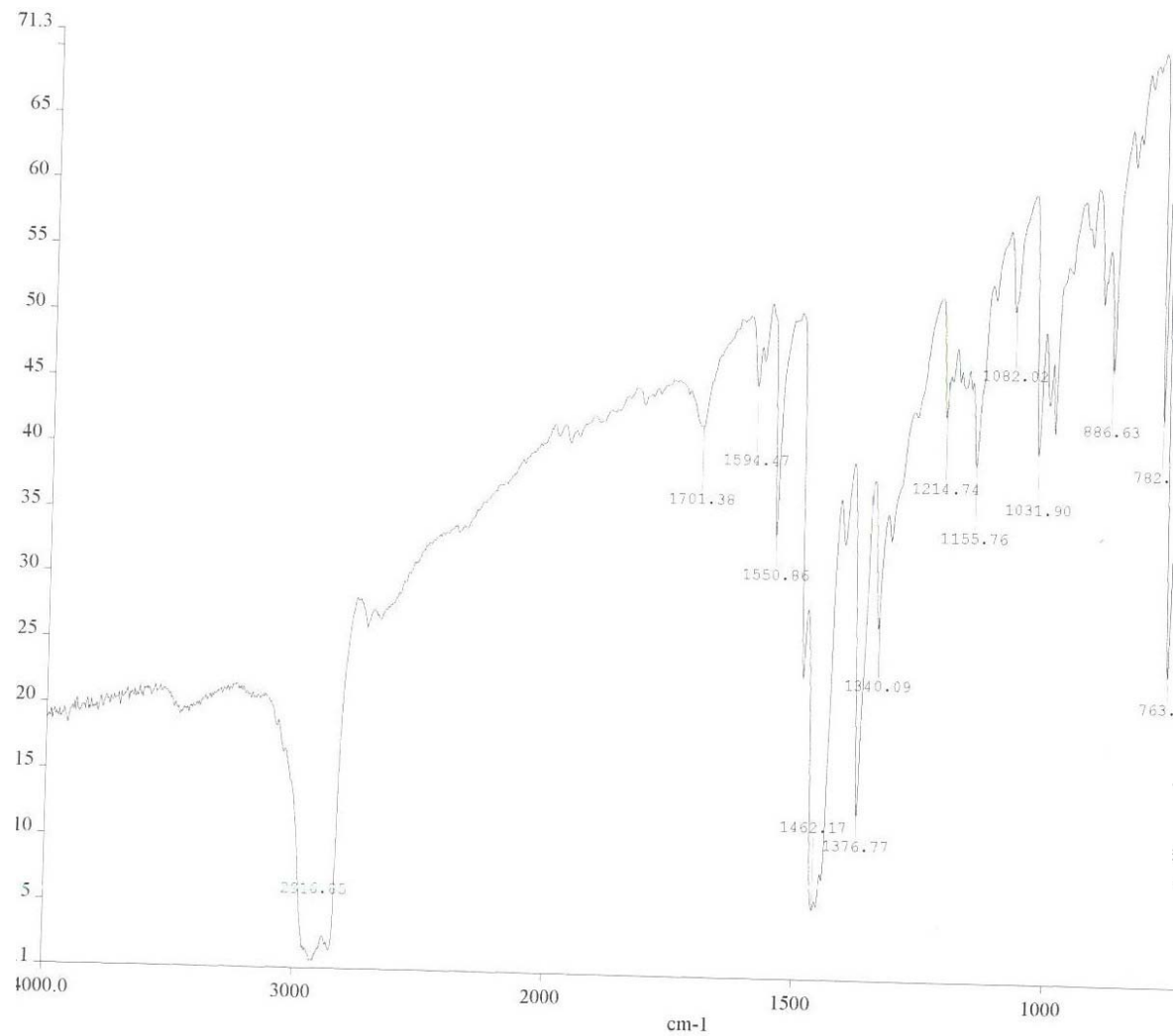


**Figure 3.5.** IR spectrum of L4.

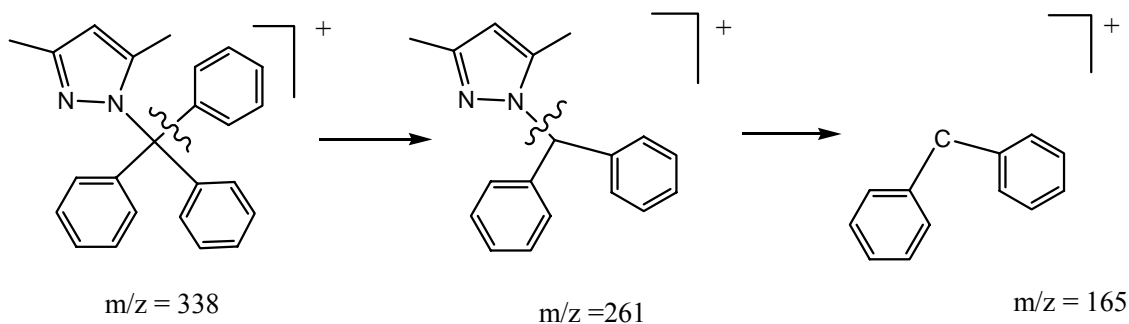


**Figure 3.6.** One possible fragmentation pattern of **L4**.

The fragmentation pattern of ligand **L4** was obtained in the same way as described for **L3**. It exhibited a molecular ion peak at  $m/z = 338$  and base peak at  $m/z = 165$ . The fragmentation pattern involved the loss of a benzene ring first with a subsequent loss of the other two rings as shown in (Fig. 3.6). This showed that the attachment of the phenyl rings to the pyrazole through a tertiary carbon is not that stable. However it is observed that the fragment having two phenyl rings attached to a carbon with an  $m/z$  value of 165 (Fig 3.6) becomes the stable fragment in agreement with the fact that the phenyl rings are the metastable ions of the ligand.<sup>7</sup>

Attempts to use ligand **L4** to obtain compound **L3** as an alternative route were unsuccessful as there was an immediate formation of suspension, which was not the desired product. This was attributed to the disintegration of **L4** back to its starting material due to the reaction being performed under reflux conditions ( $100^{\circ}\text{C}$ ) which surpassed its conditions of synthesis ( $80^{\circ}\text{C}$ ).



### 3.7 Molecular structure of L3

Single crystals of the above mentioned ligand suitable for X-ray structural analysis were obtained from recrystallization of the ligand from dichloromethane and hexane at room temperature. The molecular structure, ORTEP, of the ligand is shown in Figure 3.7. Crystal data, together with the data collection and refinement parameters are presented in Table 3.1. Selected bond lengths and angles are given in Table 3.2.

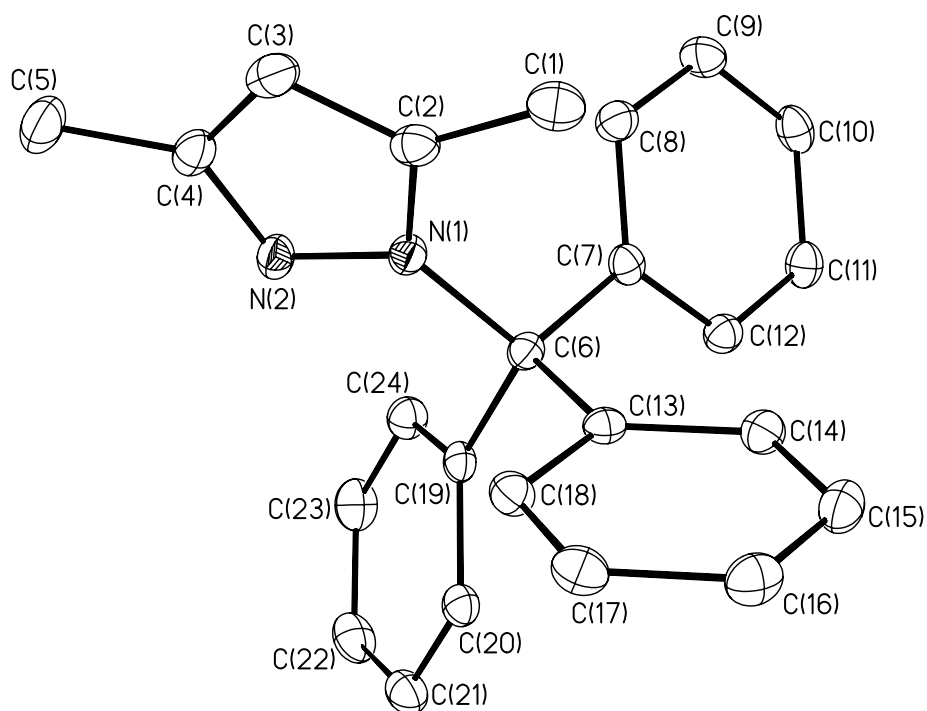


**Figure 3.7.** Molecular structure of compound L4.

**Table 3.1.** Crystal data and structure refinement for **L4**

---

Empirical formula	C <sub>24</sub> H <sub>22</sub> N <sub>2</sub>	
Formula weight	338.44	
Temperature	100(2) K	
Wavelength	0.71073 Å	
Crystal system	Monoclinic	
Space group	P2 <sub>1</sub> /c	
Unit cell dimensions	a = 9.5264(5) Å	α = 90°.
	b = 8.6992(4) Å	β = 93.961(1)°.
	c = 21.9714(11) Å	γ = 90°.
Volume	1816.47(16) Å <sup>3</sup>	
Z	4	
Density (calculated)	1.238 Mg/m <sup>3</sup>	
Absorption coefficient	0.072 mm <sup>-1</sup>	
F(000)	720	
Crystal size	0.41 x 0.27 x 0.19 mm <sup>3</sup>	
Theta range for data collection	2.14 to 26.39°.	
Index ranges	-11 ≤ h ≤ 11, -10 ≤ k ≤ 10, -27 ≤ l ≤ 27	
Reflections collected	14683	
Independent reflections	3708 [R(int) = 0.0392]	
Completeness to theta = 26.39°	99.8 %	
Absorption correction	Multi-scan with SADABS	

Max. and min. transmission	0.9864 and 0.9709
Refinement method	Full-matrix least-squares on F <sup>2</sup>
Data / restraints / parameters	3708 / 0 / 237
Goodness-of-fit on F <sup>2</sup>	1.031
Final R indices [I>2sigma(I)]	R1 = 0.0349, wR2 = 0.0906
R indices (all data)	R1 = 0.0420, wR2 = 0.0950
Largest diff. peak and hole	0.293 and -0.244 e.Å <sup>-3</sup>

---

**Table 3.2.** Selected bond lengths [Å] and angles [°] for **L4**

---

Bond lengths [Å]		Bond angles [°]	
N(1)- C(2)	1.3673(14)	N(1)-C(6)-C(7)	110.07(8)
N(1)- N(2)	1.3690(13)	N(1)-C(6)-C(13)	106.17(8)
N(1)- C(6)	1.4950(13)	N(1)-C(6)-C(19)	109.44(8)
N(2)- C(4)	1.3299(15)	N(2)-N(1)-C(6)	120.34(9)
C(1)-C(2)	1.4914(17)	C(2)-N(1)-N(2)	111.75(9)
C(6)-C(7)	1.5425(15)	C(2)-N(1)-C(6)	127.80(9)
C(6)-C(13)	1.5430(14)	C(7)-C(6)-C(19)	107.23(8)
C(6)-C(19)	1.5472(15)	C(13)-C(6)-C(19)	110.91(8)
C(7)- C(12)	1.3948(16)		

---

The molecular geometry around the achiral carbon (C6) is tetrahedral. 3,5-dimethylpyrazole and phenyl groups in this compound, possess a delocalized  $\pi$ -system with the preferred ring being the parent pyrazole. In this case the structure is found to belong to  $T_d$  group because of the identical phenyl rings not residing in the same plane as the parent pyrazole, leading to the steric repulsions being minimized. The bond angles between the substituents to the achiral carbon were found to be  $107.23(8)^\circ$  and  $110.91(8)^\circ$  for C(7)-C(6)-C(19) and C(13)-C(6)-C(19) respectively. The bond angles of N(1)-C(6)-C(19), N(1)-C(6)-C(13) and N(1)-C(6)-C(7) were found to be  $109.44(8)^\circ$ ,  $106.17(8)^\circ$  and  $110.07(8)^\circ$  suggesting a slight distortion of its geometry from conventional angle of  $109.5^\circ$ .<sup>8</sup> The presence of phenyl rings imparts some steric hindrance and hence leading to that slight distortion of the geometry. This again shows that the more bulky the molecule, the further its geometry distortion. The bond distances, N(1)-C(2), N(1)-N(2), and N(2)-C(4) were found to be  $1.3673(14)$  Å,  $1.3690(13)$  Å and  $1.3299(15)$  Å respectively and are not significantly different from those reported by Llamas *et al.*<sup>9</sup> which are in the range of  $1.3450(20)$ - $1.3230(30)$  Å. The other bond distances C(6)-C(7), C(6)-C(13) and C(6)-C(19) were found to be between  $1.5425(15)$  Å and  $1.5472(15)$  Å but longer than N(1)-C(6) ( $1.4950(13)$  Å) suggesting that the phenyl rings were further away from the parent pyrazole. The C=N bond, N(2)-C(4), was found to be shorter than C-N bond, N(1)-C(2), by  $0.0374$  Å signifying that the bond strength involved in the former is higher.

The synthesis of palladium(II) and platinum(II) complexes using ligands **L1-L3** performed. However most of the resulting complexes turned out to be insoluble in most common solvents and therefore could not be characterized fully. The IR data revealed

stretching frequencies at 3349, 1712 and 1666  $\text{cm}^{-1}$  corresponding to  $\nu(\text{N=H})$ ,  $\nu(\text{C=C})$  and  $\nu(\text{C=N})$  respectively. The microanalysis data obtained for **C1** were found to be slightly higher than expected with percentage calculated carbon content, C being 36.90 while found was 37.81. Nevertheless these data were found to be within reasonable values for the proposed formula of  $\text{ML}_2\text{X}_2$ . However it must be pointed out that these data is not conclusive.

The Figures 3.8-3.10 below shows the typical  $^1\text{H}$  NMR and IR spectra of the complexes, **1-5**, that were investigated for their biological activity.

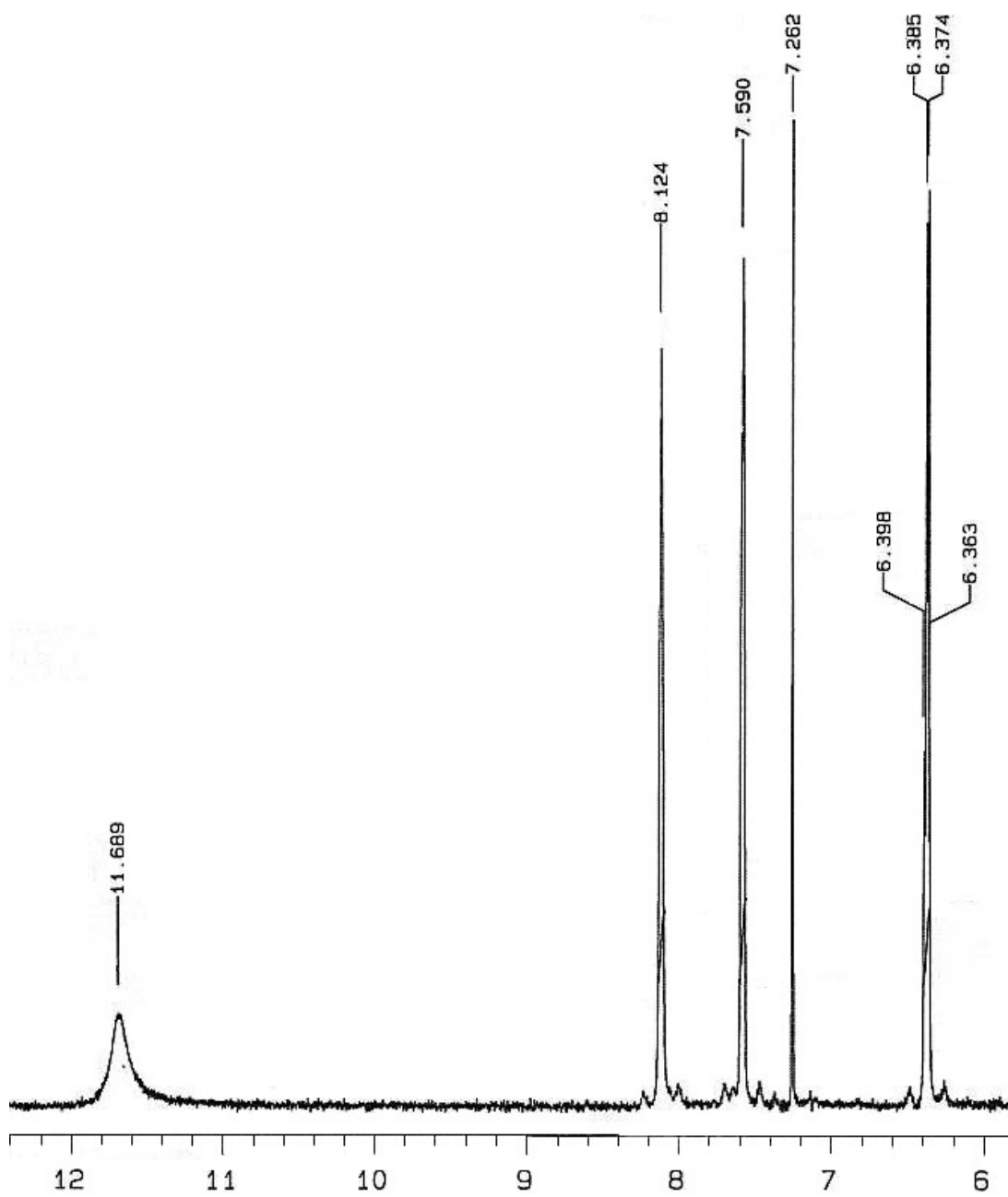


**Figure 3.8.** <sup>1</sup>H NMR spectrum of compound 1.

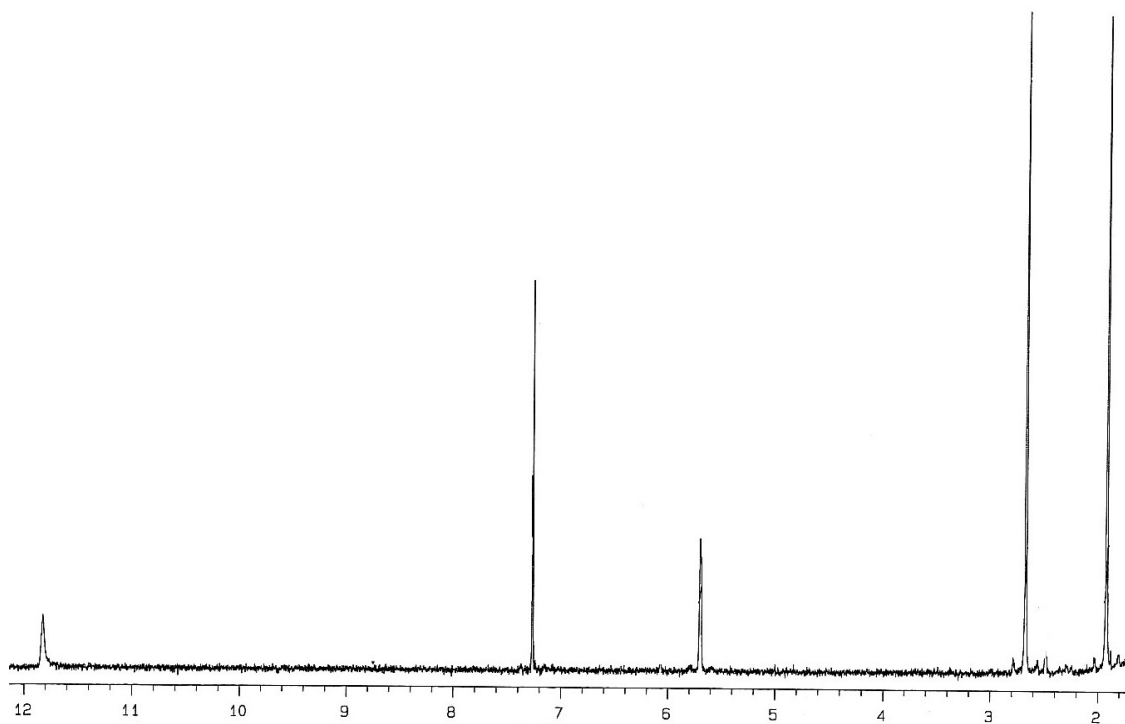


**Figure 3.9.**  $^1\text{H}$  NMR spectrum of compound 2.

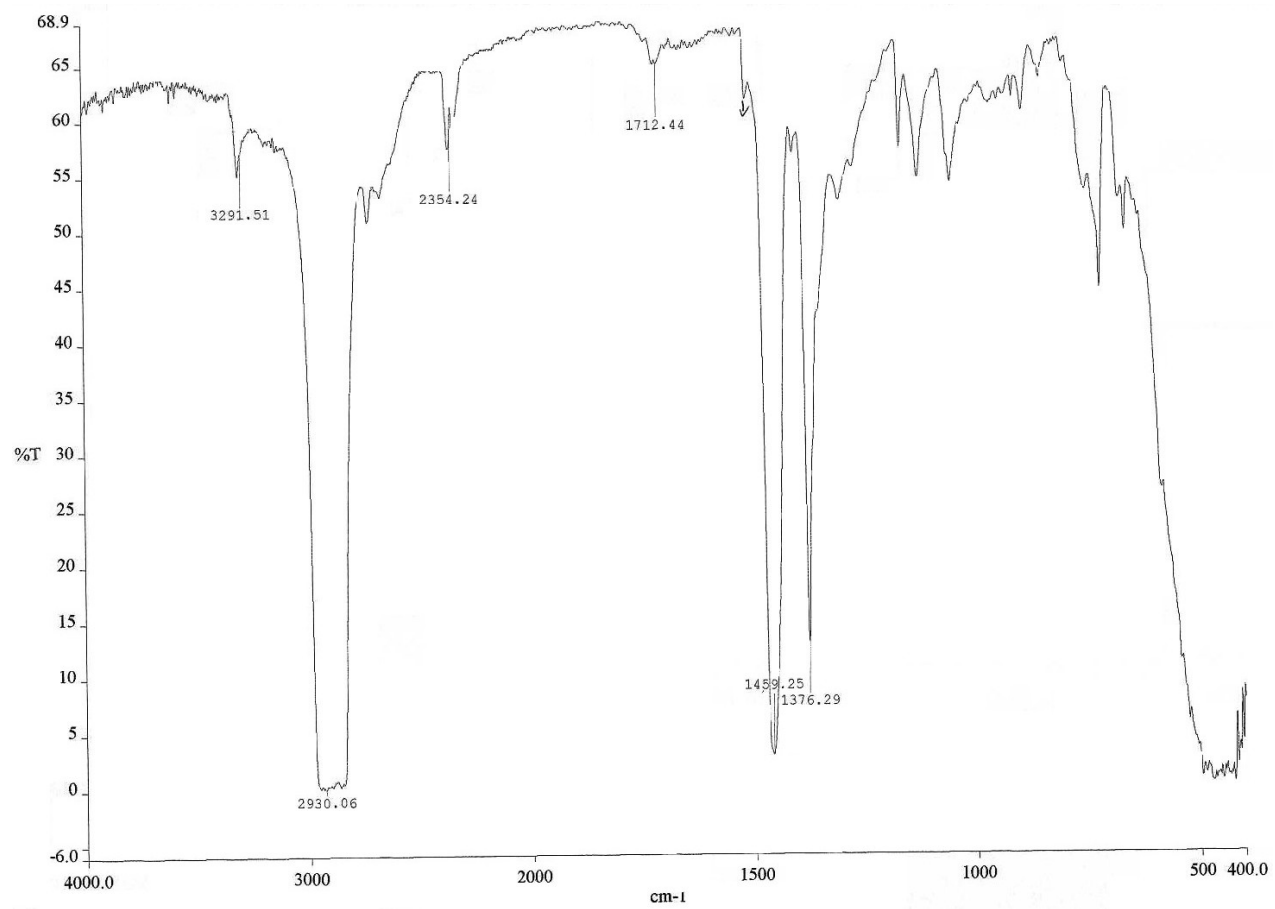


**Figure 3.10.** IR spectrum of compound 1.



### 3.8 Conclusion

Ligands **L1**, **L3** were prepared as per the reported methods and obtained in high yields, between 71-87%. In all instances they were isolated as clear oils. Attempts to use compound **L4** as a starting material in the synthesis of **L2** and **L3** were unsuccessful. This is attributed to the instability of **L4** at higher temperatures as synthesis of the former two ligands involved high temperature reflux conditions. All these compounds were characterized by a combination of analytical techniques,  $^1\text{H}$  and  $^{13}\text{C}$  NMR spectroscopy, Infrared (IR) spectroscopy, together with microanalysis in some cases. They were all found to be soluble in polar solvents, especially chlorinated organic solvents.

Despite these type of ligands having been used to synthesise pyrazolate rhodium(I) complexes as reported by Gloria *et al.*<sup>10</sup>, our efforts to synthesis the palladium and platinum analogues with a target of obtaining square planar, water soluble complexes were futile as the products obtained were insoluble solid products (yellowish in colour) and therefore could not be fully characterized. We could only postulate that the desired complexes were formed. However, it must be pointed out that the microanalysis data found were higher than expected in some cases. Nevertheless other palladium and platinum complexes, **1-5**, were successfully synthesized and fully characterized. They were obtained in moderate yields. The dichloropalladium complexes were soluble in common chlorinated organic solvents while dichloroplatinum complexes were soluble mostly in DMSO.

### 3.9 References

1. Fatma G., Oztekin A., Gokcen E., Hatice E., *Eur. J. Med. Chem.* 38 (2003) 473.
2. Chao T., Xuefeng W., Qin L., Xiaoyong W., Qiang X., Zijian G., *Inorg. Chim. Acta* 357 (2004) 95.
3. Reedijk J., *Inorg. Chim. Acta* 198 (1992) 873.
4. Li K., Darkwa J., Guzei I. A., Mapolie S. F., *J. Organomet.* 660 (2002) 108.
5. Sakai K., Yasushi T., Takuma U., Koji G., Masakatsu O., Taro T., Kazuko M., Kenji O., Kazuyuki K., *Inorg. Chim. Acta* **297** (2000) 64.
6. Moradell S., Julia L., Ana R., Marc S. R., Francesc X. A., Virtudes M., Rafael de Llorens, Angeles M., Reedijk J., Antoni L., *J. Inorg. Biochem.* 96 (2003) 493.
7. Baker J. *Mass Spectrometry*, 2<sup>nd</sup> Ed. 2000, John Willey & Sons Publishers, New York, p. 287.
8. Shriver D. F., Atkins P. W., Langford C. H., *Inorganic Chemistry*, 2<sup>nd</sup> Ed. 1994, Oxford University Press, Oxford, p. 121.
9. Llamas A. L., Foces-Foces C., Fontenas C., *Molecules*, 2 (1998) 76.
10. Gloria E., Josefina P., Ramon Y., Josep R., Xavier S., Merce F., *J. Organomet.* 605 (2000) 226.

## Chapter 4

### EVALUATION OF PALLADIUM AND PLATINUM COMPLEXES AS ANTICANCER AGENTS AND OTHER EXPERIMENTS.

#### *4.1 Introduction*

Since the discovery of the anticancer activity of cisplatin several new platinum complexes have been synthesized and tested for biological activity. Although the precise mechanism underlying antitumour action of platinum drugs is not completely understood, they are known to bind to DNA primarily by forming bifunctional adducts.<sup>1</sup> Currently there are a number of successful metallopharmaceuticals, which include carboplatin and iproplatin, for cancer treatment, indicating the utility of metal complexes as therapeutic agents. The potential antitumour activity of platinum group metal complexes is well understood. However, some tumours are resistant to treatment with cisplatin, thus there is a need to develop novel metal containing drugs, to treat this disease.

In an attempt to broaden the medical applications of such compounds, five complexes, containing either palladium or platinum, were investigated preliminarily for their activity in chinese hamster ovary (CHO) and normal human fibroblast (NHF) cell-lines. The morphological changes observed 24 h after treatment of CHO and NHF cells with the compounds showed that the treated cells reduced in volume significantly without membrane breakage. Further bio-assay performed on CHO cells indicated that the effect was both dose and time dependent.

## **4.2 Biological tests**

### *4.2.1 Cell culture and drug treatment*

CHO, NHF, MG, HeLa and Jurkat cell-lines were used in the study. The CHO cells were cultured in Hams F-12 medium containing, L-glutamine, 5% foetal calf serum (FCS) and 0.2% v/v streptomycin-penicillin at 37 °C in a humidified 5% CO<sub>2</sub> atmosphere.<sup>2</sup> The exponentially growing cells were harvested from a 25 cm<sup>2</sup> culture flask by means of trypsinisation and the cells were recovered by centrifugation. The cell pellet was re-suspended in Hams F-12 medium and the resulting cell suspension seeded at a cell density of  $2.5 \times 10^4$  cells per well in 6- well tissue culture plates and incubated for 24 h at the above conditions. Compounds to be tested were dissolved in water (or DMSO in some cases) and added to media to make a final concentration ranging from 0.02 to 1 mM. In all instances, cells supplied with media i.e. without compounds was used as the negative control (untreated cells) while cells treated with *cis*-dichlorodiammineplatinum(II) complex (cisplatin) were analysed as the positive control. Reaction of some complexes with glutathione (GSH) was achieved by mixing the (reactants) in a stoichiometric ratio of 1:2, (Pt(II):GSH) as reported in the literature<sup>3</sup> with DMSO-*d*<sub>6</sub> as the solvent.

### *4.2.2 Evaluation of cell death and apoptosis*

In most instances the treated cells were incubated for 24 h except for the time-course experiments. In the case of time course experiments, the cells were treated for different times, i.e. 0, 6, 12, and 24 h. The cells were then washed twice afterwards using PBS (phosphate buffered saline) and the cells stained for 1 h using APOPercentage<sup>TM</sup> dye

according to the supplier's instruction. The effect of the compounds on the cells (dose response), and the dye up-take by the cells were evaluated by both light microscopy and Fluorescence Activated Cell Sorting (FACS) techniques.

#### *4.2.3 Evaluation of cell cycle arrest using acridine orange*

The cells were treated and incubated as described in the above sections. After washing with PBS, the cells were trypsinised. The cells were centrifuged to obtain a pellet, which was then re-suspended in media. Then 0.1 mL of the cells in suspension were stained using acridine orange according to the suppliers' instruction. The cells were evaluated within 30 min. of staining using FACS techniques.

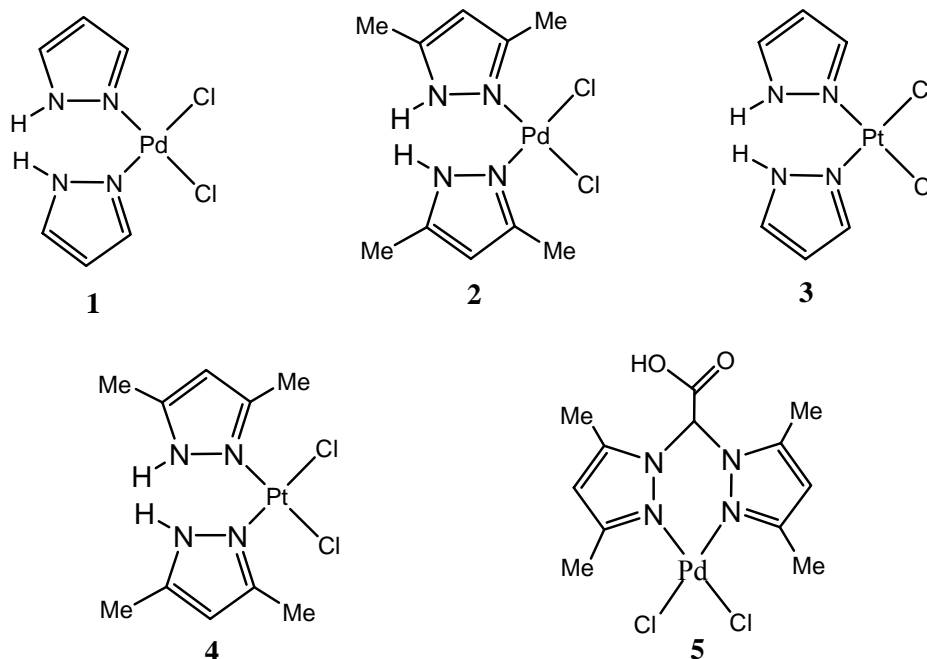
#### *4.2.4 DNA fragmentation*

For DNA fragmentation analysis,  $2.5 \times 10^4$  cell/mL were plated in six well plates. The cells were exposed to various concentrations of compounds **3** and **5** for 24 h. After treatment the cells were harvested by trypsinisation. The DNA was extracted using reported literature protocol.<sup>4</sup> The DNA was electrophoresed on a 2% agarose gel at 100 V for 1 h. The DNA was visualized by ethidium bromide staining and photographed under UV illumination.

### ***4.3 Dichloro-bis-(pyrazole)platinum(II)-glutathione, 1:2 reaction***

Complex **3** (0.010 g, 0.025 mmol) was transferred to an NMR tube and dissolved upon addition of DMSO-*d*<sub>6</sub> (0.500 ml) giving a clear yellowish solution. Glutathione (0.015 g, 0.050 mmol) was then added to this solution. Immediately there was a formation of suspension which disappeared with time to leave a clear yellowish solution. The reaction was monitored over a period of 18 h by <sup>1</sup>H NMR spectroscopy.

#### 4.4 Results and discussion



**Scheme 4.1.** Structures of compounds **1-5** that have been evaluated for their apoptotic activity.

##### 4.4.1 Morphological changes

CHO and NHF cells were exposed to various concentrations of the compounds **1-5** being investigated (section 4.2.1). The morphological changes observed showed that there was a reduction in size i.e. cell volume of the treated cells over a period of 24 h (Fig. 4.1). In addition, the decrease in cell volume was accompanied by a loss of contact with neighbouring cells as the apoptotic cells shrank and became detached from the adjacent cells. Upon staining with APOPercentage dye, the treated cells exhibited dye uptake while the negative controls (untreated cells) did not. This is a characteristic feature shown by cells dying via apoptosis. This observation is supported by the fact that cells

undergoing apoptosis, have their phosphatidylserine (PS) translocated by the enzyme flippase leading to its expression externally.<sup>5</sup> As a result, the PS trans-membrane movement as proposed by ‘flip-flop’ mechanism results in the uptake of the dye.

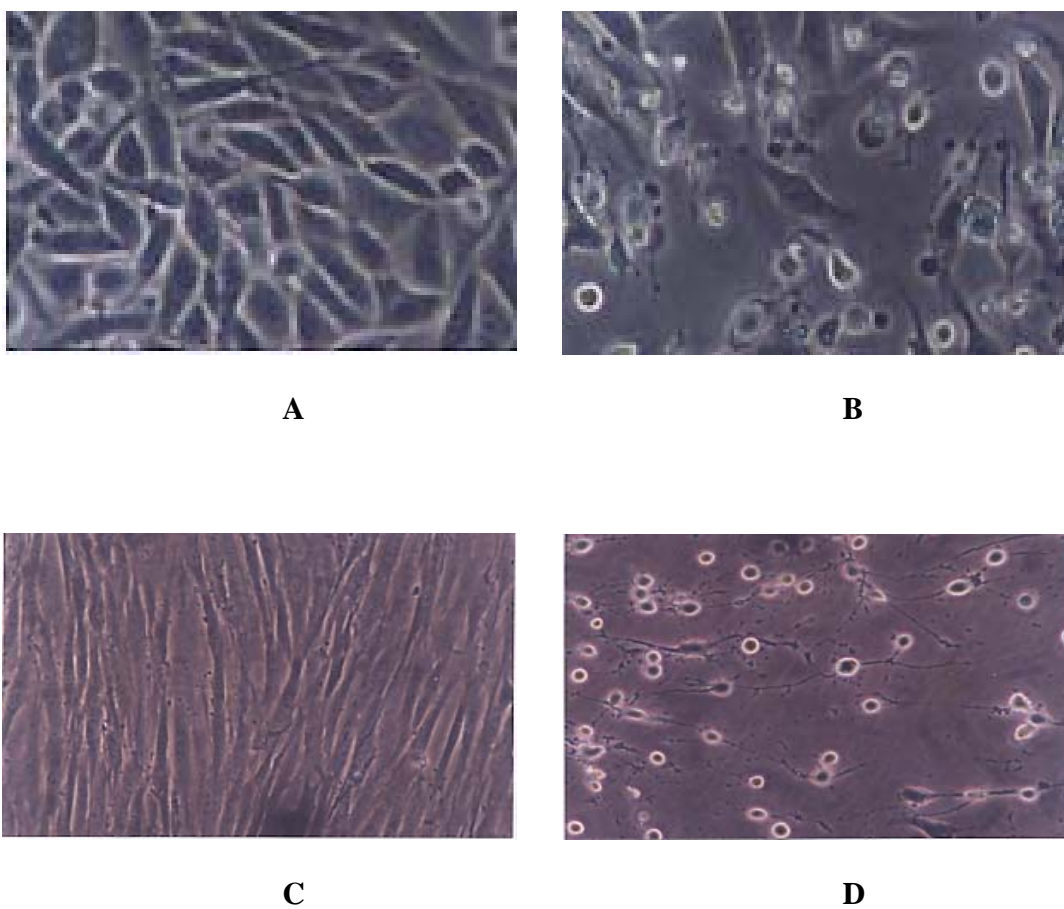
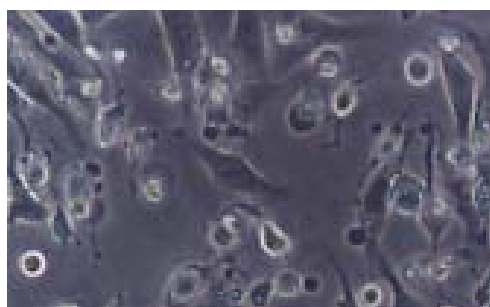


**Figure 4.1.** The morphological effects exerted by complexes on CHO and NHF cells respectively 24 h after treatment. Photographs were taken (before staining) using a Nikon inverted light microscope (20X Objective). **A** and **C** shows the untreated cells (CHO and NHF respectively) while **B** and **D** shows cells treated with 0.5 mM of compound **3** and 1 mM of compound **5** respectively.

In addition, the visible cell shrinkage observed was due to the net movement of fluid out of the cell as a result of inhibition of Na-K-Cl coupled transporter system which controls the cell volume by maintaining the osmotic balance inside and outside the cells at all times<sup>6</sup> (see Figures 4.1 and 4.2).



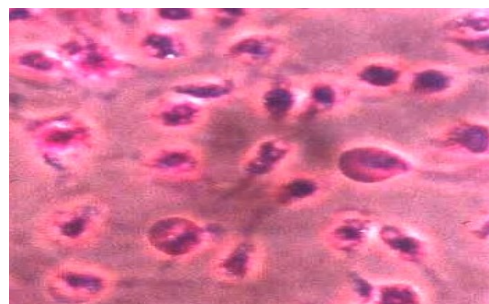
**E**



**F**



**G**



**H**

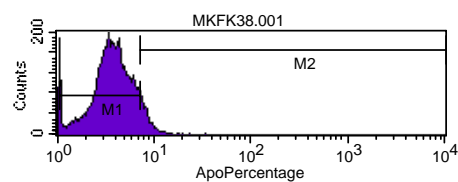
**Figure 4.2.** Photographs of treated and untreated CHO cells, APOP dye staining. The photographs show morphological effects exerted by complexes on CHO cells 24 h after treatment with complex **3** (0.5 mM). **E** and **F** show untreated and treated cells before staining while **G** and **H** show the untreated and treated (same) cells after staining. Only the treated cells stained positive with APOP dye (**H**).



#### 4.4.2 Concentration effect on the cell death, dose response

The preliminary antiproliferative activity of the palladium(II) and platinum(II) complexes synthesized were determined on CHO cell-line. The cells were incubated for 24 h with various concentrations of the compounds, ranging from 0 to 1 mM and using cisplatin as the reference. Five complexes were screened for their cytotoxicity on CHO cells, and evaluated for whether or not their cytotoxicity was by apoptosis (programmed cell death). The percentage of cell death due to the treatment with these complexes was evaluated in terms of APOPercentage<sup>TM</sup> dye uptake by the cells using FACS analysis (Fig. 4.3).

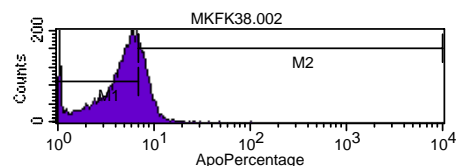
From the observation made, complexes **3**, **4** and **5** induced apoptosis significantly. In all the cases, drug treatment in the concentration range between 0 and 1 mM resulted in a dose dependent inhibition of the cell survival (Fig. 4.4). From the IC<sub>50</sub> (concentration of compound needed to inhibit cell growth by 50% against a single cell line) values obtained (Table 4.1), it clearly indicated that platinum compounds were more effective compared to palladium compounds. Complex **3** and **4** showed activity at IC<sub>50</sub> of 0.120 and 0.035 mM respectively. Complex **5** induced a 50% decrease in cell population (IC<sub>50</sub>) at 0.67 mM while the other two palladium compounds **1** and **2** showed no significant activity (Fig. 4.6). At 0.05 mM, complex **3** were found to induce apoptosis to a percentage of approximately 26% while complex **5** induced a cell death of up to ca. 22% at 0.5 mM. The difference here is attributed to the nature of the metal used. In this case platinum containing compound **3** was more active than the palladium containing compound **5** as mentioned above.



File: MKFK38.001

Untreated cells

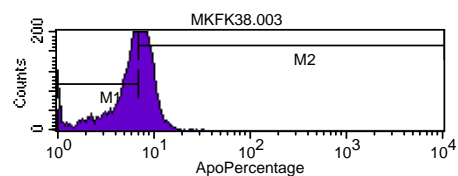
Marker	% Gated	% Total
All	100.00	100.00
M1	91.79	91.79
M2	8.21	8.21



File: MKFK38.002

Treated cells (0.05 mM)

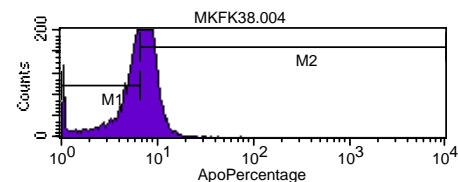
Marker	% Gated	% Total
All	100.00	100.00
M1	73.94	73.94
M2	26.06	26.06



File: MKFK38.003

Treated cells (0.10 mM)

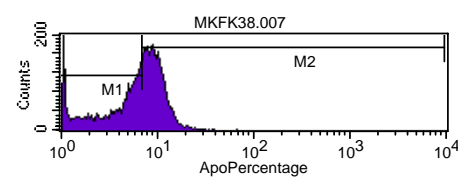
Marker	% Gated	% Total
All	100.00	100.00
M1	54.53	54.53
M2	45.47	45.47



File: MKFK38.004

Treated cells (0.15 mM)

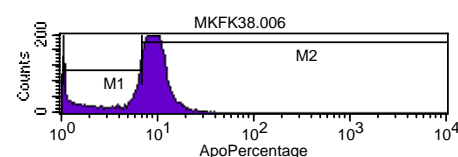
Marker	% Gated	% Total
All	100.00	100.00
M1	48.00	48.00
M2	52.00	52.00



File: MKFK38.007

Treated cells (0.20 mM)

Marker	% Gated	% Total
All	100.00	100.00
M1	47.18	47.18
M2	52.82	52.82



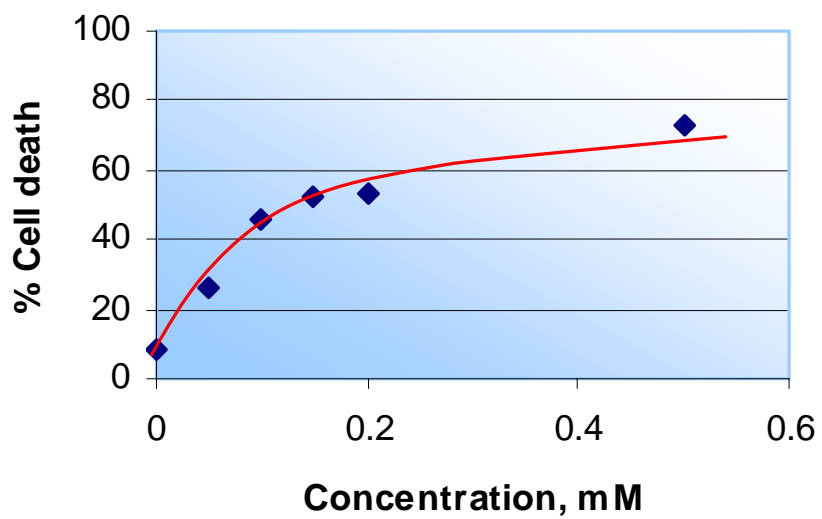
File: MKFK38.006

Treated cells (0.50 mM)

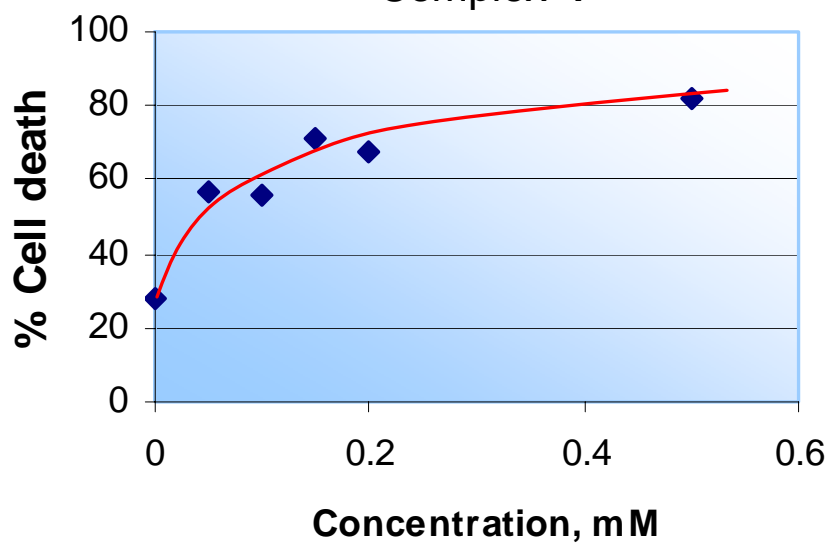
Marker	% Gated	% Total
All	100.00	100.00
M1	27.30	27.30
M2	72.70	72.70

**Figure 4.3.** FACS Analysis. Typical acquisition histograms obtained by FACS when quantifying the amount of live and dead cells. Cells in M1 are live cells while those in M2 are dead cells. Complex **3** was administered to the CHO cells for 24 h. The cells were washed with PBS and stained with APOP dye for 1 h as described in the text. The above histograms show concentration dependence of the cell death.

Complex 3



Complex 4



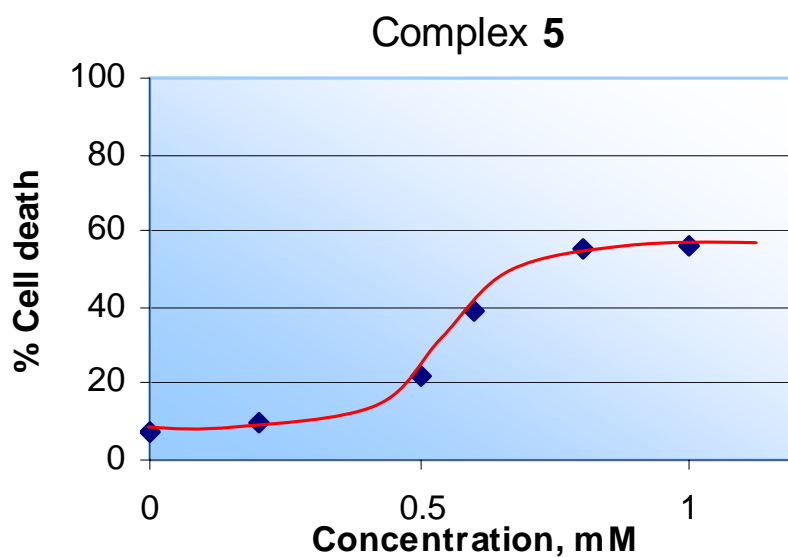


**Figure 4.4.** Graphical representation of concentration-dependent effect of the compounds **3**, **4**, and **5** on the treated CHO cells (24 h) respectively. The data was obtained by performing APOPercentage™ assay. The graphs show that increase in concentration of the compounds being tested causes an increase in cell death (by apoptosis).

**Table 4.1.** IC<sub>50</sub> values (mM) for the complexes tested in CHO cells (n.d. not detected)

Complex	IC <sub>50</sub>
<b>1</b>	n.d
<b>2</b>	n.d
<b>3</b>	0.12
<b>4</b>	0.035
<b>5</b>	0.67

The same observation was made when the activities of **2** and **4** were compared. The two complexes have the same ligand, 3,5-dimethylpyrazole, coordinated in a monodentate fashion but to different metals. Complex **4** induced a significant cell death of 57% at 0.5 mM compared to **2** which did not induce any significant cell death at the same concentration. This again serves to show the superiority of platinum complexes over palladium complexes. Despite palladium and platinum being elements of the same group and that their ionic radii are nearly the same as a result of lanthanoid contraction, their respective pyrazolic complexes exhibited varied activities with platinum compounds showing higher activity than palladium compounds. This observation is attributed to the associative substitution mechanism of the respective complexes suggesting that their kinetic behaviour is quite different even though they show similar coordinative behaviour.<sup>7</sup> Thus palladium complexes are less kinetically stable and as a result could undergo translabilization and undesired displacement of the non-leaving ligand by other nitrogen donors easily (especially those coordinated in a monodentate fashion) whereas platinum compounds are known to be kinetically inert. This implies that palladium compounds are not stable and therefore in the cellular environment will be translabilized easily by other biomolecules such as GSH and hence reacting to give other intermediates hence hindering it from forming the palladium-DNA adducts.

However, palladium compound **5** showed moderate activity compared to other palladium complexes. It exhibited an  $IC_{50}$  value of 0.67 mM. The percentage apoptotic cells increased with increase in concentration and reached ca. 56% at 1 mM. Its variation in activity with compound **2**, despite both being dichloropalladium complexes, is attributed to the ligand systems suggesting that geometric isomerisation plays an important role.

Compound **2** is monodentate system and could exist as *trans-cis* isomer in solution while compound **5** had a definite *cis* geometry imparted by the rigid ligand used. While all complexes with chloro ligand *cis* or *trans* to the bridging ligand have been reported to show good activity, it is the complexes in the *trans* configuration that are generally more active. From a mechanistic point of view, it means that compound **2** is able to form both intrastrand and interstrand DNA adducts while the latter having a rigid geometry i.e. *cis*-conformation, could only form intrastrand DNA adducts. However in this study compound **2** was less active than **5** suggesting again that compound **2** is less stable in solution hence is susceptible to translabilization compared to **5** which is favoured by SARs (section 1.4) hence its activity being higher than that of the former, **2** (Figs 4.4 and 4.6).

Another observation made is the role played by the bulkiness of the ligands, i.e. pyrazole and 3,5-dimethylpyrazole. A comparison of the activities of compounds **3** and **4** at all concentrations indicated that compound **4** is more active. Palladium compounds **1** and **2** showed similar trend with **2** being more active. However, these were thought to be significantly low values.

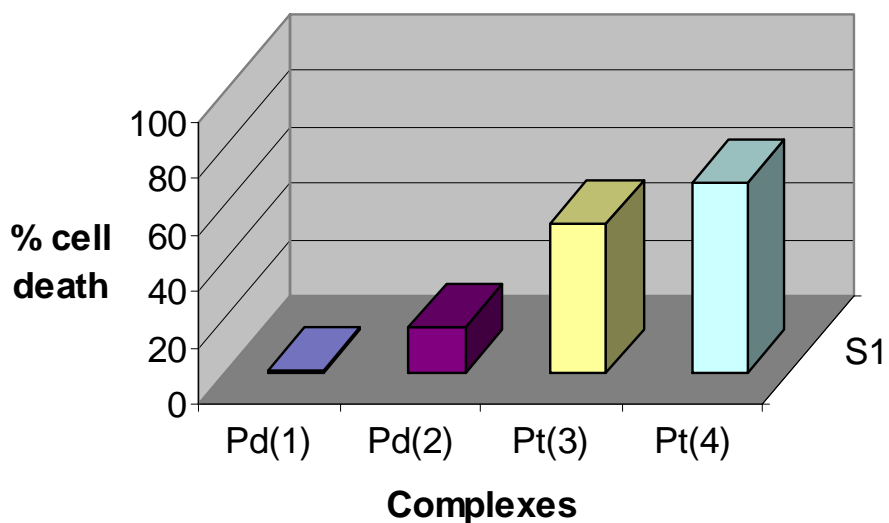


**Figure 4.5.** Comparison of the effects of ligand and the metal in the overall activity of the complexes.

From the results obtained, it was deduced that the antitumor activity of the complexes increased with the increase in bulkiness of the non-leaving ligands (Fig. 4.6). The same observation was made by Christian *et. al.* when they found dichloro-2-(2-pyridyl)benzimidazoleplatinum(II) more active than cisplatin.<sup>8</sup> Sterically hindering bulky ligands are found to reduce rapid detoxification by thiol-containing molecules. There is also a probability that such ligands prevent translabilization and undesired displacement of the non-leaving ligand by other nitrogen donors.<sup>9</sup>

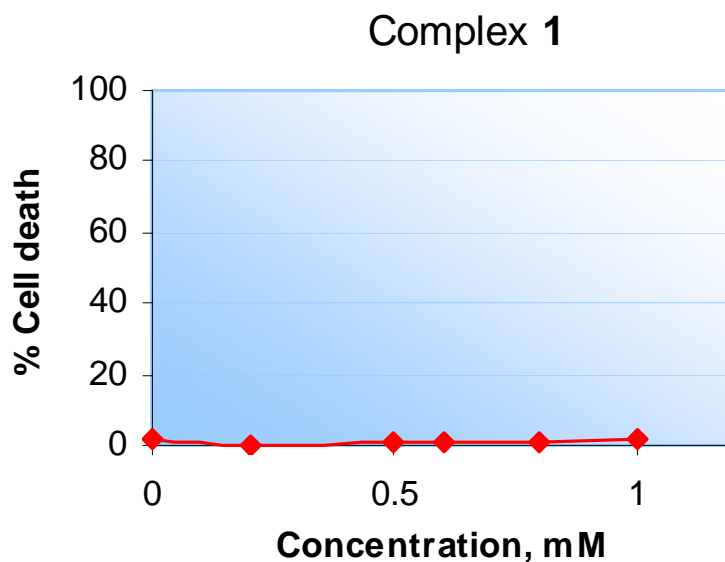
One major undoing in our study was the inability of cisplatin to induce apoptosis in the CHO cells. The cells treated with cisplatin despite showing the lack of cell multiplication, could not stain the APOPercentage<sup>TM</sup> dye. Although cisplatin is known to induce apoptosis in some cancer cells, e.g. CH1 cells, as reported by other scientists among them

Devarajan *et al.*<sup>10</sup> and Viktorsson *et al.*<sup>11</sup>, surprisingly that was not the case in our experiments on CHO cells. From the morphological changes observed using the light microscopy technique, the cells stopped multiplying and looked rigid suggesting the cells growth inhibitory effect by the chemical. In this case we found two possible explanations to this result: (1) It could imply that the cells did not undergo the flip-flop mechanism, a phenomenon that leads to the dye passing across the cell membrane into the cytoplasm suggesting that the cells died via another mechanism and not apoptosis. This means the cell death could have been as a result of effect on spindles responsible in the homeostatic process of meiosis, being stiffened by the drug. Such mechanism has been reported to be a pathway of cell death induced by the famous natural antitumor agent Taxol.<sup>12</sup> (2) It could be the fact that in respect to this cell-line, cisplatin was not a cell specific cytostatic drug. Its inhibition of cell division in G<sub>2</sub>-phase did not only lengthen this phase but could have also delayed cell death. This property of cisplatin could explain the delay/absence of apoptosis in comparison with the complexes tested.<sup>13</sup> There are also published literatures on the inability of cisplatin to induce apoptosis on some other cancer cell types, e.g. L1210.<sup>14</sup> That notwithstanding, acquisition of results on the complexes that were investigated was successful. The cytotoxic results obtained from the study performed indicated that not all the compounds exhibited a remarkable cell inhibition activity at all doses assayed. Generally there was an upward trend observed in the cell death caused by all the compounds.

Compound **1** and **2** had no substantial apoptotic property detected. This is indicated by the quasi horizontal curve in Figure 4.6. This is similar to the results reported by Sanja *et al.*<sup>15</sup> in which the K[Ru(eddp)Cl<sub>2</sub>] complex assayed for cytotoxicity against human breast



carcinoma BT-20, did not show any significant effect suggesting different ability of compounds to induce cell death in different cell lines vary. It is possible that these compounds have no significant effect on the CHO cell line used in this case but could have significant effect on other cell lines. But from the chemistry point of view, palladium complexes are known to be both thermally and kinetically unstable and thus undergo substitution reaction more readily than platinum complexes. Complex **1** and **2** could have undergone hydrolysis to afford its monofunctional reactive species before it was induced on the cells, a factor that could explain the observation made on its activity.



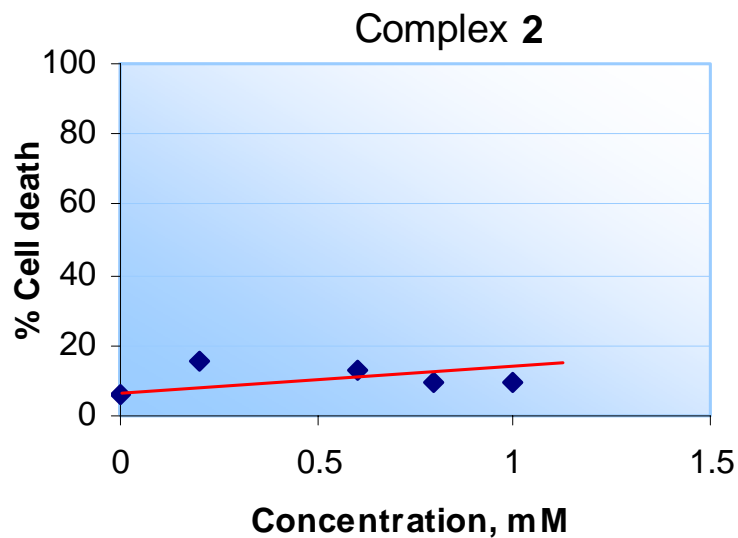


**Figure 4.6.** Graphical representation of concentration-dependent effect of the compounds **1** and **2** on CHO cells treated for 24 h respectively. No significant cell death at all concentrations (see text).

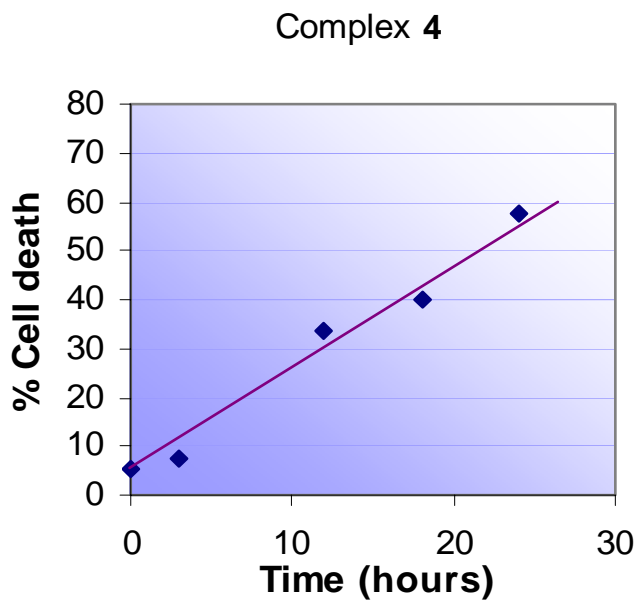
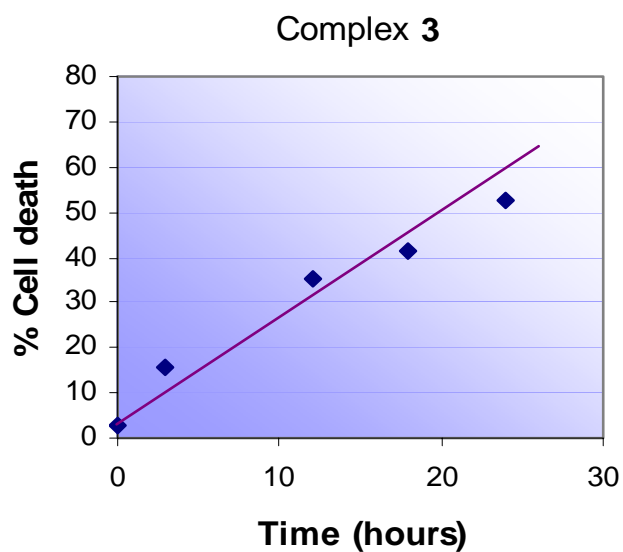
In general platinum containing compounds were also found to be more active than those of palladium. Compounds **3** and **4** were found to be the more active compared to **5**. Compound **4** is the most active. Quite apart from the screening of compounds at different concentrations, we were able to justify that the cell death was through apoptosis pathway as opposed to necrosis (lysis). This is evident from the apoptosis assay performed that indeed these compounds induced cell death via the programmed cell death.

#### 4.4.3 Time-dependent reaction courses of the compounds on the treated cells

Time-dependent reactions course of the compounds on test were done to investigate further the uptake of the drugs with time. In this case three compounds, complex **3**, **4** and **5** were used. Each compound exhibited a characteristic uptake-time curve on CHO cells, the common trend was an increase that reached equilibrium within 24 h. The uptake of the compounds was found to be slow and increasing almost linearly with time. Attempts to let the time-dependent experiment to run for more than 24 h were unsuccessful. This was attributed to prolonged incubation time thereby leading to the damage and subsequent blockage of the membrane functionality, as a result of extensive platination.<sup>16</sup> The end result was membrane damage which have could limited further analysis. A similar observation has been reported by Reile *et al.*<sup>17</sup>

It is worth noting however that in this study, the compounds were tested at different concentration i.e. minimum concentration showing significant cell death and therefore the results are not comparable. Nevertheless they registered a similar trend as mentioned earlier. Two platinum complexes, **3** and **4** were used at concentrations 0.05 mM and 0.2 mM respectively. Compound **5** (palladium containing) was used at concentration, 0.60 mM. At 0.20 mM, complex **3** showed a percentage cell death of approximately 35 in 12 h to reach approximately 52% after 24 h. Complex **4** showed a similar pattern (at 0.05 mM) with percentage cell death of approximately 34 and 58 in 12 h and 24 h respectively. Compound **5** exhibited relatively the same time-dependent course but at a higher concentration of 0.60 mM. It was found to induce a percentage cell death of approximately 27 in 12 h to reach 40% in 24 h. Of interest was how **4** induced almost the

same percentage cell death as **3** and **5** but at lower concentration, a factor that shows how a specific metal coordinated to a given ligand with certain geometry could impart activity to a compound and that increase in bulkiness of the ligand leads to higher activity (section 4.4.3).



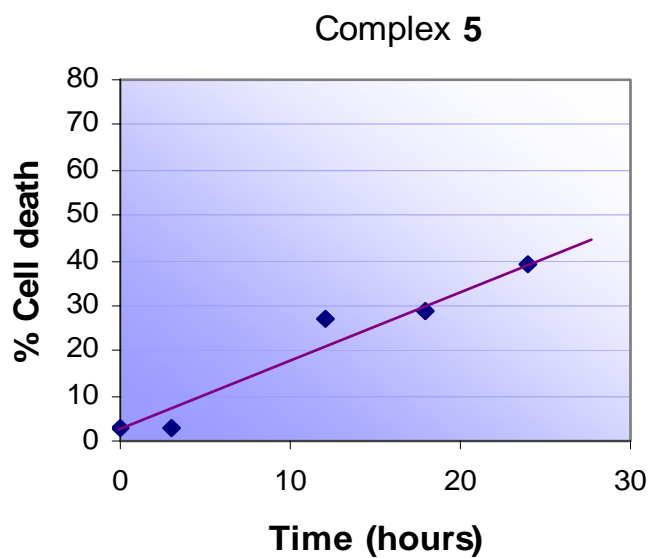


**Figure 4.7.** Graphical representation of time-dependent effect of the compounds on treated CHO cells. The treated cells (for 24 h) were stained with APOP dye and evaluated by FACS as indicated in text. The graphs show the effect of complexes **3** (0.20 mM), **4** (0.05 mM) and **5** (0.60 mM) respectively.

#### ***4.4.4 Evaluation of mechanism of cell death by DNA and RNA content measurement***

Cell cycle analysis was a useful tool in determining the effects of the compounds being tested on the CHO cells. Our studies designed to investigate the relationship between the inhibition of DNA synthesis, cytotoxicity, and cell-cycle progression suggested that the complexes used inhibit DNA transcription and replication.<sup>18</sup> We examined the effect of the complexes on the cell cycle progression and observed that almost all the treated cells did not enter the cell cycle; rather they lagged in the G<sub>1</sub>- phase. The main effect of these complexes was their ability to reduce cells in G<sub>1</sub>-phase accompanied with a simultaneous increase in cells with less than G<sub>1</sub> DNA content (Fig. 4.9). At 24 h the treated cultures contained less G<sub>1</sub>- phase cells (52.15%) and 11 times more Ap-phase (apoptotic) cells (31.10%) compared to untreated cells which had 69.86% and 2.72% respectively (Fig. 4.8).

The cell-cycle disturbances were associated with inhibition of cell proliferation in agreement with results reported by Martin *et al.*<sup>19</sup> in their cell-cycle disturbance studies. This suggests that the reduction in G<sub>1</sub>-phase cells was as a result of the accumulation of Ap-phase cells a fact that is attributed to induction of apoptosis by compounds in test. Contrary to results reported by Sorenson *et al.*<sup>20</sup> in their study of cisplatin treated CHO cells, that the cells progressed through S phase, where DNA synthesis occurs, and were arrested in the G<sub>2</sub>-phase ( see Fig 2.5, chapter 2), our results indicate that the cells in G<sub>1</sub>-phase could not encounter DNA replication (synthesis). Rather, our observation is that the cells were trapped in G<sub>1</sub>-phase and therefore paused their progress in the cycle and subsequently entered an indefinite phase, Ap-phase (31.10%). This is attributed to the

complex binding to DNA in G<sub>1</sub>-phase and therefore disrupting its programme of passing the DNA for replication in the S-phase. This then caused the cell receptors to detect the anomaly hence triggering apoptosis.

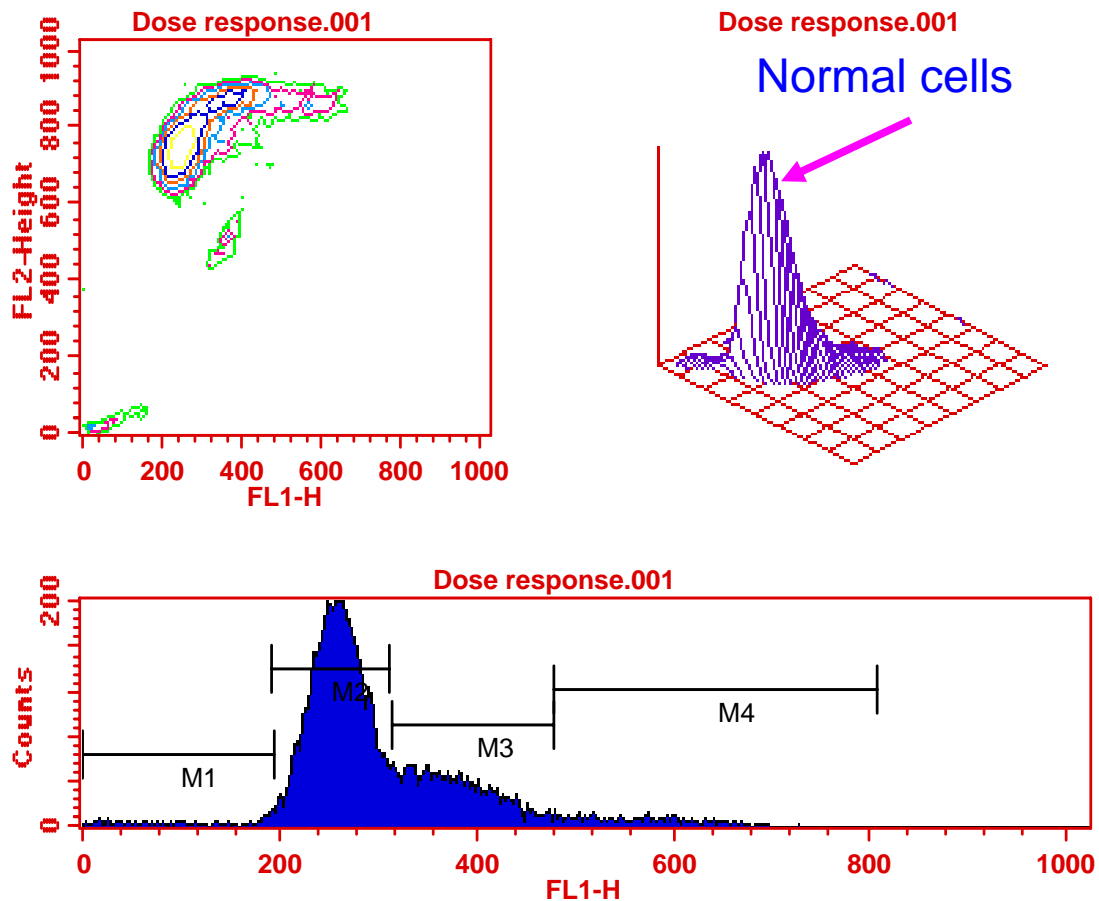


**Figure 4.8.** Differential staining of RNA and DNA with acridine orange (section 4.2.3) of control. Cell cycle progression of the untreated CHO cells after 24 h. **M1** = Ap-phase (apoptotic cells are in M1), **M2** = G<sub>1</sub>-phase, **M3** = S-phase, **M4** = G<sub>2</sub>/M-phase.

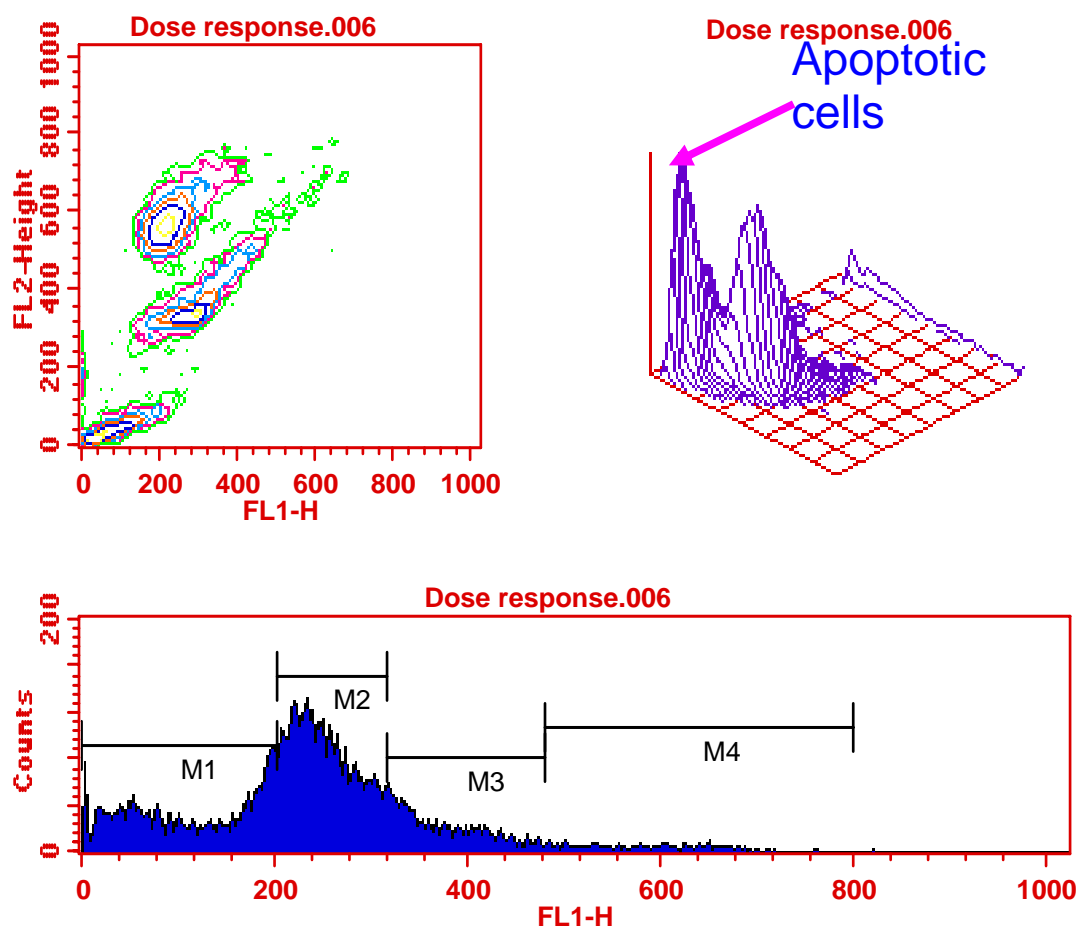


**Figure 4.9.** Differential staining of RNA and DNA with acridine orange (section 4.2.3) of treated cells. Cell cycle progression of CHO cells treated with compound **5** (0.60 mM), for 24 h. **M1** = Ap-phase (apoptotic cells are in M1), **M2** = G<sub>1</sub>-phase, **M3** = S-phase, **M4** = G<sub>2</sub>/M-phase.



#### ***4.4.5 Induction of genomic DNA cleavage***

To further characterize the apoptotic activity of the palladium and platinum compounds, two complexes **3** and **5** were used to examine the ability of these compounds to induce DNA fragmentation in CHO cells. Using agarose gel electrophoresis, the formation of the nucleosomal DNA fragments by the control and drug-treated cells was investigated. The inter-nucleosomal DNA cleavage seen was similar to those reported by Moradell *et al.*<sup>2</sup> The undigested DNA appeared as a band of large molecular size corresponding to genomic DNA in control cells whereas in the treated cells there was evidence of genomic DNA digested into smaller fragments. Results obtained from cells treated with the complex **3** (platinum containing) were more pronounced than those of **5** (palladium containing). This was an indication of DNA double-strand cleavage occurring in the linker regions between nucleosomes thereby producing fragments that are multiples of approximately 201 base pairs (Fig. 4.10). This feature is the biochemical hallmark of apoptosis.

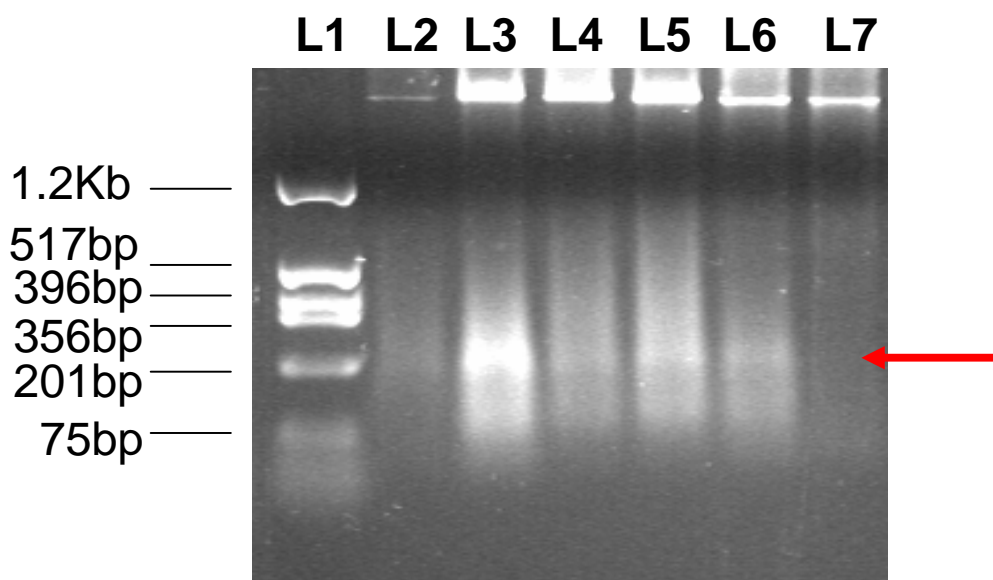


**Figure4.10.** DNA fragmentation pattern of CHO cells treated with complex **2**. Lane identification: **L1** = DNA size marker, **L2** = control cells without treatment, **L3** = treated cells, 0.05 mM, **L4** = treated cells, 0.10 mM, **L5** = treated cells, 0.15 mM, **L6** = treated cells, 0.20 mM, **L7** = treated cells 0.50 mM.

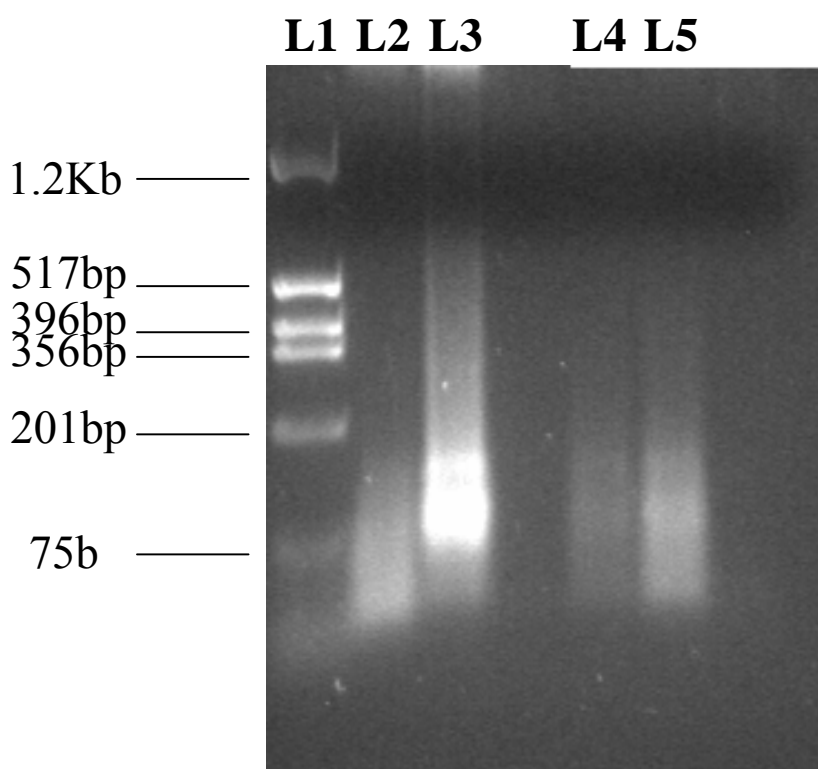


**Figure 4.11.** DNA fragmentation pattern of CHO cells treated with complex **5**. Lane identification: **L1** = DNA size marker, **L2** = control cells without treatment, **L3** = treated cells, 0.60 mM, **L4** = treated cells, 0.80 mM, **L5** = treated cells, 1 mM,

The DNA fragmentation visualized for complex **5** was not very clear as the bands appeared as smears (Fig. 4.12). It is possible that the compound could have led to an increase in membrane permeability resulting in the loss of small DNA fragments by the time of analysis and therefore could not be detected.<sup>21</sup> This occurrence would account for the slight smearing of the DNA upon gel electrophoresis. It is also possible that the experiment was run for a longer period and consequently smears observed as opposed to laddering. Similar observations were reported by Bortner *et al.*<sup>22</sup> and Schulze-Osthoff *et al.*<sup>23</sup>

#### ***4.5 Reactions of platinum(II) complex with glutathione monitored by <sup>1</sup>H NMR spectroscopy***

Cis-dichloro-bis-(pyrazole)platinum(II) (Complex **3**) was used as a representative complex in the reaction with glutathione.<sup>24</sup> The reactions were monitored by taking a <sup>1</sup>H NMR spectrum in the intervals of 1, 1.5, 3, and 18 h. For reliability, each single experiment was carried out at least twice, and always identical product signals and similar reaction proceedings were observed.

Ideally the reaction of this complex with excess GSH is a typical representation of such reaction *in vivo* where the concentration of GSH in the cell is about 8-100 mM. Of interest was to determine the rate of reaction (ligand exchange) of compounds **1-5** with GSH, since GSH is one of the biomolecules that reacts with drugs in the cells leading to acquired resistance against the drug by the cells. This study was achieved by monitoring the changes in three peaks (7.93, 7.52, and 6.39 ppm) belonging to the complex upon interaction with GSH, as reported by Kelemu *et al.*<sup>3</sup> in a similar study. This gave an indication of the typical reaction in the cell.

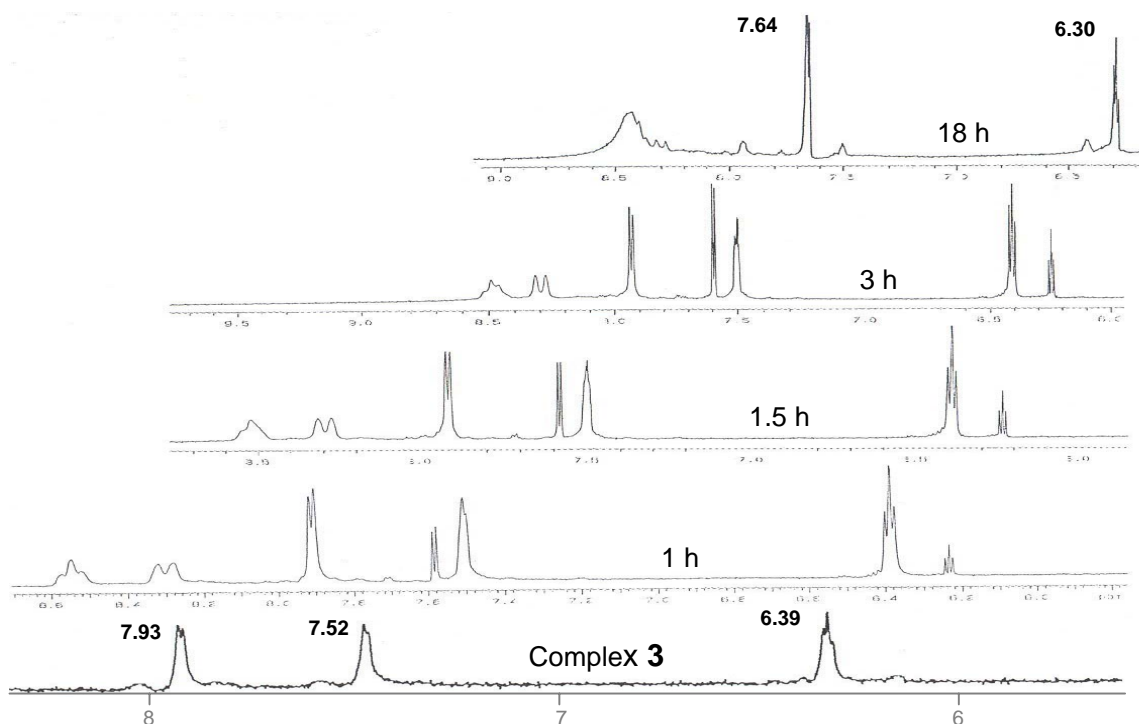


**Figure 4.12.** <sup>1</sup>H NMR spectra showing the reaction of complex **3** with GSH (ratio 1:2) at room temperature, as monitored by <sup>1</sup>H NMR. The peaks of the complex monitored are; 7.93, 7.52, and 6.39 ppm

When compound **3** was reacted with GSH, the signals recorded at time 0 h were those of the complex i.e. 7.93, 7.52, 6.39 ppm (Fig.4.14). The new peaks observed at 7.59 ppm (doublet) and 6.24 ppm (triplet) respectively after 1h, suggested formation of a secondary product, indicating that there is a ligand substitution process whereby the pyrazolic ligand system was being displaced by the glutathione. After 1.5 h, the two new peaks were more pronounced. These are typical of the third and fourth protons, **e** and **f** (Fig. 4.14) of free pyrazole ligand emerging. Eventually at 18 h, the primary starting material (complex) was completely diminished. Instead, the noticeable peaks were at 7.64 ppm (**d** and **e**) and

6.30 ppm (f) respectively (Fig. 4.14) corresponding to those of free pyrazole 7.64 and 6.36 ppm. The assignment of the peaks is summarized in Table 4.2.

One striking feature is the slow disappearance of the peak at 7.93 ppm (c). In the spectrum at 18 h it has completely disappeared. Ideally in the spectrum of free pyrazole there are three peaks, N-H, 4 H, with 3H (e) and 5H (d). When it is complexed, 3H (7.52 ppm) and 5H (7.93 ppm) protons resonates at different frequencies. They exhibit different chemical environment a factor resulting from coordination to the metal center. Thus with the ligand substitution by GSH over a period of time, the peak at 7.93 ppm disappears leaving the peaks at 7.64 ppm (3H and 5H) and 6.30 ppm (4H) of pyrazole respectively. The absence of the N-H signal is attributed to the proton undergoing deuterium exchange in solvent. Of interest is the appearance of the peaks at ca. 8.55 and 8.32 ppm after 1h of reaction. At 18 h, these peaks had merged to give one broad peak at 8.43 ppm an indication that there was a formation of a secondary product. Although the observations made are in agreement with the theoretical principals that ligand substitution reaction took place, we could not speculate on the resultant product, as the attempts to isolate the compound for structure elucidation were unsuccessful.

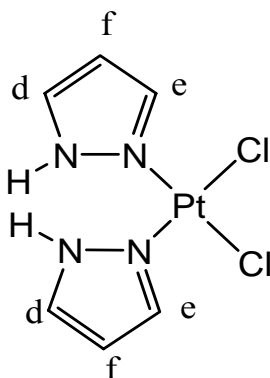


**Figure 4.13.** Cis-dichloro-bis-(pyrazole)platinum(II), **3**

**Table 4.2.** Showing the disappearance of the complex and emerging of the ligand (pyrazole) substituted by GSH.

Time (Hours)	Proton peaks of the complex disappearing			Proton peaks of the ligand (pyrazole) emerging	
	c	e	f	d	f <sup>l</sup>
0	7.93	7.52	6.40	7.60	-
1.00	7.90	7.50	6.39	7.58	6.24
1.50	7.92	7.50	6.39	7.58	6.24
3.00	7.94	7.50	6.41	7.60	6.26
18.00	-	-	-	<b>7.64</b>	<b>6.30</b>

Glutathione is known to have cysteine as one of its constituents. In this case cysteine is known to contain three possible coordination sites, the sulfhydryl, the amino and the carboxyl groups. It coordinates to platinum through the oxygen and the sulfur atoms. However, when cysteine is incorporated into a peptide, in this case GSH, it is sandwiched between glutamic acid and glycine ends. This then leads to oxygen molecule not available as a chelating site. It acts as a bidentate chelating ligand, coordinating to the platinum via the cysteinyl sulfur and nitrogen atoms (the latter, part of the peptide bond to glutamic acid).<sup>24</sup>

Our postulate is that when the sulfur is coordinated to platinum, it will labilize the *trans* aromatic amine ligand (pyrazole) leading to its replacement by glutathione molecule through formation of a Pt-S bond. Several attempts to isolate the product and perform spectroscopic analysis in order to elucidate the possible structure were unsuccessful.

#### **4.6 Conclusions**

It is well known that one of the handicaps of cancer chemotherapy is the local toxicity produced by the currently used drugs, due to their accumulation in several organs and tissues at therapeutic doses. Apoptosis is considered to be a proper physiological pathway of cell death than necrosis, because lysis of the necrotic cells leads to the production of local side effects due to the release of toxic substances from inside the cell to the extracellular environment. The complexes discussed above were studied for their induction of apoptosis and not just their cytotoxicity. The morphological changes observed showed that induced cell death occurs through apoptosis. Further analysis of the cytotoxicity activities of these complexes by flow cytometry, indicates that they are both



dose and time dependent except for complexes **1** and **2** which were considered inactive. The highest activity of most complexes was achieved after 24 h. The measurement of apoptotic cells by double staining of DNA and RNA enabled the determination of the effects of compounds on the cell cycle of the treated CHO cells. A greater population of cells were found trapped in the G<sub>1</sub>-phase with time, suggesting that DNA replication is stopped and apoptosis take place. The observation made in the DNA fragmentation experiments (especially with compound **3**) is an indication of the genomic DNA cleavage. This not only indicates apoptosis but it also shows that the complexes are able to bind to the DNA and as result stop DNA replication.

As part of our systematic research on this type of compounds, our interest was directed to the substitution of platinum by its homologue palladium for the investigation of their potential in anticancer agents research. However platinum complexes were found to be more active than the palladium complexes. In addition, complexes carrying bulkier substituents on the pyrazole ligands were more active, suggesting that with increase in bulkiness the translabilization of complexes is reduced and as a result activity increased. In general complexes exhibiting *trans* disposition were found to be more active than those in *cis* configuration except for palladium complexes. One of the reasons as to why *trans* complexes could be more active than *cis*, apart from forming intrastrand and interstrand DNA adducts, is that the different accumulation can be accounted for by the intrinsic lower polarity of *trans*-geometry (idealized D<sub>2h</sub> symmetry) with respect to *cis*-geometry (idealized C<sub>2v</sub> geometry).

The reaction of complex **3** and glutathione gave an indication of the possible reactions that occur in the cell *in vivo*. This includes the displacement of the non-leaving ligand by sulfur containing compounds.

#### 4.7 References.

1. Jana K., Oldrich V., Nicholus F., Viktor B., *J. Inorg. Biochem.* 98 (2004) 1560.
2. Moradell S., Julia L., Ana R., Marc S. R., Francesc X. A., Virtudes M., Rafael de L., Angeles M., Reedijk J., Antoni L., *J. Inorg. Biochem.* 96 (2003) 493.
3. Kelemu L., Tiesheng S., Lars I. E., *Inorg. Chem.*, 39 (2000) 1728.
4. Ken S., Yasushi T., Takuma U., Koji G., Masakatsu O., Taro Tsaboruma, K., Kenji O., Kazuyuki K., *Inorg. Chim. Acta* 297 (2000) 64.
5. Martin Z., Anne Odile H., Wiebke B., Gerard E., *Biochim. Biophys. Acta* 1551 (2001) F1.
6. Wilcock C., Hickman J. A., *Biochim. Biophys. Acta* 946 (1988) 359.
7. Micheal J. R., Sarah F., Christian M., Ina P., Bernt K., *Inorg. Chim. Acta* 350 (2003) 355.
8. Christian M., Ina P., Michael J. R., Gesche T., Jhannes E. A. W., Bernt K., *Inorg. Chim. Acta* 319 (2001) 109.
9. Fatma G., Oztekin A., Gokcen E., Hatice E., *Eur. J. Med. Chem.* 38 (2003) 473.
10. Devarajan P., Michelle S., Patricia M. C., Moon S. P., Nora E., Gilda K., Federico K., *Hear. Res.* 174 (2002) 45.
11. Viktorsson K., Jessica E., Maria C. L., Rolf L., Boris Z., Stig L., Maria C. S., *Exp. Cell Res.*, 289 (2003) 256.
12. Blagosklonny M. V., Giannakakou P., El-Deiry W. S., Kingston D. G. I., Higgs P. I., Neckers L., Fojo T., *Cancer Res.*, 57 (1997) 130.
13. Beata K., Regina O., Ewa C., Leszek S., Elzbieta Z., Justyn O., *Mutat. Res.* 558 (2004) 169.

14. Russell J., Ling C. C., *Eur. J. Cancer* 39 (2003) 2234.
15. Sanja R., Grguric S., Rosario A. V., Jose M. P., Miguel A. F., Carlos A., Ysmael A., Tibor J. S., Francisco G., *J. Inorg. Biochem.* 97 (2003) 215.
16. AnnaRita G., Maurizio A., Claudio C., Elisabetta G., Domenico O., *J. Inorg. Biochem.* 98 (2004) 73.
17. Reile H., Bernhardt G., Koch M., Schonenberger H., Hollstein M., Lux F., *Cancer Chemother. Pharmacol.* 30 (1992) 113.
18. Elizabeth R. J., Stephen J. L., *Chem. Rev.* 99 (1999) 2467.
19. Martin B. Oleksiewicz, Soren A., *J. Virol.* 71 (1997) 1386.
20. Sorenson C. M., Eastman A., *Cancer Res.* 48 (1988) 6703.
21. Ormerod M. G., O'Neill C. F., Robertson D., Harrap K. R., *Exp. Cell Res.* 211 (1994) 231.
22. Bortner C. D., Cidlowiski J. A., *Trends Cell Biol.* 5 (1995) 21.
23. Schulze-Osthoff K., Walczak H., Droge W., Krammer P.H., *J. Cell Biol.* 127 (1994) 15.
24. Bart A.J. Jansen, Brouwer J., Reedijk J., *J. Inorg. Biochem.* 89 (2002) 197.